From coastal waters to the open ocean: the variability and emissions of methane and nitrous oxide

Dissertation

zur Erlangung des Doktorgrades

der Mathematisch-Naturwissenschaftlichen Fakultät

der Christian-Albrechts-Universität zu Kiel

vorgelegt von

Xiao Ma

Kiel, 2020

Erste/r Gutachter:	Prof. Dr. Hermann Bange
Zweite/r Gutachter:	Prof. Dr. Arne Körtzinger
Tag der mündlichen Prüfung:	
Zum Druck genehmigt:	

Hiermit erkläre ich, dass ich die vorliegende Doktorarbeit selbständig und ohne unerlaubte Hilfe erstellt habe. Weder diese noch eine ähnliche Arbeit wurde an einer anderen Abteilung oder Hochschule im Rahmen eines Prüfungsverfahrens vorgelegt, veröffentlicht oder zur Veröffentlichung vorgelegt. Ferner versichere ich, dass die Arbeit unter Einhaltung der Regeln guter wissenschaftlicher Praxis der Deutschen Forschungsgemeinschaft entstanden ist.

Kiel, den 14 August 2020 ……

Xiao Ma

Table of Contents

Abstract

Methane (CH_4) and nitrous oxide (N_2O) are potent greenhouse gases which are involved in atmospheric chemistry and global warming. Oceans, especially coastal regions, are important sources of these gases. Long-term observations and field investigations on a global scale are effective tools to constrain the uncertainty of oceanic CH_4 and N_2O emissions, to assess trends and to predict potential changes in the future. In this study, the variability and emissions of CH_4 and N_2O were investigated at the Boknis Eck (BE) time-series station located in the coastal SW Baltic Sea during 2005–2017, and the results of continuous underway measurement and depth profiles of N_2O were reported from a cruise to the SW Indian Ocean. Hydroxylamine (NH_2OH), a short-lived intermediate in the nitrogen cycle and precursor of N_2O, was also measured at several locations during the same cruise, in order to decipher the N_2O production pathway in the ocean. The major findings are:

1) Dissolved CH_4 concentrations fluctuated between 2.9 and 695.6 nM, with an average of 51.2 ± 84.2 nM during 2006–2017 at the BE time-series station. In general, CH_4 concentrations were higher in the bottom water than in the surface layer, indicating the release of CH_4 from the sediments. CH_4 maxima were usually observed in the bottom water in February, June and October. Enhanced CH_4 concentrations in the upper water layer as, for example, observed in December 2014, could be explained by a major Baltic inflow of North Sea water. This event significantly promoted CH_4 emissions to the atmosphere. During 2006–2017, sea-to-air CH_4 flux densities ranged between 0.3 and 746.3 µmol m^{-2} d^{-1}, with an average of 43.8 ± 88.7 µmol m^{-2} d^{-1}, while in December 2014, the value was 3104.5 µmol m^{-2} d^{-1}. Throughout the sampling period, surface BE water was supersaturated with CH_4 and thus emitting CH_4 to the atmosphere.
2) During 2005–2017, N_2O concentrations at the BE time-series station varied between 1.2 and 37.8 nM, with an overall average of 13.9 ± 4.2 nM. N_2O concentrations showed a significant seasonal cycle with low concentrations (undersaturation) in autumn, coinciding with hypoxic/anoxic conditions in the bottom water. Relatively low N_2O concentrations were observed during October 2016–April 2017, and relatively high N_2O concentrations were observed in November 2017, but no significant N_2O trend was detected during 2005–2017. N_2O flux densities were estimated to range between -19.0 and 105.7 µmol m^{-2} d^{-1}, with an average of 3.5 ± 12.4 µmol m^{-2} d^{-1}, indicating that BE is a moderate source of atmospheric N_2O.

3) Surface N_2O concentrations in the southwestern Indian Ocean ranged between 5.8 and 8.0 nM (mean ± SD: 6.9 ± 0.6 nM). Surface waters were mostly supersaturated with respect to atmospheric equilibrium (mean ± SD: 104.1 ± 2.8%), and most of the outgassing occurred along the zonal band between 5°S and 10°S. Depths profiles showed a generally inverse relationship between N_2O and oxygen with N_2O maxima at about 1000 m. For waters above and below 1000 m, different slopes were found in the correlations between ΔN_2O (excess N_2O)/AOU (apparent oxygen utilization) and $\Delta N_2O/NO_3^-$. NH_2OH concentrations in the sampling area varied between below detection limit and 6.76 nM. Although NH_2OH concentrations were variable in the Indian Ocean, we suggest that nitrification might be the dominant pathway of N_2O formation.

In summary, the distributions and variations of CH_4 and N_2O in coastal and open ocean environments are driven by a complex interplay of various biological and physical processes, and the situation might be even more complicate in coastal waters because of the strong anthropogenic influences. Coastal waters and the open ocean are important sources of atmospheric CH_4 and N_2O, but the answer to the emerging question of how these emissions will change with the further development of global warming and ocean deoxygenation remains ambiguous.

Kurzfassung

Methan (CH_4) und Distickstoffmonoxid (N_2O) sind starke Treibhausgase, die an der Atmosphärenchemie und der globalen Erwärmung beteiligt sind. Die Ozeane, insbesondere die Küstenregionen, sind wichtige Quellen dieser Gase. Langzeitbeobachtungen und Felduntersuchungen auf globaler Ebene sind wirksame Instrumente, um die Unsicherheit der ozeanischen CH_4- und N_2O-Emissionen zu verringern, Trends abzuschätzen und potenzielle Veränderungen in der Zukunft vorherzusagen. In dieser Studie untersuchten wir die Variabilität und die Emissionen von CH_4 und N_2O an der Zeitserienstation Boknis Eck (BE) im küstennahen südwestlichen Teil der Ostsee im Zeitraum 2005-2017 und berichten über die Ergebnisse kontinuierlicher ‚Underway'-Messungen und Tiefenprofile von N_2O von einer Forschungsfahrt in den südwestlichen Indischen Ozean. Hydroxylamin (NH_2OH), ein kurzlebiges Zwischenprodukt im Stickstoffkeislauf und Vorläufer von N_2O, wurde ebenfalls während derselben Fahrt gemessen, um den N_2O-Produktionsweg im Ozean zu entschlüsseln. Die wichtigsten Ergebnisse sind:

1) Die gelösten CH_4-Konzentrationen schwankten zwischen 2,9 und 695,6 nM, mit einem Durchschnitt von 51,2 ± 84,2 nM im Zeitraum 2006-2017 an der BE-Zeitserienstation. Im Allgemeinen waren die CH_4-Konzentrationen im Bodenwasser höher als in der Oberflächenschicht, was auf die Freisetzung von CH_4 aus den Sedimenten hinweist. CH_4-Höchstwerte wurden gewöhnlich im Februar, Juni und Oktober im Bodenwasser beobachtet. Erhöhte CH_4-Konzentrationen in der oberen Wasserschicht, wie sie z.B. im Dezember 2014 beobachtet wurden, könnten durch einen starken Einstrom von Nordseewasser erklärt werden. Dieses Ereignis verstärkte die CH_4-Emissionen in die Atmosphäre signifikant. Im Zeitraum 2006-2017 lagen die ozeanischen CH_4- Emissionen zwischen 0,3 und 746,3 µmol m^{-2} d^{-1}, mit einem Mittelwert von 43,8 ± 88,7 µmol m^{-2} d^{-1}, während im Dezember 2014 der Wert 3104,5 µmol m^{-2} d^{-1} betrug. Während des gesamten Probenahmezeitraums war das Oberflächenwasser an der Zeitserienstation BE mit CH_4 übersättigt und gab somit CH_4 an die Atmosphäre ab.

2) Im Zeitraum 2005-2017 schwankten die N_2O-Konzentrationen an der BE-Zeitserienstation zwischen 1,2 und 37,8 nM, mit einem Gesamtmittelwert von 13,9 ± 4,2 nM. Die N_2O-Konzentrationen zeigten einen signifikanten saisonalen Zyklus mit geringen Konzentrationen (Untersättigung) im Herbst, der mit hypoxischen/anoxischen Bedingungen im Bodenwasser einherging. Wir beobachteten relativ niedrige N_2O-Konzentrationen in den Monaten Oktober 2016 bis April 2017 und relativ hohe N_2O-Konzentrationen im November 2017, aber im Zeitraum 2005-2017 wurde kein signifikanter N_2O-Trend festgestellt. Die N_2O-Emissionen wurden auf einen Bereich

zwischen -19,0 und 105,7 µmol m^{-2} d^{-1} geschätzt, mit einem Durchschnitt von 3,5 ± 12,4 µmol m^{-2} d^{-1}, was darauf hinweist, dass BE eine mäßige Quelle für atmosphärisches N_2O ist.

3) Die N_2O-Oberflächenkonzentrationen im südwestlichen Indischen Ozean lagen zwischen 5,8 und 8,0 nM (Mittelwert ± SD: 6,9 ± 0,6 nM). Das Oberflächenwasser war in Bezug auf den atmosphärischen Gleichgewichtswert größtenteils übersättigt (Mittelwert ± SD: 104,1 ± 2,8%) und die stärksten Emissionen erfolgten entlang eines Bandes zwischen 5°S und 10°S. Die Tiefenprofile zeigten eine im Allgemeinen umgekehrte Beziehung zwischen N_2O und Sauerstoff mit N_2O-Maxima bei etwa 1000 m Tiefe. Für Wassermassen oberhalb und unterhalb von 1000 m wurden unterschiedliche Steigungen in den Korrelationen zwischen ΔN_2O (N_2O-Überschuss)/AOU (scheinbarer Sauerstoffverbrauch) und $\Delta N_2O/NO_3^-$ gefunden. Die NH_2OH-Konzentrationen schwankten zwischen unterhalb der Nachweisgrenze und 6,76 nM. Obwohl die NH_2OH-Konzentrationen im Indischen Ozean variabel waren, vermuten wir, dass Nitrifikation der dominierende Pfad der N_2O-Bildung sein könnte.

Zusammenfassend lässt sich sagen, dass die Verteilungen und Variationen von CH_4 und N_2O in Küstengewässern und im offenen Ozean durch ein komplexes Zusammenspiel verschiedener biologischer und physikalische Prozesse bestimmt werden und dass dieses Zusammenspiel in Küstengewässern aufgrund der starken anthropogenen Einflüsse noch komplizierter sein könnte. Die Küstengewässer und der offene Ozean sind wichtige Quellen für atmosphärisches CH_4 und N_2O, aber die Antwort auf die aufkommende Frage, wie sich diese Emissionen mit der weiteren Entwicklung der globalen Erwärmung und der Vergrößerung der Sauerstoffminimumzonen in den Weltozeanenverändern werden, bleibt unklar.

Introduction

1 Greenhouse gases (CH_4 and N_2O) and climate change

The Earth is experiencing a series of unprecedented environmental changes due to extensive human activities. Global warming, for example, has been demonstrated by long-term temperature measurements and decreasing glaciers and ice coverage in polar regions (see e.g. Haeberli, 1990; Karl et al., 1991; Haeberli and Beniston, 1998; Pollack et al., 1998; Dyurgerov et al., 2000; Soruco et al., 2009; Thompson, 2010). The sharp increase in temperature has profound impact on global climate, ecosystems and human society. As a consequence, sea level rise, regional changes in precipitation, more frequent extreme weather conditions and coral bleaching, etc. have been reported over the past decades (see e.g. Pandolfi et al., 2011; Schiermeier, 2011; Munday et al., 2012; Zhai and Liu, 2012; Cazenave et al., 2014). Ocean acidification and deoxygenation can be associated with global warming as well (Keeling et al., 2010; Six et al., 2013; Levin, 2018).

Greenhouse gases (GHGs) play a dominating role in global warming. They can hinder infrared radiations from being emitted to the outer space and hence trap heat in the atmosphere. The development of global warming is closely linked to the increase of GHG mole fractions in the atmosphere. Besides water vapor (H_2O) and carbon dioxide (CO_2), methane (CH_4) and nitrous oxide (N_2O) are important GHGs which significantly contribute to radiative forcing (Kweku et al., 2017).

CH_4 is the most abundant hydrocarbon compound in the atmosphere, with a life time of about 9.1 years (Prather et al., 2012). As a potent GHG, CH_4 is much stronger than CO_2 in capturing heat on a single molecule basis (Lelieveld et al., 1993; IPCC, 2013). In 2016, the radiative forcing due to CH_4 was 0.5 W m^{-2}, which is approximately 25 % that of CO_2 (WMO, 2018). Compared to CH_4, N_2O is much more effective in trapping heat on a single molecule basis (Khalil, 1999). As one of the most important long-lived GHGs, the lifetime of N_2O was estimated to be 116 ± 9 years (Prather et al., 2015). Due to its relatively high global warming potential (GWP) and long lifetime, the contribution of N_2O to radiative forcing reached 0.19 W m^{-2} in 2016, 10% the value of CO_2 (WMO, 2018).

Atmospheric mole fractions of N_2O have been increasing steadily at a rate of around 0.8 ppb yr^{-1}, reaching ~330 ppb nowadays (AGAGE, https://agage.mit.edu/), which is approximately 20% higher than pre-industrial revolution (IPCC, 2013). Excessive usage of fertilizers, combustion of fossil fuels, and wastewater treatment are strong anthropogenic sources of N_2O (Davidson, 2009; Kampschreur et al., 2009; Ussiri and Lal, 2013). CH_4 mole fractions in the atmosphere have increased by about 150% since 1750,

reaching ~1850 ppb nowadays (IPCC, 2013). The increasing trend in mole fractions of atmospheric CH_4 has been lasting for decades. However, the significant increase seemed to have ceased during 2000–2007 (AGAGE, https://agage.mit.edu/). Worden et al. (2017) suggested a decline of CH_4 in biomass burning emissions and an increase in fossil fuel emissions, reconciling the changes in atmospheric CH_4 and its isotopic composition. The renewed growth after 2007 was attributed to enhanced wetland or agricultural emissions (primarily from ruminant animals) (Nisbet et al., 2016; Schaefer et al., 2016; Wolf et al., 2017). Dalsoren et al. (2016) compared observations and model results and attributed recent CH_4 changes to an increase in anthropogenic emissions from East Asia and reduced lifetime. However, the uncertainty in the global CH_4 budget remains considerable, and the potential causes for recent CH_4 trends are still controversially discussed.

Atmospheric CH_4 and N_2O also affect the evolution of stratospheric ozone. CH_4 is an important source of stratospheric water vapor and HO radicals, which, on one hand, increases the HO_X-ozone loss, and on the other hand, sequesters NO_x, thereby reducing the ozone loss in the mid-stratosphere (Randeniya et al., 2002). It is also involved in chlorine deactivation into HCl, and the overall increase of ozone in the extratropics via strengthening of the circulation and changes in chemistry (WMO, 2018). N_2O emissions are primary sources of NO radicals (Wayne, 1991), which can catalytically destroy ozone (Crutzen, 1970; Johnston, 1971). Due to the decrease in the atmospheric mole fractions of other ozone-depleting substances, such as CFC11 and CFC12, the impact of CH_4 and N_2O on stratospheric ozone will be enhanced in the future. N_2O is even considered as the single most important threat of ozone in the 21st century (Ravishankara et al., 2009). Increasing GHG mole fractions (CO_2 and CH_4) can alleviate the post-volcanic chemical ozone destruction due to the cooling of the upper stratosphere (Klobas et al., 2017; Naik et al., 2017). Butler et al. (2016) suggested that extratropical ozone could either remain weakly depleted or even increase well above the historical levels, depending on the future CH_4 and N_2O scenarios. Global ozone is expected to restore to above pre-1980 levels due to future projected increases in GHG emissions (WMO, 2018).

2 Methane (CH_4)

2.1 CH_4 emissions from the ocean

The ocean covers about two thirds of the Earth's surface, but its contribution to CH_4 in the atmosphere is minor (Fig. 1). The oceanic CH_4 emissions were estimated to range from 5 to 25 Tg yr^{-1}, equivalent to about 1–3 % of total CH_4 emissions (Saunois et al., 2016). The global CH_4 flux is disproportionately high from shallow coastal waters. The total CH_4 emitted from continental shelves and estuaries is approximately 13 Tg yr^{-1} and

1–7 Tg yr^{-1}, respectively (Bange et al., 1994; Upstill-Goddard et al., 2000; Middelburg et al., 2002; Borges et al., 2016). Only recently, Weber et al. (2019), by using machine-learning models, were able to narrow the range of global oceanic CH_4 emissions down to 6–12 Tg yr^{-1}, but again highlighted the dominating role of near-shore environments as a source of atmospheric CH_4.

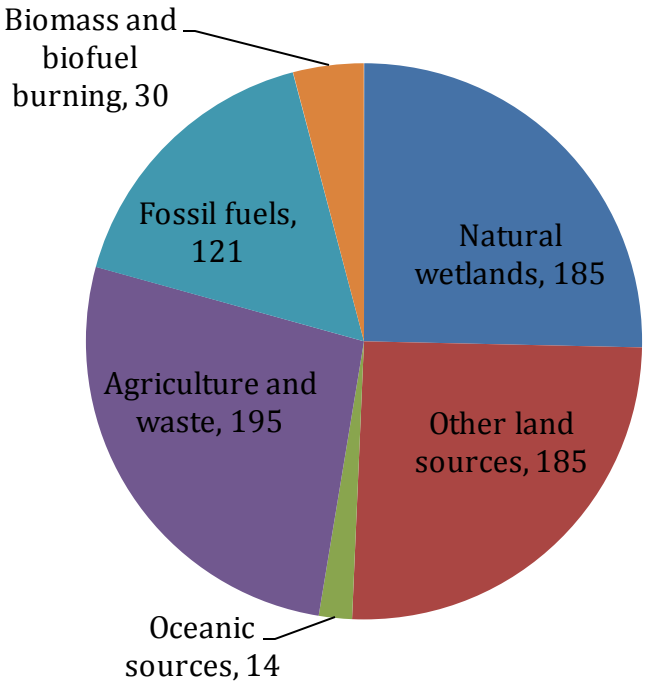

Fig. 1 Global CH_4 emissions by source type in Tg CH_4 yr^{-1} from Saunois et al., 2016. Natural wetlands, other land sources and oceanic sources are considered as natural sources. Biomass and biofuel burning, fossil fuels and agriculture and waste are considered as anthropogenic sources.

Sediments are traditionally thought to be the major source of the oceanic CH_4. Sedimentary CH_4 is produced microbiologically under anoxic conditions (Barnes and Goldberg, 1976). There are also various abiotic oceanic CH_4 sources, such as hydrothermal systems, the serpentinization reaction, decomposition of CH_4 clathrate hydrates, diagenesis of organic carbon, etc. (Reeburgh, 2007). The benthic-originated CH_4 can reach the atmosphere via ebullition, which is fast but only significant in regions where sufficient sedimentary methanogenesis is combined with shallow water depths (see e.g. Lohrberg et al., 2020). Another pathway is diffusion, but this pathway is constrained by effective aerobic and anaerobic CH_4 oxidation in the water column and sediments (Whiticar and Faber, 1986). Even in coastal waters where hot spots for CH_4 emissions are found, see for example the southwestern Baltic Sea, more CH_4 is oxidized

than it is evading to the atmosphere (Steinle et al., 2017). The ocean could be considered as a giant reactor which rapidly consumes CH_4 from various benthic sources (Reeburgh, 2007).

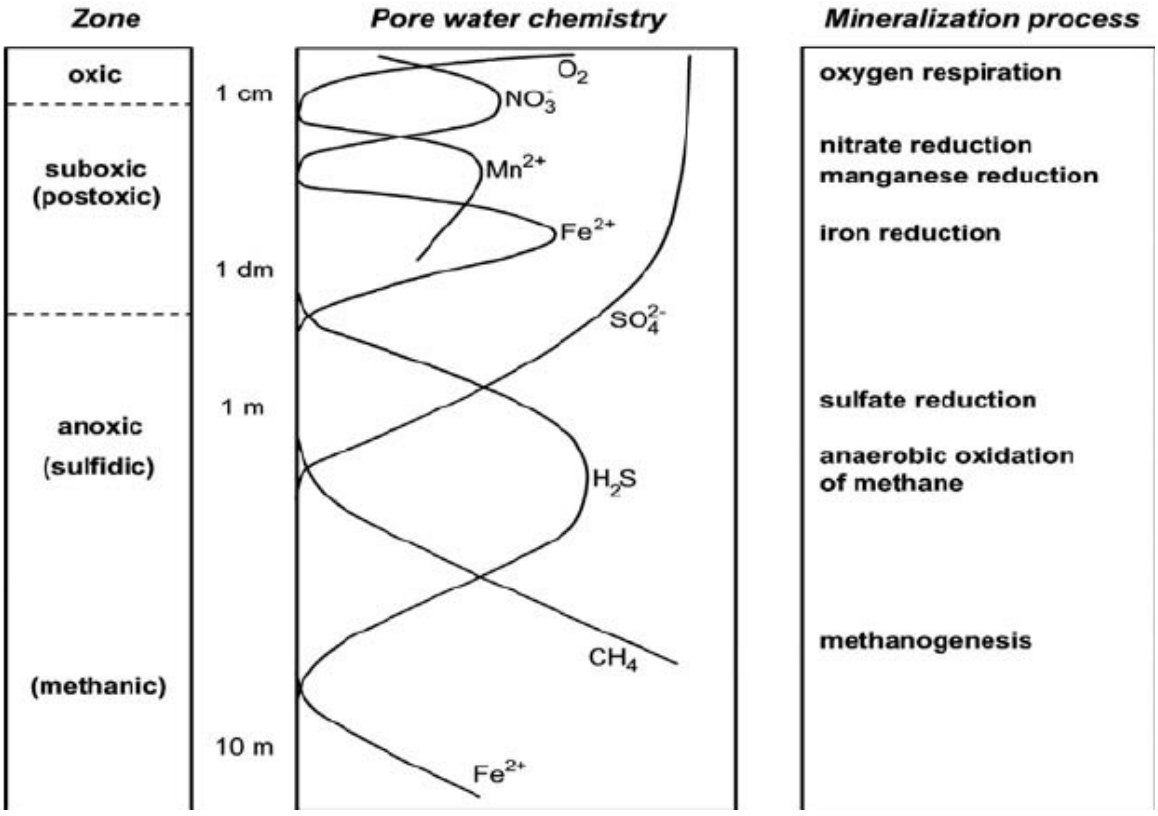

Fig. 2 Simplified sequence of microbial redox processes in stratified sediments (from Jørgensen and Kasten, 2006).

2.2 Ocean CH_4 paradox

Methanogenesis occurs only under strict anoxic conditions when sulfate is reduced (Fig. 2). Methanogens can utilize substrates such as H_2 and CO_2, formate, methanol, methylamines, and acetate to produce CH_4 anaerobically (Blaut, 1994; Ferry, 2010). However, the surface ocean, with the presence of high oxygen (O_2) and sulfate (SO_4^{2-}) concentrations, is generally close to equilibrium or slightly supersaturated with respect to the atmospheric CH_4. This counter-intuitive phenomenon is termed the "ocean CH_4 paradox", which plays an essential role in air-sea CH_4 exchange. The excess CH_4 is usually associated with anaerobic micro environments, such as found in sinking particles, digestive tracts of zooplankton and fishes, in which methanogenesis can take place (Karl and Tilbrook, 1994; de Angelis and Lee, 1994; Schmale et al., 2018; Stawiarski et al.,

2019). It has been suggested that some methanogens are tolerant to O_2 and thus might remain active under oxic conditions (Angel et al., 2011), and there has been accumulating evidence that CH_4 can be produced aerobically by archaea, algae, plants, animals and even human (Table 1; Keppler et al., 2006, 2016; Ghyczy et al., 2008; Lenhart et al, 2012, 2015; Tuboly et al., 2013). A recent study by Bizic et al. (2020) confirmed that cyanobacteria can produce CH_4 at substantial rates under oxic conditions with or without light. Several marine algae (*Emiliania huxleyi, Phaeocystis globosa* and *Chrysochromulina* sp.) have been also proved capable of CH_4 production (Lenhart et al, 2016; Klintzsch et al., 2019; Hartmann et al., 2020). Methylphosphonate (MPn) decomposition has been suggested as a potential source of dissolved CH_4 in oxygenated water, especially under phosphorus starvation condition (Karl et al., 2008). Furthermore, a C–P lyase pathway was proposed to catalyse CH_4 production from marine dissolved organic matter (Kamat et al., 2013; Repeta et al., 2016). Another alternative substrate for aerobic methanogenesis is dimethylsulfoniopropionate (DMSP) and its degradation products dimethyl sulfide (DMS) or dimethyl sulfoxide (DMSO), and several CH_4 formation pathways have been proposed (Damm et al., 2008, 2010; Florez-Leiva et al., 2013; Zindler et al., 2013). Besides, abiotic methanogenesis can readily produce CH_4 under oxidative conditions (Althoff et al., 2014; Li et al., 2020). Damm et al. (2015) reported CH_4 release from sea ice into the ocean via brine drainage in winter and spring, and thus suggested that sea ice is a potential source of CH_4 in Arctic surface water. The above-mentioned CH_4 sources might help to elucidate CH_4 supersaturation in oxic waters. However, some CH_4 pathways are still controversial, and it remains uncertain whether these sources are sufficient to maintain the CH_4 oversaturation in surface ocean. Further investigations are required to quantify their contributions comprehensively. The "ocean CH_4 paradox" still remains enigmatic.

Table 1. A complication of potential CH_4 pathways in the oxygenated surface ocean

Potential CH_4 source	Findings	Reference
Anaerobic micro environment	CH_4 release from sinking particles	Karl and Tilbrook, 1994
	Methanogenesis within zooplanktondigestive tracts	de Angelis and Lee, 1994
	In situ biogenic origin from CO_2 reduction	Schmale et al., 2018
	Zooplankton grazing and potential substrates of organic sulfur compounds	Stawiarski et al., 2019

Marine algae	*Emiliania huxleyi* produce CH_4 with bicarbonate and the sulphur-bound methyl group of methionine as carbon precursors	Lenhart et al, 2016
	Three marine phytoplankton (*Emiliania huxleyi, Phaeocystis globosa* and *Chrysochromulina* sp.) are involved in CH_4 production under oxic conditions	Klintzsch et al., 2019
	Photoautotroph community is an important driver for CH_4 production in oxic surface waters	Hartmann et al., 2020
Decomposition of organic sulfur compounds	Proposed CH_4 production as a by-product of methylphosphonate (MPn) decomposition in phosphate-stressed waters	Karl et al., 2008
	Potential coupling of methanogenesis with DMSP degradation processes in aerobic stratified seawater	Damm et al., 2008
	Methylated compounds (such as DMSP and its degradation products) serve as the bacterial C source in low N:P waters and forms CH_4 as a metabolic by-product	Damm et al., 2010
	CH_4 formation via demethylation of DMS due to an increase in the dissolved methyl group	Florez-Leiva et al., 2013;
	Algae derived DMSP and DMSO might serve as important substrates for methanogens	Zindler et al., 2013
	CH_4 formation via cleavage of the C–P bond catalyzed by a novel enzyme	Kamat et al., 2013
	Aerobic bacterial degradation of phosphonate esters in dissolved organic matter releases CH_4	Repeta et al., 2016
	MPn degradation through the C-P lyase pathway is an important source and a common production pathway of CH_4	Sosa et al., 2020
	Aerobic CH_4 formation from MPn degradation driven by MPn-utilizing microorganisms	Ye et al., 2020
Abiotic methanogenesis	Oxidation of methyl sulphides and demethylation of sulphoxides	Althoff et al., 2014
	Abiotic methane photoproduction from chromophoric dissolved organic matter (CDOM)	Li et al., 2020
Sea ice	CH_4 release via brine drainage triggered by sea ice freezing and melting	Damm et al., 2015

3 Nitrous oxide (N_2O)

3.1 N_2O pathways in the ocean

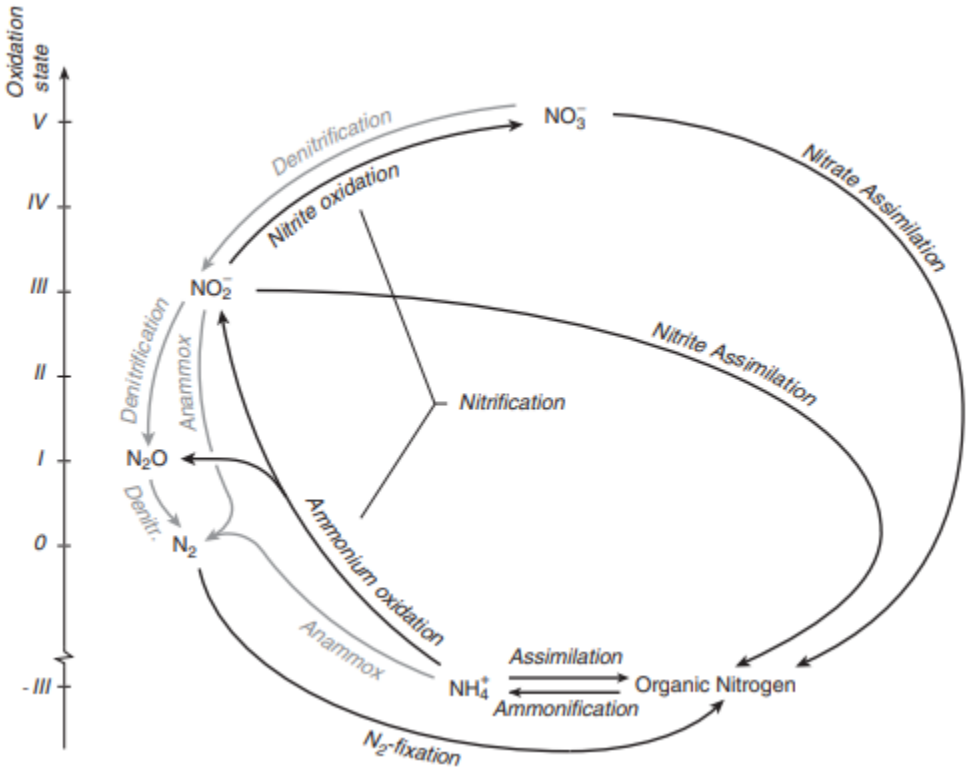

Fig. 3. Major chemical forms and transformations of nitrogen in the marine environment (from Gruber 2008). Processes shown in black lines take place under oxic conditions and processes shown in grey lines take place under suboxic/anoxic conditions.

There are several microbial processes that mediate marine N_2O production and consumption, of which the most important are nitrification and denitrification (Fig. 3). Nitrification is a series of reactions that transform ammonia (NH_3) to nitrite (NO_2^-) and then NO_2^- to nitrate (NO_3^-). During NH_3 oxidation, N_2O is produced as a side product. Denitrification is the sequential reduction of NO_3^- to dinitrogen, during which N_2O is produced as an intermediate. These two processes are primarily constrained by O_2 concentration and microbiological activity.

Generally, both nitrification and denitrification are favourable under suboxic conditions, but nitrification has a higher tolerance of O_2 compared to denitrification (Fig. 4). When O_2 is almost 0, N_2O is consumed via denitrification. Please note that nitrification and denitrification can occur at the same low O_2 concentrations and there are no clear O_2

thresholds for both processes. In the subsurface ocean where the waters are oxygenated, nitrification is presumably the dominating N_2O source (Nevison et al., 2003; Ma et al., 2020), however, in continental shelf sediments and oxygen minimum zone (OMZ), denitrification usually plays a more important role (Naqvi et al., 2000; Farías et al., 2009; Ji et al., 2015). The situation in coastal waters might be more complicated because of the regular shifting between oxic and anoxic conditions as a result of eutrophication and seasonal stratification (see for example, Boknis Eck).

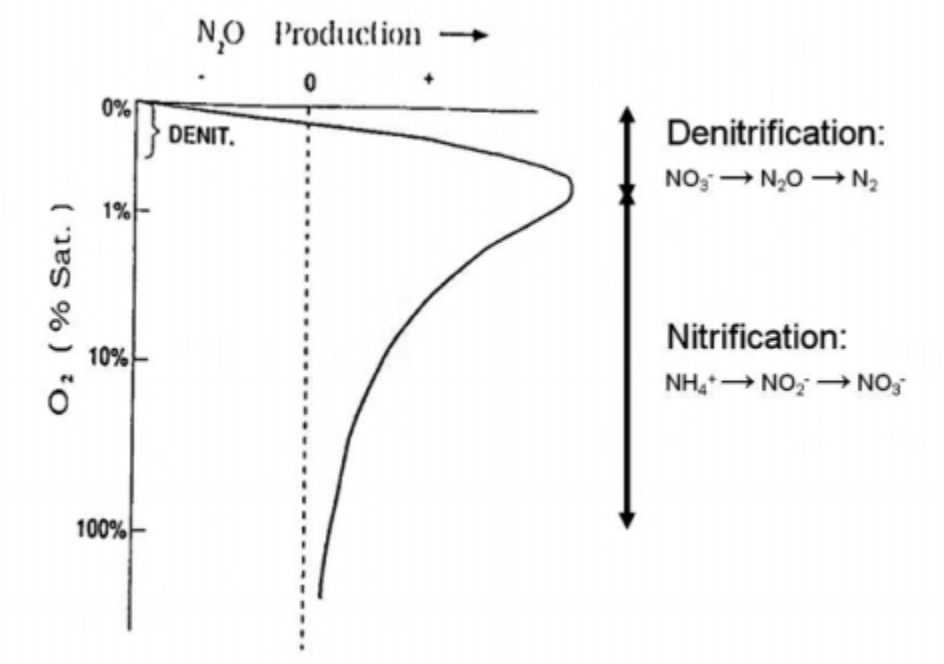

Fig. 4. N_2O production versus O_2 saturation in the ocean (from Bange et al., 2010).

Traditionally NH_3 oxidation was thought to be exclusively performed by ammonia-oxidizing bacteria (AOB) (Frame and Casciotti, 2010; Goreau et al., 1980), but recent studies indicate that ammonia-oxidizing archaea (AOA) play a dominant role in marine environment and direct evidence for N_2O production via AOA has been provided (Santoro et al., 2011; Löscher et al., 2012; Berg et al., 2015). AOA and AOB belong to different domains of life and there are evidences for niche differentiation between AOA and AOB with respect to environmental factors. For example, AOA (*Candidatus Nitrosopumilus maritimus*) has a higher NH_3 affinity than AOB (Martens-Habbena et al., 2009), which provides a convincing explanation for the dominance of AOA in marine environments, where NH_3 is present at nanomolar concentrations. Kitzinger et al. (2020) also reported the contrasting life strategies of NOB (Nitrospinae) and AOA. They found that Nitrospinae mainly assimilate organic-N compounds urea and cyanate, while AOA mainly assimilate ammonia. The N_2O yield, i.e. the ratio of N_2O to NO_x^- (= NO_2^-+NO_3^-)

produced or NH_3 consumed via nitrification, can be used to indicate likely N_2O sources. N_2O yield from AOB cultures ranges from 0.1 % to 8 %, depending on the available NH_4^+ and O_2 concentrations; however, N_2O yields of AOA cultures are generally lower (0.04–0.3%), and NH_4^+ and O_2 concentrations have little or no effect (Prosser et al., 2020). This is consistent with the assumption that N_2O produced by AOA derives only from abiotic reactions of intermediate compounds (Kozlowski et al., 2016), but this conclusion is challenged by the enzymatic N_2O production reported in *Nitrosocosmicus oleophilus* (Jung et al., 2019). There are breakthroughs for our knowledge on N_2O production during NH_3 oxidation, but some key questions in N_2O pathways mediated by AOA/AOB remain ambiguous.

Besides bacterial and archaea, microalgae are also capable of N_2O production (Guieysse et al., 2013; Plouviez et al., 2017). Guieysse et al. (2013) demonstrated N_2O formation in axenic *Chlorella vulgaris* cultures and a nitrite reduction pathway has been proposed. They found enhanced N_2O production in dark with NO_2^- addition, and suggest that N_2O might be formed via the precursor of nitric oxide (NO) or nitroxyl (HNO). Plouviez et al. (2019) compiled various studies acknowledging algal N_2O synthesis and identified several potential microalgal N_2O pathways. Due to the ubiquitous presence of microalgae in natural ecosystems, N_2O emission from microalgae could be a potentially important but so far unaccounted N_2O source worldwide (Plouviez et al., 2019).

Complete denitrification (= dentrification including the last step of N_2O reduction to N_2) is traditionally considered as the only known N_2O consumption pathway in the ocean. Recently, Farías et al. (2013) found that N_2O can be directly transformed into particular organic nitrogen (PON) via biological assimilation. This process can take place under extreme biogeochemical conditions and even at very low N_2O concentrations. Biological N_2O fixation could provide a globally significant sink for atmospheric and oceanic N_2O and also a potential source of oceanic fixed nitrogen (Farías et al., 2013).

3.2 The role of hydroxylamine in N_2O pathways

Hydroxylamine (NH_2OH) is a short-lived compound in the nitrogen cycle, with a life time of only a few hours in seawater (Fiadeiro et al., 1967; Butler and Gordon, 1986). The primary analysis of NH_2OH in natural waters relied on chemical conversion (Fiadeiro et al., 1967) or spectrophotometric methods (Johnson, 1968). Several oxidants were proposed to convert NH_2OH to N_2O and their measurements are usually combined. In fresh water, the oxidant of hypochlorite is used for the determination of NH_2OH (Seike et al., 2004), but it is not applicable for brackish water because of the interference of halogen compounds. Kato et al. (2017) adjusted the measurement by the addition of

phenol, which can scavenge bromide in seawater. The improved method can quantify NH_2OH in natural seawater with a wide range of salinity with a detection limit of 0.2 μg N L^{-1}. Another gentle oxidant used to convert NH_2OH to N_2O is Fe (III) (Von Breymann et al., 1982; Butler and Gordon, 1986), which is suitable for both fresh and brackish water conditions. Kock and Bange (2013) optimized the NH_2OH conversion with this oxidant by adding sulfanilamide to suppress the undesired side reactions induced by NO_2^-, and the detection limit dropped to approximately 0.6 nmol L^{-1} (Ma et al., 2020).

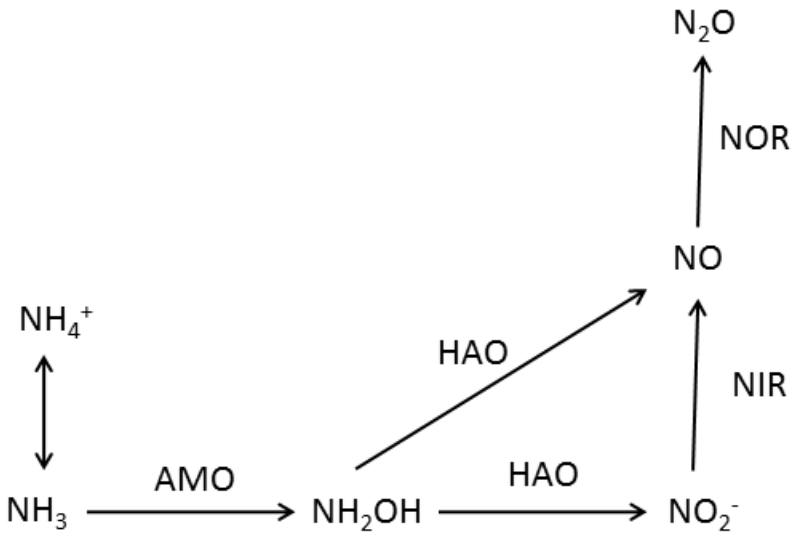

Fig. 5. Specific pathways for N_2O production in bacteria. AMO, ammonia monooxygenase; HAO, hydroxylamine oxidoreductase; NIR, nitrite reductase; NOR, nitric oxide reductase (modified from Stein 2011).

NH_2OH plays an important role in AOB-mediated nitrogen cycle. AOBs are capable of not only nitrification but also denitrification, termed nitrifier-denitrification (Wrage 2001). The prevailing view of the first step of nitrification is that AOB use two enzymes, ammonia monooxygenase (AMO) and hydroxylamine oxidoreductase (HAO) to oxidize NH_3 to NO_2^- via NH_2OH (Fig. 5). Caranto and Lancaster (2017) suggest that nitric oxide (NO) is an additional obligate intermediate in the aerobic NH_2OH oxidation pathway, which necessitate the involvement of the third enzyme in NH_3 oxidation. During the dissimilatory NO_2^- reduction pathway, NO_2^- derived from nitrification is reduced by nitrite reductase (NIR). Both enzymatic pathways share NO as an intermediate, which is then reduced to N_2O by NO reductase (NOR; Stein 2011). HNO is proposed as the alternative intermediate of enzymatic NH_2OH oxidation (Anderson, 1964; Ritchie and Nicholas, 1972) which could dimerize and dehydrate to form N_2O and H_2O (Bonner and Hughes, 1988; Shafirovich and Lymar, 2002). Caranto et al. (2016) reported that the

enzyme *cytochrome P460* can convert NH_2OH to N_2O quantitatively under aerobic conditions, thereby establishing a direct enzymatic link between nitrification and N_2O formation via NH_2OH, which implies that N_2O production by AOBs are independent from nitrifier-denitrification (White and Lehnert, 2016). Terada et al. (2017) investigated the AOB activities in a partial nitrifying bioreactor and proposed a hybrid N_2O production pathway (NH_2OH interact with NO_2^-), which could be another potential N_2O source via NH_2OH. Korth et al. (2019) reported positive correlations between NH_2OH and N_2O/ NO_3^- in the open ocean, and suggested that NH_2OH is a potential indicator for nitrification in oxic oceanic environments.

Although AOA is capable of NH_3 oxidation to NO_2^-, little is known about the NH_3 oxidation pathways. AOA contain genome sequences for homologs of the bacterial AMO, but the lack of genes encoding the AOB-like HAO complex suggests either a novel enzyme for the oxidation of NH_2OH or a completely new pathway without NH_2OH. Vajrala et al. (2013) detected NH_2OH production and consumption during NH_3 oxidation by AOA (*Nitrosopumilus maritimus*), and proposed that this process seems mechanistically similar to the one mediated by AOB with NH_2OH as an intermediate. The isotopic signature indicated that the N_2O produced by AOA is not derived from the reduction of NO_2^-, and thus AOA is probably conducting NH_3 oxidation with a novel enzyme complex (Vajrala et al., 2013). Kozlowski et al. (2016) proposed a NH_2OH oxidation pathway in AOA catalyzed by a putative copper-based enzyme, with NO involved in hybrid N_2O production. In the presence of O_2, NO and NH_2OH can be rapidly converted to N_2O abiotically (Stieglmeier et al., 2014; Kozlowski et al., 2016). This process has implicitly been assumed intracellular, but Liu et al. (2017) reported abiotic conversion of extracellular NH_2OH to N_2O during NH_3 oxidation. The studies mentioned above were performed in well-mixed systems in which the environmental conditions are constant. In natural environments, however, the conditions will be transient, which could potentially lead to metabolic imbalance that may result in the accumulation of intermediates (Prosser et al., 2020). Biological N_2O production is highly dynamic in response to N-imbalance imposed on a system, and it is difficult to assess N_2O production through specific reactions linked to NH_2OH oxidation. These studies provide plausible evidence that NH_2OH may be an intermediate in archaeal nitrification, but the microbial/abiotic pathways and the role of NH_2OH in these processes are not fully understood.

NH_2OH is also reported to be involved in dissimilatory nitrate reduction to ammonium (DNRA), an anaerobic process which transforms NO_3^- to NO_2^- and then to NH_4^+. Einsle et al. (2002) proposed that NH_2OH is formed as an intermediate during nitrite reduction. However, other studies point out that nitrite reduction to ammonium is mediated by a

pentaheme cytochrome C nitrite reductase (*nrfA*) without producing any intermediate nitrogen compound (Einsle et al., 1999). There are other nitrite reduction pathways during which *nrfA* can use NH_2OH as alternative substrate (Simon et al., 2011). There have been numerous reports suggesting that organisms carrying out DNRA can produce N_2O in both field and culture conditions (Giblin et al., 2013), but there is only few information on the mechanisms and controls for NH_2OH and N_2O production.

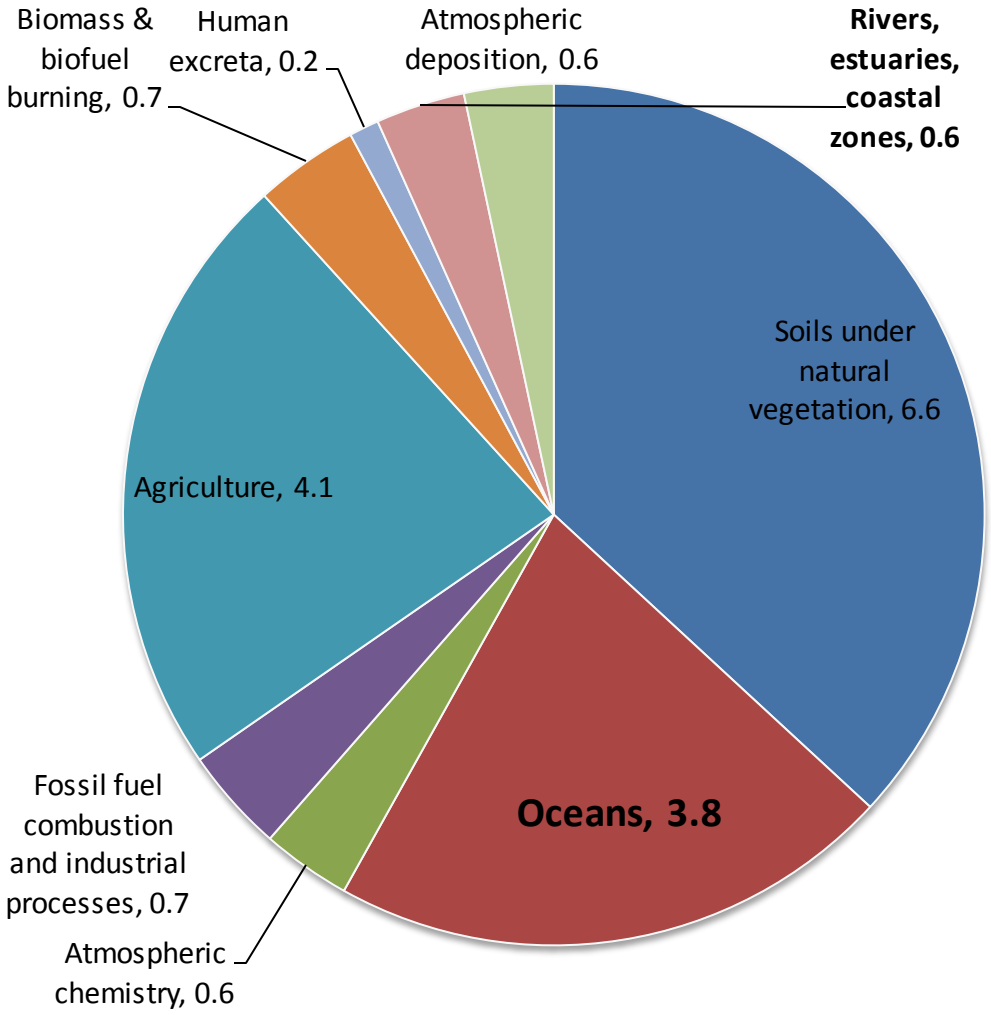

Fig. 6 Global N_2O emissions by source type in Tg N yr^{-1} from IPCC, 2013. Natural sources are soils under natural vegetation, oceans and atmospheric chemistry. Anthropogenic sources are fossil fuel combustion and industrial processes, agriculture, biomass & biofuel burning, human excreta, rivers, estuaries, coastal zones and atmospheric deposition. Please note that oceans and rivers, estuaries, coastal zones are separated.

To sum up, current studies indicate that chemical reactions involving NH_2OH may play an important role in N_2O production, especially during NH_3 oxidation. Due to the short lifetime of NH_2OH in natural seawater, the presence of NH_2OH is strongly indicative of in situ production. Effective measurement of NH_2OH is of great importance to understand the mechanisms of N_2O formation.

3.3 N_2O emissions from the ocean

The global annual emissions of N_2O was estimated to range from 16.1 to 18.7 Tg N yr^{-1} with about one third emitted from the ocean (Fig. 6, Saikawa et al., 2014; Thompson et al., 2014). Yang et al. (2020) estimated a mean annual oceanic N_2O flux of 4.2 ± 1.0 Tg $N{\cdot}yr^{-1}$, which largely reduces the uncertainty reported by IPCC (2013). Due to the strong influence of human activities, coastal waters, continental shelves and estuaries are considered as hot spots of N_2O emissions (see e.g. Naqvi, et al., 2000; Bange 2006; Arevalo-Martínez et al., 2015; Farías et al., 2015; Ma et al., 2016).

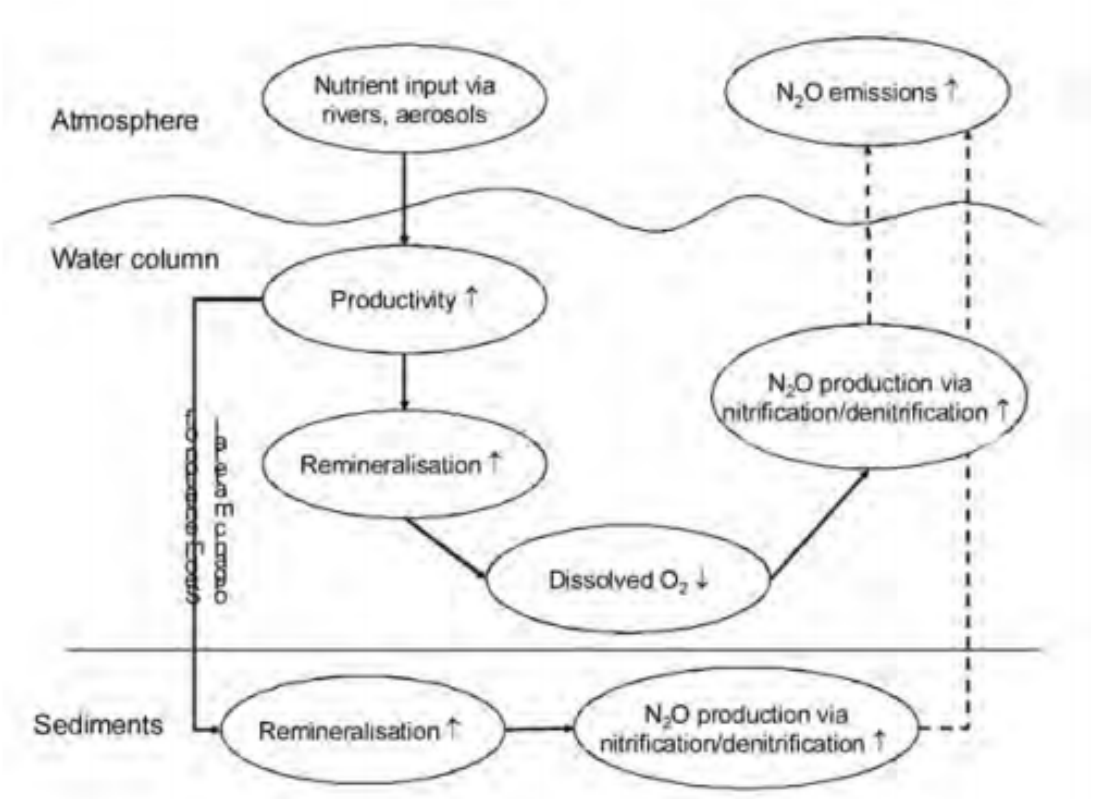

Fig. 7 Simplified scheme of the impact of nutrients input on N_2O emission in coastal areas (from Bange et al., 2010). Up and down arrows within the ovals stand for increase or decrease, respectively.

Strong anthropogenic nitrogen inputs can stimulate N_2O production and emissions from coastal areas (Fig. 7). On the one hand, eutrophication promotes primary productivity and leads to O_2 depletion in the water column, which is conducive to form N_2O (see section 3.1); on the other hand, excessive nutrients provide sufficient substrates for nitrification/denitrification and thus enhance N_2O production/emission directly. Besides, global warming results in higher surface water temperature, and the prolonged and reinforced stratification prevents O_2 supply from vertical mixing, leading to expanding hypoxia in the water column (e.g. see Carstensen et al., 2014; Lennartz et al., 2014). Since N_2O production is closely linked to the dissolved O_2 concentrations in seawater, it is well-accepted that the oceanic N_2O emissions, especially in coastal waters, will increase in future (Naqvi et al., 2000; Bange, 2006).

Besides, ocean acidification also exerts an influence on N_2O production. Studies from multiple marine environments indicate that microbial nitrification, mediated either by AOA or AOB, was inhibited when pH was reduced (Huesemann et al., 2002; Beman et al., 2011; Rees et al., 2016). This could be explained by the pH-driven shift in the NH_3:NH_4^+ equilibrium. During the first step of nitrification, NH_3 oxidation organisms prefer NH_3 as substrate, which becomes substantially less abundant relative to NH_4^+ in a more acidified ocean (pK of NH_3/NH_4^+ is ~9.2, Gehlen et al., 2011). As a result, nitrification rates could drop by 3–44% within the next few decades and thus affecting oceanic N_2O production and emissions (Beman et al., 2011). Considering the dominant role of nitrification in oxygenated open ocean, Rees et al. (2016) estimated a maximum reduction of 0.82 Tg N y^{-1} for the oceanic N_2O production by the end of the 21st century. However, this conclusion was achieved without the direct measurement of N_2O production. In contrast, although nitrification rates decreased when pH was reduced, Breider et al. (2019) found that N_2O production rates increased significantly in seawater. During nitrification N_2O is produced as a side product. It was suggested by Breider et al. (2019) that N_2O production rates via nitrification and nitrification rates are probably uncoupled, and the inhibition of nitrification, therefore, does not necessarily lead to a decrease in N_2O production. Breider et al. (2019) estimated that ocean acidification could increase marine N_2O production via nitrification by 185–491% by the end of the century. As for denitrification, Wan et al. (2016) reported that increasing CO_2 concentrations could decrease nitrogen removal efficiency via denitrification, but increase N_2O production. The negative influence of CO_2 on denitrifying microbes was attributed to the inhibition of intracellular electron transport and consumption. Similarly, Jung et al. (2019) found increased N_2O emissions from acidification via enzymatic denitrification, although different mechanisms were proposed for AOA and AOB. However, these incubation experiments were conducted in artificially controlled

environments and whether the results are reproducible in natural seawater remains unclear. Frame et al. (2017) reported enhanced N_2O yields of NH_3 oxidizers by acidification in a lake and a marine environment, and proposed a hybrid N_2O formation pathway (i.e. the combination of NH_4^+ and NO_2^- derived N). Ocean acidification can influence N_2O production in different ways, including changing the NH_3 oxidizer community composition (Bowen et al., 2013), altering the activity of the N_2O-producing enzymes or the genes encoding the enzymes, and by shifting of the chemical equilibrium (NH_3/NH_4^+) related to N_2O production. The response of the oceans to rising atmospheric CO_2 concentrations will not be homogenous. Generally oceanic N_2O production and emissions are likely to increase in the future as a result of ocean acidification.

4 Motivation and thesis outline

Ocean deoxygenation plays a significant role for the biogeochemical cycles of carbon and nitrogen. The spatial distribution and temporal variability of trace gases (CH_4 and N_2O) are not homogenous, and strongly depends on the region, depth and microbial activity that affect the production/consumption in different O_2 regimes. Therefore, the future response of CH_4 and N_2O emissions on ocean deoxygenation remain ambiguous, especially in coastal waters where severe eutrophication and expanding hypoxia occur. Long-term observation is an effective tool to explore the variability in trace gas concentrations and emissions under significant environmental changes.

The Baltic Sea is not only a hot spot of greenhouse gas emissions, but is expected to experience significant environmental changes in view of ongoing eutrophication, ocean acidification, warming and stratification. In order to monitor the variability of the dissolved CH_4/N_2O concentrations, as well as to predict the future trends of their emissions, especially under warming and deoxygenation, long-term observations were conducted at the Boknis Eck time-series station in the southwestern Baltic Sea. Chapters 2 and 3 are focusing on CH_4 and N_2O, respectively. The following questions were addressed:

- What are the potential environmental controls of the seasonal variations in dissolved CH_4/N_2O concentrations?
- Are there any special events affecting the CH_4/N_2O variability and what are the potential causes?
- Are there significant CH_4/N_2O trends during the long-term observations?
- How strong is the southwestern Baltic Sea as a CH_4/N_2O source?

Chapter 2: 'A decade of methane measurements at the Boknis Eck Time-series Station in the Eckernförde Bay (southwestern Baltic Sea)': ms published in *Biogeosciences, 17, 3427–3438, 2020*.

Xiao Ma, Mingshuang Sun, Sinikka T. Lennartz, and Hermann W. Bange

Author Contribution: XM, MS, STL and HWB designed the study and participated in the fieldwork. CH_4 measurements and data processing were performed by XM, MS and STL. XM wrote the article with contributions from MS, STL and HWB.

Chapter 3: 'A multi-year observation of nitrous oxide at the Boknis Eck Time-series Station in the Eckernförde Bay (southwestern Baltic Sea)': ms published in *Biogeosciences, 16, 4097–4111, 2019*.

Xiao Ma, Sinikka T. Lennartz, and Hermann W. Bange

Author Contribution: XM, STL, and HWB designed the study and participated in the fieldwork. N_2O measurements and data processing were done by XM and STL. XM wrote the article with contributions from STL and HWB.

The Indian Ocean is of great importance in the global N_2O budget. However, this area is largely undersampled. An analysis of the N_2O distribution and ΔN_2O/AOU and $\Delta N_2O/NO_3^-$ relationships in the Southwest Indian Ocean is presented in Chapter 4 'Nitrous oxide and hydroxylamine measurements in the southwest Indian Ocean'. The surface ocean distribution of N_2O was investigated with a continuous underway system and complemented with depth profiles from several locations. The potential correlation between N_2O and NH_2OH were also discussed. This chapter has been published in *Journal of Marine Systems, 209, 103062, 2020*.

Xiao Ma, Hermann W. Bange, Gesa K. Eirund, Damian L. Arévalo-Martínez

Author Contribution: XM, DLA and HWB designed the study. XM and GKE took the N_2O/NH_2OH samples and measured the depth profiles. XM calculated the N_2O concentrations and analyzed the water masses. DLA analyzed the underwater measurements and calculated the sea-to-air fluxes of N_2O. XM and DLA wrote the paper with contributions from GKE and HWB.

References

AGAGE, the Advanced Global Atmospheric Gases Experiment, https://agage.mit.edu/

Althoff, F., Benzing, K., Comba, P., McRoberts, C., Boyd, D. R., Greiner, S., and Keppler, F.: Abiotic methanogenesis from organosulphur compounds under ambient conditions. Nature Communications, 5(1), 1–9, 2014.

Anderson, J. H.: The copper-catalysed oxidation of hydroxylamine. Analyst, 89(1058), 357–362, 1964.

Angel, R., Matthies, D., and Conrad, R.: Activation of Methanogenesis in Arid Biological Soil Crusts Despite the Presence of Oxygen, Plos One, 6, e20453, https://doi.org/10.1371/journal.pone.0020453, 2011.

Arevalo-Martínez, D. L., Kock, A., Löscher, C. R., Schmitz, R. A., and Bange, H. W.: Massive nitrous oxide emissions from the tropical South Pacific Ocean. Nature Geoscience, 8(7), 530–533, 2015.

Bange, H. W., Bartell, U. H., Rapsomanikis, S. and Andreae, M. O.: Methane in the Baltic and North seas and a reassessment of the marine emissions of methane. Global Biogeochem. Cycles 8, 465–480, 1994.

Bange, H. W.: Nitrous oxide and methane in European coastal waters. Estuarine, Coastal and Shelf Science, 70(3), 361–374, 2006.

Bange, H. W., Freing, A., Kock, A., and Löscher, C. R.: Marine pathways to nitrous oxide. In Nitrous oxide and climate change (pp. 40–66). Routledge, 2010.

Barnes, R. O. and Goldberg, E. D.: Methane production and consumption in anoxic marine sediments. Geology 4, 297–300, 1976.

Beman, J. M., Chow, C. E., King, A. L., Feng, Y., Fuhrman, J. A., Andersson, A., Bates, N. R., Popp, B. N., and Hutchins, D. A.: Global declines in oceanic nitrification rates as a consequence of ocean acidification. Proceedings of the National Academy of Sciences, 108(1), 208–213, 2011.

Berg, C., Vandieken, V., Thamdrup, B., and Jürgens, K.: Significance of archaeal nitrification in hypoxic waters of the Baltic Sea. The ISME journal, 9(6), 1319–1332, 2015.

Bizic, M., Klintzsch, T., Ionescu, D., Hindiyeh, M. Y., Gunthel, M., Muro-Pastor, A. M., Eckert, W., Urich, T., Keppler, F., and Grossart, H. P.: Aquatic and terrestrial cyanobacteria produce methane, Science Advances, 6, 2020.

Blaut, M.: Metabolism of methanogens. Antonie Van Leeuwenhoek, 66(1–3), 187–208, 1994.

Bonner, F. T., and Hughes, M. N.: The aqueous solution chemistry of nitrogen in low positive oxidation states. Comments on Inorganic Chemistry, 7(4), 215–234, 1988.

Borges, A. V., Champenois, W., Gypens, N., Delille, B., and Harlay, J.: Massive marine methane emissions from near-shore shallow coastal areas. Scientific reports, 6, 27908, 2016.

Bowen, J. L., Kearns, P. J., Holcomb, M., and Ward, B. B.: Acidification alters the composition of ammonia-oxidizing microbial assemblages in marine mesocosms. Marine Ecology Progress Series, 492, 1–8, 2013.

Breider, F., Yoshikawa, C., Makabe, A., Toyoda, S., Wakita, M., Matsui, Y., Kawagucci, S., Fujiki, T., Harada, N., and Yoshida, N.: Response of N_2O production rate to ocean acidification in the western North Pacific. Nature Climate Change, 9(12), 954–958, 2019.

Butler, J. H., and Gordon, L. I.: An improved gas chromatographic method for the measurement of hydroxylamine in marine and fresh waters. Marine Chemistry, 19(3), 229–243, 1986.

Butler, A. H., Daniel, J. S., Portmann, R. W., Ravishankara, A. R., Young, P. J., Fahey, D. W., and Rosenlof, K. H.: Diverse policy implications for future ozone and surface UV in a changing climate, Environ. Res. Lett., 11, doi:10.1088/1748-9326/11/6/064017, 2016.

Caranto, J. D., Vilbert, A. C., and Lancaster, K. M.: Nitrosomonas europaea cytochrome P460 is a direct link between nitrification and nitrous oxide emission. Proceedings of the National Academy of Sciences, 113(51), 14704–14709, 2016.

Caranto, J. D., and Lancaster, K. M.: Nitric oxide is an obligate bacterial nitrification intermediate produced by hydroxylamine oxidoreductase. Proceedings of the National Academy of Sciences, 114(31), 8217–8222, 2017.

Carstensen, J., Andersen, J. H., Gustafsson, B. G., and Conley, D. J.: Deoxygenation of the Baltic Sea during the last century. Proceedings of the National Academy of Sciences, 111(15), 5628–5633, 2014.

Cazenave, A., Dieng, H. B., Meyssignac, B., Von Schuckmann, K., Decharme, B., and Berthier, E.: The rate of sea-level rise. Nature Climate Change, 4(5), 358–361, 2014.

Crutzen, P. J.: The influence of nitrogen oxides on the atmospheric ozone content. Quarterly Journal of the Royal Meteorological Society, 96(408), 320–325, 1970.

Dalsoren, S. B., Myhre, C. L., Myhre, G., Gomez-Pelaez, A. J., Sovde, O. A., Isaksen, I. S. A., Weiss, R. F., and Harth, C. M.: Atmospheric methane evolution the last 40 years, Atmos. Chem. Phys., 16(5), 3099–3126, doi:10.5194/acp-16-3099-2016, 2016.

Damm, E., Kiene, R., Schwarz, J., Falck, E., and Dieckmann, G.: Methane cycling in Arctic shelf water and its relationship with phytoplankton biomass and DMSP, Mar. Chem., 109, 45–59, 2008.

Damm, E., Helmke, E., Thoms, S., Schauer, U., Nöthig, E., Bakker, K., and Kiene, R. P.: Methane production in aerobic oligotrophic surface water in the central Arctic Ocean, Biogeosciences, 7, 1099–1108, doi:10.5194/bg-7-1099-2010, 2010.

Damm, E., Rudels, B., Schauer, U., Mau, S., and Dieckmann, G.: Methane excess in Arctic surface water-triggered by sea ice formation and melting, Scientific Reports, 5, 2015.

Davidson, E. A.: The contribution of manure and fertilizer nitrogen to atmospheric nitrous oxide since 1860. Nature Geoscience, 2(9), 659–662, 2009.

de Angelis, M. A., and Lee, C.: Methane production during zooplankton grazing on marine phytoplankton. Limnology and Oceanography, 39(6), 1298–1308, 1994.

Dyurgerov, M. B., and Meier, M. F.: Twentieth century climate change: evidence from small glaciers. Proceedings of the National Academy of Sciences, 97(4), 1406-1411, 2000.

Einsle, O., Messerschmidt, A., Stach, P., Bourenkov, G. P., Bartunik, H. D., Huber, R., and Kroneck, P.M.: Structure of cytochrome c nitrite reductase. Nature 400: 476–480, http:// dx.doi.org/10.1038/22802, 1999.

Einsle, O., Messerschmidt, A., Huber, R., Kroneck, P. M., and Neese, F.: Mechanism of the six-electron reduction of nitrite to ammonia by cytochrome c nitrite reductase. Journal of the American Chemical Society, 124(39), 11737–11745, 2002.

Farías, L., Castro-González, M., Cornejo, M., Charpentier, J., Faúndez, J., Boontanon, N., and Yoshida, N.: Denitrification and nitrous oxide cycling within the upper oxycline of the eastern tropical South Pacific oxygen minimum zone, Limnol. Oceanogr., 54, 132–144, 557 https://doi.org/10.4319/lo.2009.54.1.0132, 2009.

Farías, L., Faúndez, J., Fernandez, C., Cornejo, M., Sanhueza, S., and Carrasco, C.: Biological N_2O fixation in the Eastern South Pacific Ocean and marine cyanobacterial cultures. PLoS One, 8(5), 2013.

Farías, L., Besoain, V., and García-Loyola, S.: Presence of nitrous oxide hotspots in the coastal upwelling area off central Chile: an analysis of temporal variability based on ten years of a biogeochemical time series. Environmental Research Letters, 10(4), 044017, 2015.

Ferry, J. G.: How to make a living by exhaling methane. Annual review of microbiology, 64, 453–473, 2010.

Fiadeiro, M., Solorzano, L., and Strickland, J. D. H.: Hydroxylamine in seawater. Limnology and Oceanography, 12(3), 555–556, 1967.

Florez-Leiva, L., Damm, E., and Farías, L.: Methane production induced by dimethylsulfide in surface water of an upwelling ecosystem. Progress in oceanography, 112, 38–48, 2013.

Frame, C. H. and Casciotti, K. L.: Biogeochemical controls and isotopic signatures of nitrous oxide production by a marine ammonia-oxidizing bacterium, Biogeosciences, 7, 2695–2709, doi:10.5194/bg-7-2695-2010, 2010.

Frame, C. H., Lau, E., Nolan IV, E. J., Goepfert, T. J., and Lehmann, M. F.: Acidification enhances hybrid N_2O production associated with aquatic ammonia-oxidizing microorganisms. Frontiers in microbiology, 7, 2104, 2017.

Gehlen, M., Gruber, N., Gangstø, R., Bopp, L., and Oschlies, A.: Biogeochemical consequences of ocean acidification and feedbacks to the earth system. Ocean acidification, 1, 230–248, 2011.

Ghyczy, M., Torday, C., Kaszaki, J., Szabo, A., Czobel, M., and Boros, M.: Hypoxia-induced generation of methane in mitochondria and eukaryotic cells–An alternative approach to methanogenesis, Cell. Physiol. Biochem., 21, 251–258, 2008.

Giblin, A. E., Tobias, C. R., Song, B., Weston, N., Banta, G. T., and Rivera-Monroy, V. H.: The importance of dissimilatory nitrate reduction to ammonium (DNRA) in the nitrogen cycle of coastal ecosystems. Oceanography, 26(3), 124–131, 2013.

Goreau, T. J., Kaplan, W. A., Wofsy, S. C., McElroy, M. B., Valois, F. W., and Watson, S. W.: Production of NO_2^- and N_2O by Nitrifying Bacteria at Reduced Concentrations of Oxygen, Appl. Environ. Microb., 40, 526–532, 1980.

Gruber, N.: The marine nitrogen cycle: overview and challenges. Nitrogen in the marine environment, 2, 1–50, 2008.

Guieysse, B., Plouviez, M., Coilhac, M., and Cazali, L.: Nitrous Oxide (N_2O) production in axenic Chlorella vulgaris microalgae cultures: evidence, putative pathways, and potential environmental impacts. Biogeosciences, 10(10), 6737, 2013.

Haeberli, W.: Glacier and permafrost signals of 20th-century warming. Annals of Glaciology, 14, 99–101, 1990.

Haeberli, W., and Beniston, M.: Climate change and its impacts on glaciers and permafrost in the Alps. Ambio, 27(4), 258–265, 1998.

Hartmann, J. F., Gunthel, M., Klintzsch, T., Kirillin, G., Grossart, H. P., Keppler, F., and Isenbeck-Schroter, M.: High Spatiotemporal Dynamics of Methane Production and Emission in Oxic Surface Water, Environmental Science & Technology, 54, 1451–1463, 2020.

Huesemann, M. H., Skillman, A. D., and Crecelius, E. A.: The inhibition of marine nitrification by ocean disposal of carbon dioxide. Marine Pollution Bulletin, 44(2), 142–148, 2002.

IPCC: Climate Change 2013: The physical science basis. Contribution of Working Group I to the fifth assessment report of the Intergovernmental Panel on Climate Change, Cambridge University Press, Cambridge, UK and New York, NY, TS17 2013.

Ji, Q., Babbin, A. R., Jayakumar, A., Oleynik, S., and Ward, B. B.: Nitrous oxide production by nitrification and denitrification in the Eastern Tropical South Pacific oxygen minimum zone. Geophysical Research Letters, 42(24), 10–755, 2015.

Johnson, D. P.: Spectrophotometric determination of oximes and unsubstituted hydroxylamine. Analytical Chemistry, 40(3), 646–648, 1968.

Johnston, H.: Reduction of stratospheric ozone by nitrogen oxide catalysts from supersonic transport exhaust. Science, 173(3996), 517–522, 1971.

Jørgensen, B., and Kasten, S.: Sulfur Cycling and Methane Oxidation. 10.1007/3-540-32144-6_8, 2006.

Jung, M. Y., Gwak, J. H., Rohe, L., Giesemann, A., Kim, J. G., Well, R., Madsen, E. L., Herbold, C. W., Wagner, M., and Rhee, S. K.: Indications for enzymatic denitrification to

N_2O at low pH in an ammonia-oxidizing archaeon. The ISME journal, 13(10), 2633–2638, 2019.

Kamat, S. S., Williams, H. J., Dangott, L. J., Chakrabarti, M., and Raushel, F. M.: The catalytic mechanism for aerobic formation of methane by bacteria, Nature, 497, 132–136, doi:10.1038/nature12061, 2013.

Kampschreur, M. J., Temmink, H., Kleerebezem, R., Jetten, M. S., and van Loosdrecht, M. C.: Nitrous oxide emission during wastewater treatment. Water research, 43(17), 4093–4103, 2009.

Karl, T. R., Kukla, G., Razuvayev, V. N., Changery, M. J., Quayle, R. G., Heim Jr, R. R., Easterling, D. R., and Fu, C. B.: Global warming: Evidence for asymmetric diurnal temperature change. Geophysical Research Letters, 18(12), 2253–2256, 1991.

Karl, D. M. and Tilbrook, B. D.: Production and transport of methane in oceanic particulate organic matter, Nature, 368, 732–734, 1994.

Karl, D. M., Beversdorf, L., Björkman, K. M., Church, M. J., Martinez, A., and Delong, E. F.: Aerobic production of methane in the sea. Nature Geoscience, 1(7), 473, 2008.

Kato, T., Sugahara, S., Murakami, M., Senga, Y., Egawa, M., Kamiya, H., Omata, K., and Seike, Y.: Sensitive Method for the Oxidation-determination of Trace Hydroxylamine in Environmental Water Using Hypochlorite Followed by Gas Chromatography. Analytical Sciences, 33(6), 691–695, 2017.

Keeling, R. F., Körtzinger, A., and Gruber, N.: Ocean deoxygenation in a warming world. Annual review of marine science, 2, 199–229, 2010.

Keppler, F., Hamilton, J. T. G., Braß, M. and Röckmann, T.: Methane emissions from terrestrial plants under aerobic conditions. Nature 439, 187–191, 2006.

Keppler, F., Schiller, A, Ehehalt, R., Greule, M., Hartmann, J., and Polag, D.: Stable isotope and high precision concentration measurements confirm that all humans produce and exhale methane. J. Breath Res. 10, 016003, 2016.

Khalil, M. A. K.: Non-CO_2 greenhouse gases in the atmosphere. Annual Review of Energy and the Environment, 24(1), 645–661, 1999.

Kitzinger, K., Marchant, H. K., Bristow, L. A., Herbold, C. W., Padilla, C. C., Kidane, A. T., Littmann, S., Daims, H., Pjevac, P., Stewart, F. J., Wagner, M., and Kuypers, M. M. M.:

Single cell analyses reveal contrasting life strategies of the two main nitrifiers in the ocean, Nature Communications, 11, 2020.

Klintzsch, T., Langer, G., Nehrke, G., Wieland, A., Lenhart, K., and Keppler, F.: Methane production by three widespread marine phytoplankton species: release rates, precursor compounds, and potential relevance for the environment. Biogeosciences, 16(20), 4129–4144, 2019.

Klobas, J. E., Wilmouth, D. M., Weisenstein, D. K., Anderson, J. G., and Salawitch, R. J.: Ozone depletion following future volcanic eruptions, Geophys. Res. Lett., 44, doi:10.1002/2017GL073972, 2017.

Kock, A., and Bange, H. W.: Nitrite removal improves hydroxylamine analysis in aqueous solution by conversion with iron (III). Environmental Chemistry, 10(1), 64–71, 2013.

Korth, F., Kock, A., Arévalo-Martínez, D. L., and Bange, H. W.: Hydroxylamine as a potential indicator of nitrification in the open ocean. Geophysical Research Letters, 46(4), 2158–2166, 2019.

Kozlowski, J. A., Stieglmeier, M., Schleper, C., Klotz, M. G., and Stein, L. Y.: Pathways and key intermediates required for obligate aerobic ammonia-dependent chemolithotrophy in bacteria and Thaumarchaeota. The ISME Journal, 10(8), 1836, 2016.

Kweku, D. W., Bismark, O., Maxwell, A., Desmond, K. A., Danso, K. B., Oti-Mensah, E. A., Quachie, A. T., and Adormaa, B. B.: Greenhouse effect: greenhouse gases and their impact on global warming. Journal of Scientific Research and Reports, 1–9, 2017.

Lelieveld, J., Crutzen, P. J., and Brühl, C.: Climate effects of atmospheric methane. Chemosphere, 26(1–4), 739–768, 1993.

Lenhart, K., Bunge, M., Ratering, S., Neu, T. R., Schüttmann, I., Greule, M., Kammann, C., Schnell, S., Müller, C., Zorn, H., and Keppler, F.: Evidence for methane production by saprotrophic fungi. Nat. Commun. 3, 1046, 2012.

Lenhart, K., Althoff, F., Greule, M., and Keppler, F.: Technical Note: Methionine, a precursor of methane in living plants, Biogeosciences, 12, 1907–1914, https://doi.org/10.5194/bg-12-1907-2015, 2015.

Lenhart, K., Klintzsch, T., Langer, G., Nehrke, G., Bunge, M., Schnell, S., and Keppler, F.: Evidence for methane production by the marine algae Emiliania huxleyi. Biogeosciences, 13(10), 3163–3174, 2016.

Lennartz, S. T., Lehmann, A., Herrford, J., Malien, F., Hansen, H. P., Biester, H., and Bange, H. W.: Long-term trends at the Time Series Station Boknis Eck (Baltic Sea), 1957–2013: does climate change counteract the decline in eutrophication? Biogeosciences, 11, 6323–6339, 2014.

Li, Y., Fichot, C. G., Geng, L., Scarratt, M. G., and Xie, H.: The contribution of methane photoproduction to the oceanic methane paradox. Geophysical Research Letters, e2020GL088362, 2020.

Liu, S., Han, P., Hink, L., Prosser, J. I., Wagner, M., and Bruggemann, N.: Abiotic conversion of extracellular NH_2OH contributes to N_2O emission during ammonia oxidation. Environmental science & technology, 51(22), 13122–13132, 2017.

Lohrberg, A., Schmale, O., Ostrovsky, I., Niemann, H., Held, P., and Schneider von Deimling, J.: Discovery and quantification of a widespread methane ebullition event in a coastal inlet (Baltic Sea) using a novel sonar strategy, Sci. Rep.-UK, 10, 4393, https://doi.org/10.1038/s41598-020-60283-0, 2020.

Löscher, C., Kock, A., Koenneke, M., LaRoche, J., Bange, H. W., and Schmitz, R. A.: Production of oceanic nitrous oxide by ammonia-oxidizing archaea. Biogeosciences, 9, 2419–2429, 2012.

Ma, X., Zhang, G. L., Liu, S. M., Wang, L., Li, P. P., Gu, P. P., and Sun, M. S.: Distributions and fluxes of nitrous oxide in lower reaches of Yellow River and its estuary: impact of water-sediment regulation. Estuarine, Coastal and Shelf Science, 168, 22–28, 2016.

Ma, X., Bange, H. W., Eirund, G. K., and Arévalo-Martínez, D. L.: Nitrous oxide and hydroxylamine measurements in the Southwest Indian Ocean. Journal of Marine Systems, 103062, 2020.

Martens-Habbena, W., Berube, P. M., Urakawa, H., José, R., and Stahl, D. A.: Ammonia oxidation kinetics determine niche separation of nitrifying Archaea and Bacteria. Nature, 461(7266), 976, 2009.

Middelburg, J. J., Nieuwenhuize, J., Iversen, N., Høgh, N., De Wilde, H., Helder, W., Seifert, R., and Christof, O.: Methane distribution in European tidal estuaries. Biogeochemistry 59, 95–119, 2002.

Munday, P. L., McCormick, M. I., and Nilsson, G. E.: Impact of global warming and rising CO_2 levels on coral reef fishes: what hope for the future? Journal of Experimental Biology, 215(22), 3865–3873, 2012.

Naik V., Horowitz, L. W., Schwarzkopf, M. D., and Lin, M.: Impact of volcanic aerosols on stratospheric ozone recovery, J. Geophys. Res. Atmos., 122, doi:10.1002/2016JD025808, 2017.

Naqvi, S. W. A., Jayakumar, D. A., Narvekar, P. V., Naik, H., Sarma, V. V. S. S., D'souza, W., Joseph, S., and George, M. D.: Increased marine production of N_2O due to intensifying anoxia on the Indian continental shelf. Nature, 408(6810), 346–349, 2000.

Nevison, C., Butler, J. H., and Elkins, J. W.: Global distribution of N_2O and the ΔN_2O-AOU yield in the subsurface ocean. Global Biogeochemical Cycles, 17(4), 2003.

Nisbet, E. G., Dlugokencky, E. J., Manning, M. R., Lowry, D., Fisher, R. E., France, J. L., Michel, S. E., Miller, J. B., White, J. W. C., Vaughn, B., Bousquet, P., Pyle, J. A., Warwick, N. J., Cain, M., Brownlow, R., Zazzeri, G., Lanoiselle, M., Manning, A. C., Gloor, E., Worthy, D. E. J., Brunke, E. G., Labuschagne, C., Wolff, E. W.,and Ganesan, A. L.: Rising atmospheric methane: 2007-2014 growth and isotopic shift, Global Biogeochem. Cycles, 30(9), 1356–1370, doi:10.1002/2016gb005406, 2016.

Pandolfi, J. M., Connolly, S. R., Marshall, D. J., and Cohen, A. L.: Projecting coral reef futures under global warming and ocean acidification. Science, 333(6041), 418–422, 2011.

Plouviez, M., Shilton, A., Packer, M. A., and Guieysse, B.: N_2O emissions during microalgae outdoor cultivation in 50 L column photobioreactors. Algal research, 26, 348–353, 2017.

Plouviez, M., Shilton, A., Packer, M. A., and Guieysse, B.: Nitrous oxide emissions from microalgae: potential pathways and significance. Journal of applied phycology, 31(1), 1–8, 2019.

Pollack, H. N., Huang, S., and Shen, P. Y.: Climate change record in subsurface temperatures: a global perspective. Science, 282(5387), 279–281, 1998.

Prather, M. J., Hsu, J., DeLuca, N. M., Jackman, C. H., Oman, L. D., Douglass, A. R., Fleming, E. L., Strahan, S. E., Steenrod, S. D., Søvde, O. A., Isaksen, I. S., Froidevaux, L., and Funke, B.: Measuring and modeling the lifetime of nitrous oxide including its variability. Journal of Geophysical Research: Atmospheres, 120(11), 5693-5705, 2015.

Prosser, J. I., Hink, L., Gubry-Rangin, C., and Nicol, G. W.: Nitrous oxide production by ammonia oxidizers: Physiological diversity, niche differentiation and potential mitigation strategies. Global Change Biology, 26(1), 103–118, 2020.

Randeniya, L., Vohrolik, P. F., and Plumb, I. C.: Stratospheric ozone depletion at northern mid latitudes in the 21st century: The importance of future concentrations of greenhouse gases nitrous oxide and methane, Geophys. Res. Lett., 29 (4), doi:10.1029/2001GL014295, 2002.

Ravishankara, A. R., Daniel, J. S., and Portmann, R. W.: Nitrous oxide (N_2O): the dominant ozone-depleting substance emitted in the 21st century. Science, 326(5949), 123–125, 2009.

Reeburgh, W. S.: Oceanic methane biogeochemistry. Chemical reviews, 107(2), 486–513, 2007.

Rees, A. P., Brown, I. J., Jayakumar, A., and Ward, B. B.: The inhibition of N_2O production by ocean acidification in cold temperate and polar waters. Deep Sea Research Part II: Topical Studies in Oceanography, 127, 93–101, 2016.

Repeta, D. J., Ferrón, S., Sosa, O. A., Johnson, C. G., Repeta, L. D., Acker, M., Delong, E. F., and Karl, D. M.: Marine methane paradox explained by bacterial degradation of dissolved organic matter. Nature Geoscience, 9(12), 884, 2016.

Ritchie, G. A. F., and Nicholas, D. J. D.: Identification of the sources of nitrous oxide produced by oxidative and reductive processes in Nitrosomonas europaea. Biochemical Journal, 126(5), 1181–1191, 1972.

Saikawa, E., Prinn, R. G., Dlugokencky, E., Ishijima, K., Dutton, G. S., Hall, B. D., Langenfelds, R., et al.:Global and Regional Emissions Estimates for N_2O. Atmospheric Chemistry and Physics 14, no. 9: 4617–4641, 2014.

Santoro, A. E., Buchwald, C., McIlvin, M. R., and Casciotti, K. L.: Isotopic signature of N_2O produced by marine ammonia-oxidizing archaea. Science, 333(6047), 1282–1285, 2011.

Saunois, M., Bousquet, P., Poulter, B., Peregon, A., Ciais, P., Canadell, J. G., Dlugokencky, E. J., Etiope, G., Bastviken, D., Houweling, S., Janssens-Maenhout, G., Tubiello, F. N., Castaldi, S., Jackson, R. B., Alexe, M., Arora, V. K., Beerling, D. J., Bergamaschi, P., Blake, D. R., Brailsford, G., Brovkin, V., Bruhwiler, L., Crevoisier, C., Crill, P., Covey, K., Curry, C., Frankenberg, C., Gedney, N., Hoglund-Isaksson, L., Ishizawa, M., Ito, A., Joos, F., Kim, H. S., Kleinen, T., Krummel, P., Lamarque, J. F., Langenfelds, R., Locatelli, R., Machida, T., Maksyutov, S., McDonald, K. C., Marshall, J., Melton, J. R., Morino, I., Naik, V., O'Doherty, S., Parmentier, F. J. W., Patra, P. K., Peng, C. H., Peng, S. S., Peters, G. P., Pison, I., Prigent, C., Prinn, R., Ramonet, M., Riley, W. J., Saito, M., Santini, M., Schroeder, R., Simpson, I. J., Spahni, R., Steele, P., Takizawa, A., Thornton, B. F., Tian, H. Q., Tohjima, Y., Viovy, N.,

Voulgarakis, A., van Weele, M., van der Werf, G. R., Weiss, R., Wiedinmyer, C., Wilton, D. J., Wiltshire, A.,Worthy, D.,Wunch, D., Xu, X. Y., Yoshida, Y., Zhang, B.W., Zhang, Z., and Zhu, Q.: The global methane budget 2000–2012, Earth Syst. Sci. Data, 8, 697–751, https://doi.org/10.5194/essd-8-697-2016, 2016.

Schaefer, H., Fletcher, S. E. M., Veidt, C., Lassey, K. R., Brailsford, G. W., Bromley, T. M., Dlugokencky, E. J., Michel, S. E., Miller, J. B., Levin, I., Lowe, D. C., Martin, R. J., Vaughn, B. H., and White, J. W. C.: A 21st-century shift from fossil-fuel to biogenic methane emissions indicated by $^{13}CH_4$, Science, 352(6281), 80–84, doi:10.1126/science.aad2705, 2016.

Schiermeier, Q.: Increased flood risk linked to global warming: likelihood of extreme rainfall may have been doubled by rising greenhouse-gas levels. Nature, 470(7334), 316–317, 2011.

Schmale, O., Wäge, J., Mohrholz, V.,Wasmund, N., Gräwe, U., Rehder, G., Labrenz, M., and Loick-Wilde, N.: The contribution of zooplankton to methane supersaturation in the oxygenated upper waters of the central Baltic Sea, Limnol. Oceanogr., 63, 412–430, 2018.

Seike, Y., Fukumori, R., Senga, Y., Oka, H., Fujinaga, K., and Okumura, M.: A simple and sensitive method for the determination of hydroxylamine in fresh-water samples using hypochlorite followed by gas chromatography. Analytical Sciences, 20(1), 139–142, 2004.

Shafirovich, V., and Lymar, S. V.: Nitroxyl and its anion in aqueous solutions: spin states, protic equilibria, and reactivities toward oxygen and nitric oxide. Proceedings of the National Academy of Sciences, 99(11), 7340–7345, 2002.

Simon, J., Kern, M., Hermann, B., Einsle, O., and Butt, J. N.: Physiological function and catalytic versatility of bacterial multihaem cytochromes c involved in nitrogen and sulfur cycling. Biochemical Society Transactions 39: 1864–1870, http://dx.doi.org/10.1042/BST20110713, 2011.

Six, K. D., Kloster, S., Ilyina, T., Archer, S. D., Zhang, K., and Maier-Reimer, E.: Global warming amplified by reduced sulphur fluxes as a result of ocean acidification. Nature Climate Change, 3(11), 975–978, 2013.

Soruco, A., Vincent, C., Francou, B., and Gonzalez, J. F.: Glacier decline between 1963 and 2006 in the Cordillera Real, Bolivia. Geophysical Research Letters, 36(3), 2009.

Sosa, O. A., Burrell, T. J., Wilson, S. T., Foreman, R. K., Karl, D. M., and Repeta, D. J.: Phosphonate cycling supports methane and ethylene supersaturation in the phosphate-depleted western North Atlantic Ocean. Limnology and Oceanography, 2020.

Stawiarski, B., Otto, S., Thiel, V., Gräwe, U., Loick-Wilde, N.,Wittenborn, A. K., Schloemer, S., Wäge, J., Rehder, G., Labrenz, M., Wasmund, N., and Schmale, O.: Controls on zooplankton methane production in the central Baltic Sea, Biogeosciences, 16, 1–16, https://doi.org/10.5194/bg-16-1-2019, 2019.

Stein, L. Y.: Surveying N_2O-producing pathways in bacteria. In Methods in enzymology (Vol. 486, pp. 131–152). Academic press, 2011.

Steinle, L., Maltby, J., Treude, T., Kock, A., Bange, H. W., Engbersen, N., Zopfi, J., Lehmann, M. F., and Niemann, H.: Effects of low oxygen concentrations on aerobic methane oxidation in seasonally hypoxic coastal waters, Biogeosciences, 14, 1631–1645, https://doi.org/10.5194/bg-14-1631-2017, 2017.

Stieglmeier, M., Mooshammer, M., Kitzler, B., Wanek, W., Zechmeister-Boltenstern, S., Richter, A., and Schleper, C.: Aerobic nitrous oxide production through N-nitrosating hybrid formation in ammonia-oxidizing archaea. The ISME Journal, 8(5), 1135, 2014.

Terada, A., Sugawara, S., Hojo, K., Takeuchi, Y., Riya, S., Harper Jr, W. F., Yamamoto, T., Kuroiwa, M., Isobe, K., Katsuyama, Chie, Suwa, Y., Koba, K., Hosomi, M.: Hybrid nitrous oxide production from a partial nitrifying bioreactor: hydroxylamine interactions with nitrite. Environmental science & technology, 51(5), 2748–2756, 2017.

Thompson, L. G.: Climate change: The evidence and our options. The Behavior Analyst, 33(2), 153–170, 2010.

Thompson, R. L., Ishijima, K., Saikawa, E., Corazza, M., Karstens, U., Patra, P. K., et al.: TransCom N_2O model inter-comparison, Part 2: Atmospheric inversion estimates of N_2O emissions. Atmospheric Chemistry and Physics, 14, 6177–6194, 2014.

Tuboly, E., Szabó, A., Garab, D., Bartha, G., Janovszky, Á., Ero"s, G., et al.: Methane biogenesis during sodium azide-induced chemical hypoxia in rats. Am. J. Physiol. Physiol. 304, C207–C214, 2013.

Upstill-Goddard, R. C., Barnes, J., Frost, T., Punshon, S. and Owens, N. J. P.: Methane in the southern North Sea: low-salinity inputs, estuarine removal, and atmospheric flux. Global Biogeochem. Cycles 14, 1205–1217, 2000.

Ussiri D., and Lal R.: Global Sources of Nitrous Oxide. In: Soil Emission of Nitrous Oxide and its Mitigation. Springer, Dordrecht, 2013.

Vajrala, N., Martens-Habbena, W., Sayavedra-Soto, L. A., Schauer, A., Bottomley, P. J., Stahl, D. A., and Arp, D. J.: Hydroxylamine as an intermediate in ammonia oxidation by globally abundant marine archaea. Proceedings of the National Academy of Sciences, 110(3), 1006–1011, 2013.

Von Breymann, M. T., De Angelis, M. A., and Gordon, L. I.: Gas chromatography with electron capture detection for determination of hydroxylamine in seawater. Analytical Chemistry, 54(7), 1209–1210, 1982.

Wan, R., Chen, Y., Zheng, X., Su, Y., and Li, M.: Effect of CO_2 on microbial denitrification via inhibiting electron transport and consumption. Environmental science & technology, 50(18), 9915–9922, 2016.

Wayne R. P.: Chemistry of Atmospheres, 1991 (Oxford Univ. Press, Oxford, ed. 3, 2000), p. 775.

Weber, T., Wiseman, N. A., and Kock, A.: Global ocean methane emissions dominated by shallow coastal waters. Nature communications, 10(1), 1–10, 2019.

White, C. J., and Lehnert, N.: Is there a pathway for N_2O production from hydroxylamine oxidoreductase in ammonia-oxidizing bacteria? Proceedings of the National Academy of Sciences, 113(51), 14474–14476, 2016.

Whiticar, M. J., and Faber, E.: Methane oxidation in sediment and water column environments—isotope evidence. Organic geochemistry, 10(4–6), 759–768, 1986.

WMO: Scientific assessment of ozone depletion: 2018, World Meteorological Organization, Geneva, Switzerland, Global Ozone Research and Monitoring Project–Report No. 58, 588 pp., 2018.

Wolf, J., Asrar, G. R., and West, T. O.: Revised methane emissions factors and spatially distributed annual carbon fluxes for global livestock, Carbon Balance Manag., 12(1), 16, doi:10.1186/s13021-017-0084-y, 2017.

Worden, J. R., Bloom, A. A., Pandey, S., Jiang, Z., Worden, H. M., Walker, T. W., Houweling, S., and Röckmann, T.: Reduced biomass burning emissions reconcile conflicting estimates of the post-2006 atmospheric methane budget, Nat. Commun., 8(1), 2227, doi:10.1038/s41467-017-02246-0, 2017.

Wrage, N., Velthof, G. L., Van Beusichem, M. L., and Oenema, O.: Role of nitrifier denitrification in the production of nitrous oxide. Soil biology and Biochemistry, 33(12–13), 1723–1732, 2001.

Yang, S., Chang, B. X., Warner, M. J., Weber, T. S., Bourbonnais, A. M., Santoro, A. E., Kock, A., Sonnerup, R. E., Bullister, J. L., Wilson, S. T., and Bianchi, D.: Global reconstruction reduces the uncertainty of oceanic nitrous oxide emissions and reveals a vigorous seasonal cycle, Proceedings of the National Academy of Sciences, doi: 10.1073/pnas.1921914117, 2020. 201921914, 2020.

Ye, W. W., Wang, X. L., Zhang, X. H., and Zhang, G. L.: Methane production in oxic seawater of the western North Pacific and its marginal seas. Limnology and Oceanography, 2020.

Zindler, C., Bracher, A., Marandino, C. A., Taylor, B., Torrecilla, E., Kock, A., and Bange, H. W.: Sulphur compounds, methane, and phytoplankton: interactions along a north-south transit in the western Pacific Ocean, Biogeosciences, 10, 3297–3311, doi:10.5194/bg-10-3297-2013, 2013.

Zhai, P. M., and Liu, J.: Extreme weather/climate events and disaster prevention and mitigation under global warming background. Engineering Sciences, 14(9), 55–63, 2012.

Chapter 2

A decade of methane measurements at the Boknis Eck Time-series Station in the Eckernförde Bay (southwestern Baltic Sea)

Biogeosciences, 17, 3427–3438, 2020
https://doi.org/10.5194/bg-17-3427-2020

Biogeosciences
Open Access
EGU

A decade of methane measurements at the Boknis Eck Time Series Station in Eckernförde Bay (southwestern Baltic Sea)

Xiao Ma[1], **Mingshuang Sun**[1], **Sinikka T. Lennartz**[1,a], **and Hermann W. Bange**[1]

[1]GEOMAR Helmholtz Centre for Ocean Research Kiel, Düsternbrooker Weg 20, 24105 Kiel, Germany
[a]now at: ICBM, University of Oldenburg, Oldenburg, Germany

Correspondence: Xiao Ma (mxiao@geomar.de)

Received: 25 March 2020 – Discussion started: 30 March 2020
Revised: 4 June 2020 – Accepted: 10 June 2020 – Published: 6 July 2020

Abstract. Coastal areas contribute significantly to the emissions of methane (CH_4) from the ocean. In order to decipher its temporal variability in the whole water column, dissolved CH_4 was measured on a monthly basis at the Boknis Eck Time Series Station (BE) located in Eckernförde Bay (SW Baltic Sea) from 2006 to 2017. BE has a water depth of about 28 m, and dissolved CH_4 was measured at six water depths ranging from 0 to 25 m. In general, CH_4 concentrations increased with depth, indicating a sedimentary release of CH_4. Pronounced enhancement of the CH_4 concentrations in the bottom layer (15–25 m) was found during February, May–June and October. CH_4 was not correlated with Chlorophyll *a* or O_2 over the measurement period. Unusually high CH_4 concentrations (of up to 696 nM) were sporadically observed in the upper layer (0–10 m; e.g., in November 2013 and December 2014) and coincided with major Baltic inflow (MBI) events. Surface CH_4 concentrations were always supersaturated throughout the monitoring period, indicating that Eckernförde Bay is an intense but highly variable source of atmospheric CH_4. We did not detect significant temporal trends in CH_4 concentrations or emissions, despite ongoing environmental changes such as warming and deoxygenation in Eckernförde Bay. Overall, the CH_4 variability at BE is driven by a complex interplay of various biological and physical processes.

1 Introduction

Methane (CH_4) is an atmospheric trace gas which contributes significantly to global warming (IPCC, 2013) and the evolution of stratospheric ozone (WMO, 2018). Atmospheric CH_4 mole fractions have been increasing by about 150 % since the industrial revolution (IPCC, 2013).

The oceanic release of CH_4 to the atmosphere plays a minor role in the global atmospheric CH_4 budget (Saunois et al., 2016). However, coastal areas have been identified as hotspots of CH_4 emissions (see e.g., Bange et al., 1994; Upstill-Goddard et al., 2000; Borges et al., 2016). Dissolved CH_4 in coastal waters mainly results from the interplay of (i) sedimentary sources such as anaerobic methanogenesis during the decomposition of organic matter (Xiao et al., 2018; Dale et al., 2019) or seepage from oil and natural gas reservoirs (Bernard et al., 1976; Hovland et al., 1993; Judd et al., 2002) and (ii) microbial CH_4 consumption which occurs under oxic conditions in the water column and under anoxic conditions in the sediments (Pimenov et al., 2013; Steinle et al., 2017; Egger et al., 2018). Only recently, Weber et al. (2019) estimated the global oceanic CH_4 emissions to range from 6 to 12 Tg yr^{-1}, of which about 0.8–3.8 Tg yr^{-1} was attributed to coastal waters. Occasional studies of the CH_4 production and consumption pathways in coastal waters and the associated CH_4 emissions to the atmosphere have received increasing attention during the last few decades (Bange et al., 1994; Reeburgh, 2007; Naqvi et al., 2010). However, time-series measurements of CH_4 which would allow for identifying short- and long-term trends in view of the ongoing environmental changes in coastal regions (such as eutrophication, warming and deoxygenation) are still sparse. In this paper we present the monthly measurements of CH_4 from a time-series station in Eckernförde Bay (Baltic Sea) during 2006–2017.

Due to severe eutrophication, sediments in Eckernförde Bay receive large amounts of organic matter (Smetacek et al.,

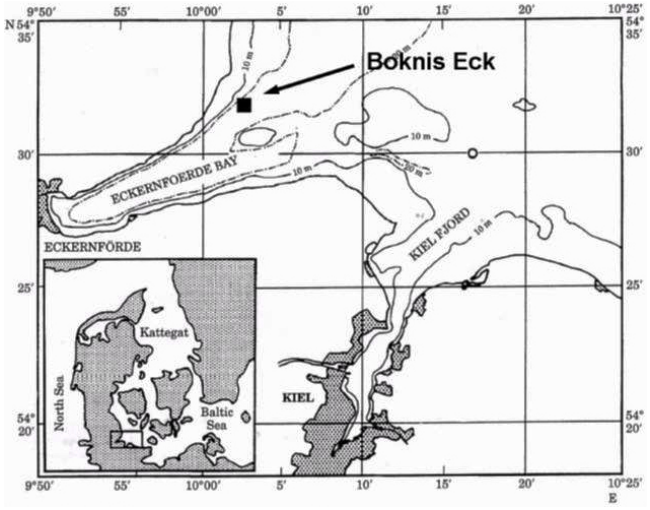

Figure 1. Location (black square) of the Boknis Eck Time Series Station in Eckernförde Bay, southwestern Baltic Sea (from Hansen et al., 1999).

1987; Oris et al., 1996; Nittrouer et al., 1998) and thus are active sites of CH_4 formation (Schmaljohann, 1996; Whiticar, 2002; Treude et al., 2005; Maltby et al., 2018). Seasonal and inter-annual CH_4 variations in concentration, saturation and air–sea flux density were investigated for more than a decade. The aim of this study was to assess the seasonal dynamics of and the environmental controls on CH_4 variability in Eckernförde Bay which is affected by high nutrient concentrations, increasing water temperatures and ongoing loss of dissolved oxygen (Lennartz et al., 2014).

2 Study site

The Boknis Eck Time Series Station (BE) is one of the oldest continuously conducted marine time-series stations in the world. The first sampling took place in 1957 and has been conducted on a monthly base with only minor interruptions since then (Lennartz et al., 2014). It is situated in Eckernförde Bay in the southwestern (SW) Baltic Sea, with a depth of approximately 28 m (Fig. 1). The sediments in the Bay are characterized by a high organic matter load and sedimentation rate (Orsi et al., 1996; Whiticar, 2002), which is closely associated with the spring and autumn algae blooms (Smetacek, 1985).

The Baltic Sea has only a limited water exchange with the North Sea through the Kattegat, which makes this area very sensitive to climate change and anthropogenic impacts. As a result of global warming, the increasing trend for the global sea surface (<75 m) temperatures (SSTs) was about 0.11 °C per decade (IPCC, 2013), while a net SST increase of 1.35 °C was observed in the Baltic Sea during 1982–2006, which is one of the most rapid temperature increments in large marine ecosystems (Belkin, 2009). Lennartz et al. (2014) reported a warming trend of up to 0.2 °C per decade at BE for the period of 1957–2013. Nutrients in the Baltic Sea had been increasing until the 1980s as a result of intensive agricultural and industrial activities and then started to decline due to effective wastewater control (HELCOM, 2018). However, hypoxia and anoxia have been increasing in the Baltic Sea during the past several decades (Conley et al., 2011; Carstensen et al., 2014). Similar trends in nutrients and O_2 were also detected at BE (Lennartz et al., 2014), indicating that Eckernförde Bay is representative of the biogeochemical setting of the SW Baltic Sea. In concert with the declining nutrient concentrations, Chlorophyll *a* concentrations at BE were declining as well (Lennartz et al., 2014).

Located close to the bottleneck of the water exchange between the North Sea and the Baltic Sea, BE is also sensitive to hydrographic fluctuations such as inflows of saline North Sea water. There is no riverine input to Eckernförde Bay, and thus, the saline water inflow from the North Sea plays a dominant role in the hydrographic setting at BE. Because the inflowing North Sea water has a higher salinity compared to Baltic Sea water, a pronounced summer stratification occurs which leads to the development of a pycnocline at about a 15 m water depth. The seasonal stratification occurs usually from mid-March until mid-September. During this period, vertical mixing is restricted and bacterial decomposition of organic material in the deep layer causes pronounced hypoxia and sporadically occurring anoxia during late summer (Lennartz et al., 2014). Pronounced phytoplankton blooms occur regularly in autumn (September–November) and spring (February–March) and to a lesser extent during summer (July–August; Smetacek et al., 1985).

3 Methods

3.1 Sample collection and measurement

Monthly sampling of CH_4 from BE started in June 2006. Seawater was collected from six depths (1, 5, 10, 15, 20 and 25 m) with 5 L Niskin bottles mounted on a CTD rosette. Brown glass vials of 20 mL were filled in triplicates without any bubbles. The vials were sealed immediately with rubber stoppers and aluminum caps. These samples were poisoned with 50 µL of saturated aqueous mercury chloride ($HgCl_2$) solution as soon as possible and then stored in a cool, dark place until measurement. The storage time of the samples before the measurements was less than 3 months.

A static headspace-equilibrium method was adopted for the CH_4 measurements. A 10 mL helium (99.9999 %, Air Liquide, Düsseldorf, Germany) headspace was created inside the vial with a gas-tight syringe (VICI Precision Sampling, Baton Rouge, LA, USA). The sample was vibrated with a vortex mixer (G560E, Scientific Industries Inc., NY, USA) for approximately 20 s and then left for at least 2 h to reach the CH_4 equilibrium between air and water phases. A

9.5 mL subsample of headspace was injected into a gas chromatograph equipped with a flame ionization detector (GC-FID; Hewlett-Packard 5890 Series II, Agilent Technologies, Santa Clara, CA, USA). Separation took place on a packed column (stainless steel, 1.8 m length, packed with Molsieve 5A, Grace, Columbia, Maryland, USA). Standard gas mixtures with varying mole fractions of CH_4 in synthetic air (Deuste Steininger GmbH, Mühlhausen, Germany, and Westfalen AG, Münster, Germany) were used daily to calibrate the response of the FID before measurements. The concentrations of standard gases were adjusted for every measurement to make sure that the values of the samples fall in the range of the calibration curves. The standard gas mixtures were calibrated against NOAA primary gas standard mixtures in the laboratory of the Max Planck Institute for Biogeochemistry in Jena, Germany. Further details about the measurements and calculations of the dissolved CH_4 concentration can be found in Bange et al. (2010). The mean precision of the CH_4 measurements, calculated as the median of the estimated standard errors (see David, 1951) from all triplicate measurements, was ± 1.3 nM. Samples with an estimated standard error of $>10\,\%$ were omitted. Dissolved O_2 concentrations were measured with Winkler titrations, and Chlorophyll *a* concentrations were measured with a fluorometer (Grasshoff et al., 1999). Secchi depth was measured with a white disk (~ 30 cm in diameter). Sea levels were measured at Kiel-Holtenau, which is about 15 km away from BE (http://www.boos.org/, last access: 2 July 2020). A more comprehensive overview of temperature, salinity, dissolved O_2 and Chlorophyll *a* as well as other parameters at BE can be found in Lennartz et al. (2014).

3.2 Calculation of saturation and air–sea flux density

The CH_4 saturation (S_{CH_4}; %) was calculated as

$$S_{CH_4} = 100 \times CH_{4,obs}/CH_{4\,eq.}, \quad (1)$$

where $CH_{4,obs}$ and $CH_{4\,eq.}$ are the observed and equilibrium concentrations of CH_4 in seawater, respectively. $CH_{4\,eq.}$ was calculated with the in situ temperature and salinity of seawater (Wiesenburg and Guinasso, 1979) and the dry mole fraction of atmospheric CH_4 at the time of sampling, which was derived from the monthly atmospheric CH_4 data measured at Mace Head, Ireland (AGAGE, http://agage.mit.edu/, last access: 2 July 2020).

The air–sea CH_4 flux density (F_{CH_4}; $\mu mol\,m^{-2}\,d^{-1}$) was calculated as

$$F_{CH_4} = k \times (CH_{4,obs} - CH_{4\,eq.}), \quad (2)$$

where k ($cm\,h^{-1}$) is the gas transfer velocity calculated with the equation given by Nightingale et al. (2000), as a function of the wind speed and the Schmidt number (Sc). Sc was computed with the empirical equations for the kinematic viscosity of seawater (Siedler and Peters, 1986) and the diffusion coefficients of CH_4 in water (Jähne et al., 1987). Wind speed data were recorded at Kiel Lighthouse (https://www.geomar.de/service/wetter/, last access: 2 July 2020), which is approximately 20 km away from BE. The wind speeds were normalized to the height of 10 m (u_{10}) with the method given by Hsu et al. (1994).

4 Results and discussion

4.1 Seasonal variations in environmental parameters and dissolved CH_4

Seasonal hypoxia was observed every year at BE during 2006–2017 (Fig. 2). O_2 depletion was detected in the bottom layer ($\sim$ 15–25 m) during July–October with minimum O_2 concentrations usually occurring in September (Fig. 3). Lennartz et al. (2014) found a significant decrease in dissolved O_2 concentrations in the bottom water at BE over the past several decades and suggested that temperature-enhanced O_2 consumption and a prolonged stratification period might be the causes of deoxygenation. Anoxia with the presence of hydrogen sulfide (H_2S, identified from the strong smell) in the period of concurrent CH_4 measurements was found in the autumn of 2007, 2014 and 2016. The anoxic event in 2016 lasted from September until November and was the longest ever recorded at BE. In September 2017, a pronounced undersaturation of O_2 ($\sim 50\,\%$) was observed in surface water (Fig. 2). The low temperature together with enhanced salinity in the surface water in September 2017 suggests the occurrence of an upwelling event, which transported O_2-depleted and colder bottom waters to the surface. An upwelling signal was also present in the nutrient concentrations (not shown) but was less pronounced than in temperature and dissolved O_2 concentrations. Similar events were also detected in September 2011 and 2012.

Enhanced Chlorophyll *a* concentrations, which can be used to indicate phytoplankton blooms, were usually observed in spring or autumn but not in every year (Fig. 2). Seasonal variations in Chlorophyll *a* concentrations were generally consistent with the annual plankton succession reported by Smetacek (1985). During 2006–2017, high Chlorophyll *a* concentrations were usually found in the upper layers in March (Fig. 3), which is different from the seasonality during 1960–2013 when, on average, high concentrations occupied the whole water column (Lennartz et al., 2014). Another difference is that no prevailing "winter dormancy" of biological activity was observed: Chlorophyll *a* concentrations usually remained high throughout the autumn–spring period. In November and December 2006 and March 2012, when high Chlorophyll *a* concentrations were observed all over the water column, nutrients and temperature were generally higher. Although the overall correlation between Chlorophyll *a* and nutrients (NO_3^-; $r^2 = 0.01$, $p < 0.01$, $n = 674$) or temperature ($r^2 = 0.02$, $p < 0.0001$, $n = 671$) is poor, nutrients or temper-

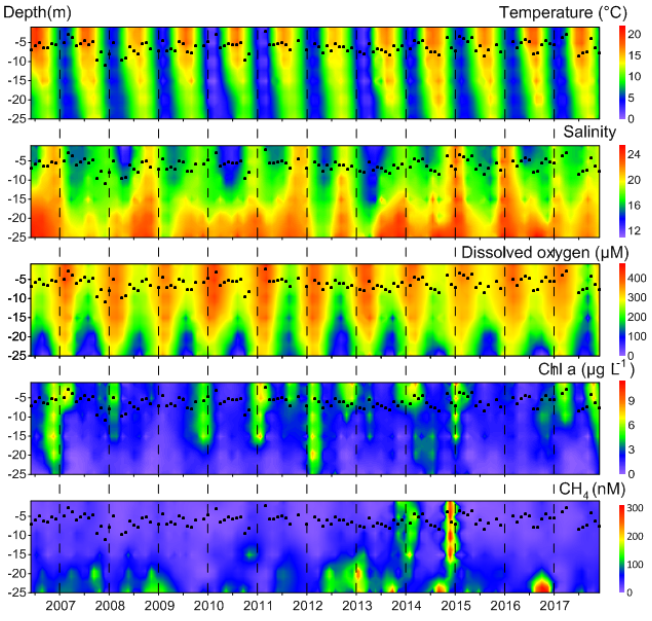

Figure 2. Distributions of temperature, salinity, dissolved O_2, Chlorophyll *a* and CH_4 at BE during 2006–2017. Black dots indicate the monthly measurements of Secchi depth. To get a better visualization, the maximum color bar for CH_4 concentration is 300 nM, but some of the actual concentrations are higher (for example, in December 2014 and in autumn 2016).

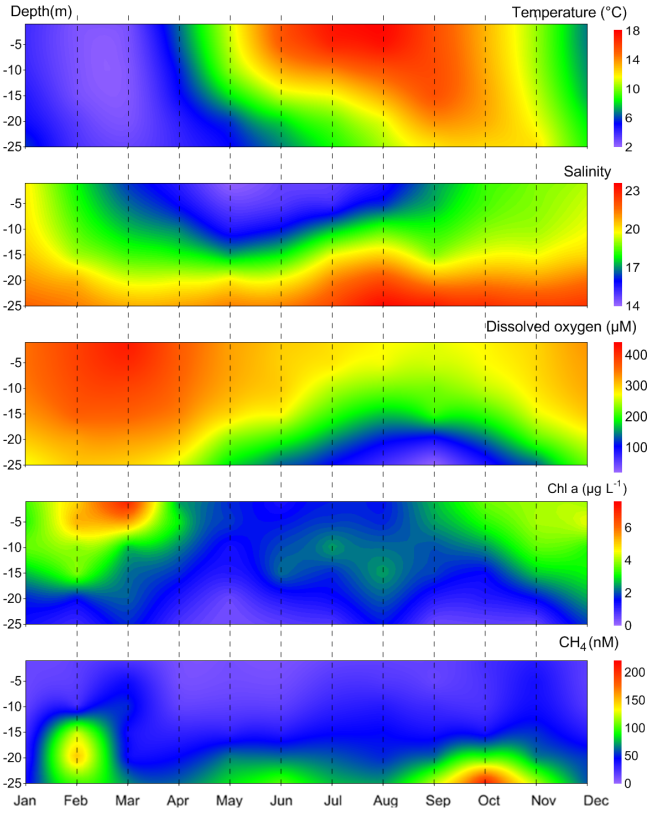

Figure 3. Mean seasonal variations in temperature, salinity, dissolved O_2, Chlorophyll *a* and CH_4 at BE during 2006–2017. CH_4 concentrations in December 2014 were excluded in plotting.

ature might be potential environmental controls on Chlorophyll *a* distribution. As a proxy for water transparency, the Secchi depth was lowest in March indicating a high turbidity, coincident with the Chlorophyll *a* maximum. Chlorophyll *a* concentrations and Secchi depths have been decreasing over the past decades in the Baltic Sea (Sandén and Håkansson, 1996; Fleming-Lehtinen and Laamanen, 2012; Lennartz et al., 2014), but this trend cannot be identified from the median slope at BE during 2006–2017.

CH_4 concentrations at BE showed strong seasonal and inter-annual variability (Fig. 2, Table 1). During 2006–2017, dissolved CH_4 concentrations ranged between 2.9 and 695.6 nM, with an average of 51.2 ± 84.2 nM. High concentrations were generally observed in the bottom layer ($\sim$ 15–25 m). Enhanced CH_4 concentrations were mainly observed during February, May–June and October (Fig. 3). Steinle et al. (2017) measured aerobic CH_4 oxidation at BE and found that the lowest rates occurred in winter, which might be one of the reasons for the enhanced CH_4 concentrations in February.

The CH_4 accumulation in May and June can be linked to enhanced methanogenesis fueled by organic matter from the spring algae bloom. Capelle et al. (2019) found a positive correlation between mean monthly CH_4 concentrations and Chlorophyll *a* concentrations in the upper layers of time-series measurements from Saanich Inlet. Bange et al. (2010) also reported correlations between seasonal CH_4 variation and Chlorophyll *a* or Secchi depth, albeit with a time lag of 1 month, at BE during 2006–2008. Although we did not detect such relationships for the extended measurements during 2006–2017, in 2009 and 2016, when no spring algae blooms were detected, CH_4 concentrations in the following summer months were lower than average (Fig. 2).

Maximum CH_4 concentrations were usually observed in October, at the end of the seasonal hypoxia (Fig. 3). Due to the long-lasting anoxic event, strong CH_4 accumulations were observed in autumn 2016 ($\sim$ 600 nM), which are the highest in the bottom layer during 2006–2017. Prevailing for several months, the depletion of bottom O_2 concentrations exerts a strong influence on the underlying sediment. Maltby et al. (2018) detected a shoaling of the sulfate reduction zone in autumn and enhanced methanogenesis in the sediments at BE. Reindl and Bolalek (2012) found similar variations in sedimentary CH_4 release in the coastal Baltic Sea. In situ production in the anoxic bottom water might be a potential CH_4 source as well (Scranton and Farrington, 1977; Levipan et al., 2007). We, therefore, suggest that the accumulation of CH_4 in the bottom water in October is caused by its release from the sediments and in situ production in the overlying water column in combination with the pronounced water col-

Table 1. Annual mean (arithmetic average ± standard deviation) of water temperature, salinity, wind speed and dissolved CH_4 concentrations at BE during 2006–2017. Water temperatures, salinity and CH_4 concentrations were averaged over the water column (0–25 m). Wind speeds were recorded at Kiel Lighthouse.

Year	Temperature (°C)	Salinity	Wind speed (u_{10}, m s^{-1})	CH_4 (nM)
2006	9.19 ± 5.75	20.14 ± 3.11	7.5 ± 2.6	39.3 ± 38.1
2007	9.68 ± 4.55	17.78 ± 2.14	7.5 ± 2.5	44.9 ± 45.5
2008	10.11 ± 4.20	19.14 ± 3.43	6.2 ± 2.1	36.9 ± 41.9
2009	9.20 ± 4.81	18.36 ± 2.22	7.3 ± 2.3	27.8 ± 26.2
2010	8.47 ± 5.20	17.80 ± 3.22	5.5 ± 2.7	34.8 ± 39.3
2011	8.74 ± 5.16	19.14 ± 2.78	6.8 ± 3.1	36.9 ± 29.1
2012	9.47 ± 3.89	18.67 ± 2.63	8.7 ± 2.1	46.4 ± 44.3
2013	9.04 ± 5.45	17.89 ± 3.74	5.9 ± 2.8	67.7 ± 83.1
2014	10.38 ± 4.93	19.17 ± 2.79	7.0 ± 3.3	101.4 ± 183.3
2015	9.19 ± 4.28	19.71 ± 3.30	6.1 ± 2.8	35.7 ± 36.3
2016	10.09 ± 4.71	18.80 ± 3.19	5.9 ± 1.7	52.6 ± 111.4
2017	10.21 ± 4.86	19.50 ± 2.11	6.8 ± 2.4	30.5 ± 22.9

umn stratification during autumn which prevents ventilation of CH_4 to the surface layer.

4.2 Enhanced CH_4 concentrations in the upper water layer

In agreement with Schmale et al. (2010) and Bange et al. (2010), we found that CH_4 concentrations generally increase with water depth, indicating a prevailing release of CH_4 from the sediments into the water column in the Baltic Sea (see Sect. 4.1). Nonetheless, unusual high CH_4 concentrations in the upper layers were detected sporadically at BE during 2006–2017 (Fig. 2). In November 2013 and March 2014, average CH_4 concentrations in the upper waters were 187.2±13.9 nM (1–10 m) and 217.8±1.4 nM (5–10 m), which are about 16 and 5 times higher than those found in the bottom layers, respectively (Fig. 4). The most striking event occurred in December 2014, when CH_4 concentrations in the upper layer (1–15 m) were as high as 692.6 ± 3.4 nM (19 890 ± 115 %), whereas dissolved CH_4 in the bottom layer (20–25 m) was ∼ 50 nM. The surface CH_4 concentration in December 2014 was the highest observed during 2006–2017. In December 2014, a major Baltic inflow (MBI) event occurred, carrying large amounts of saline and oxygenated water from the North Sea into the Baltic Sea (Mohrholz et al., 2015). Dissolved CH_4 concentrations in the surface North Sea were much lower than in Eckernförde Bay (Bange et al., 1994; Rehder et al., 1998), and therefore a direct CH_4 contribution from the North Sea by oxygenated waters seems unlikely. We hypothesize that this inflow substituted the lower part of the water column which had high CH_4 concentration throughout the water depth before, as opposed to, e.g., an in situ production of CH_4 at the surface being responsible for the observed concentration profile anomaly. The MBI is the third-strongest event ever recorded, and an unusual outflow period was detected in Eckernförde Bay: sea levels declined from mid-November, reached a minimum on 10 December and then began to increase with the inflow (Fig. 5). The sampling at BE took place on 16 December, during the main inflow period. Extreme weather conditions (wind speed >15 m s^{-1}) were observed several days before the sampling date, and storm-generated waves and currents could have affected the sediment structures in Eckernförde Bay (Oris et al., 1996). Currents across the seabed can result in pressure gradients that drive porewater flow within the permeable sediments (Ahmerkamp et al., 2015), which might be a potential CH_4 source. Sediment resuspension might also contribute to enhanced CH_4 release, but we did not observe a significant decline in Secchi depths in December 2014 (Fig. 2). The significant decrease in sea level alleviated the static pressure on the sediments. Enhanced CH_4 release from the sediments, via gas bubbles or exchange from porewater, may have led to the accumulation of CH_4 in the water column. Similar hydrostatic pressure effects were also reported in tidal systems such as mangrove creeks and estuaries (see e.g., Barnes et al., 2006; Maher et al., 2015; Sturm et al., 2017). Atmospheric pressure also contributes to the overall pressure on the sediments, but it is not recorded at BE and thus was omitted. Although the water level fluctuation of ±1 m (Fig. 5) seems rather small compared to the water depth (28 m), it might exert a strong influence on the sediments. Water level fluctuation, when there was no strong wind or inflow event, was approximately ±0.2 m in Eckernförde Bay. Lohrberg et al. (2020) detected a change in water level (±0.5 m) and air pressure (±1500 Pa, equivalent to approximately ±0.15 m of water level fluctuation) during a weak storm in the autumn of 2014. The fluctuation in hydrostatic pressure induced a pronounced CH_4 ebullition event in Eckernförde Bay, and a sedimentary CH_4 flux of 1916 µmol m^{-2} d^{-1} was estimated (Lohrberg et al., 2020). This value is generally in good agreement with the sharp increase in the sea-to-air CH_4 fluxes in December 2014 (see Sect. 4.3). The outflow period of the MBI in 2014 lasted for almost a month, and bulk ebullitions and supersaturated water with CH_4 could be anticipated. During the inflow period, large amounts of North Sea water flooded into Eckernförde Bay and presumably pushed the CH_4-enriched water to the surface. A negative correlation was found between salinity and CH_4 concentration in the water column (Fig. 4a; $r^2 = 0.84$, $p = 0.01$, $n = 6$), indicating that vertical CH_4 distributions were linked to the mixing of saline water in the bottom and less-saline water in the upper layers. We suggest that CH_4 release driven by hydrostatic pressure fluctuations and the MBI-associated mixing are responsible for the abnormal CH_4 profile in December 2014.

The CH_4 anomaly in November 2013 can be linked to saline water inflow as well. Nausch et al. (2014) reported the occurrence of an inflow event from 27 October to 7 November in 2013. The sampling at BE took place on 5 November, and an increase in salinity was detected in the bottom water (Fig. 4b). The rapid transition from hypoxic (9.8 µM L^{-1},

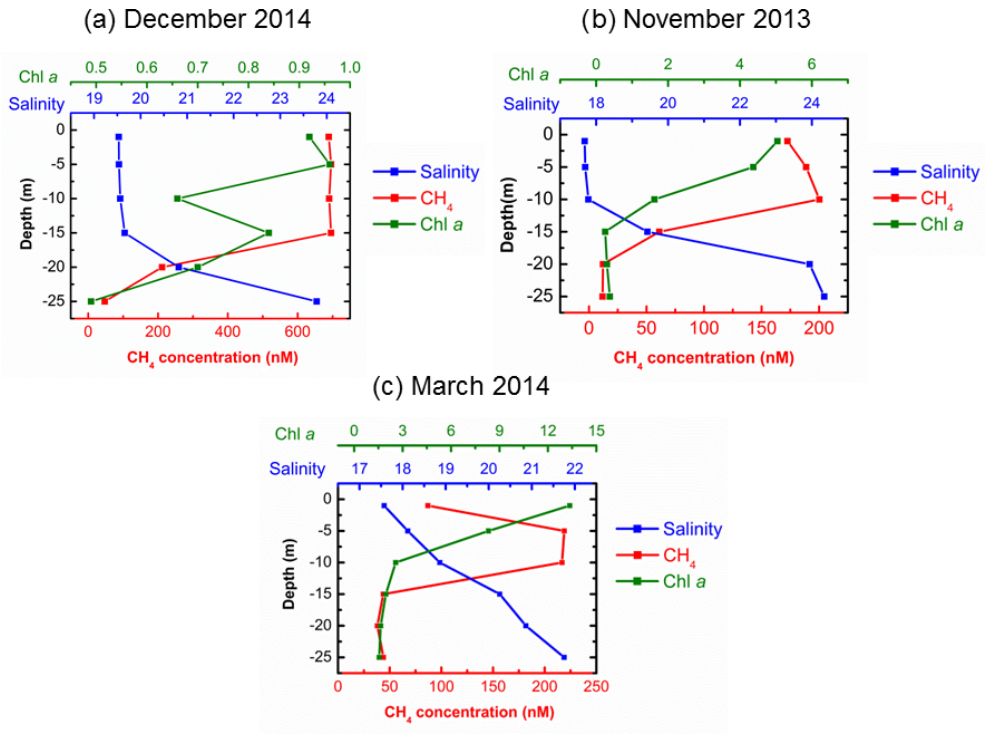

Figure 4. Vertical distribution of Chlorophyll *a*, salinity and CH_4 concentrations in the water column in December 2014 **(a)**, November 2013 **(b)** and March 2014 **(c)**.

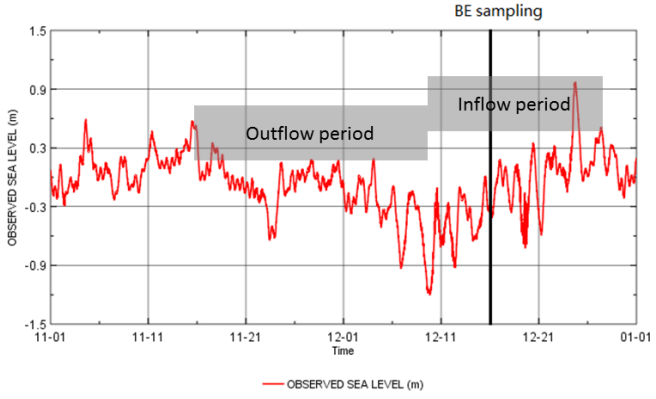

Figure 5. Sea level variations in November and December 2014. The black line indicates the occurrence of BE sampling in December 2014.

25 m in October) to oxic (239.2 µM L^{-1}, 25 m in November) conditions in the bottom layer also supports the occurrence of the inflow (Fig. 2). Steinle et al. (2017) found a change in the temperature optimum of aerobic CH_4-oxidizing bacteria (MOB) in November 2013 at BE and linked it to a displacement of the local MOB community as a result of saltwater injection. Although enhanced CH_4 concentrations and high net methanogenesis rates were detected in the sediments in November 2013 (Maltby et al., 2018), the saline inflow with less dissolved CH_4 was sandwiched between the sediments and the upper-layer waters. As a result, we also found a negative salinity–CH_4 correlation in the water column (Fig. 4b; $r^2 = 0.86$, $p<0.01$, $n = 6$). This inflow event was much weaker than the MBI in December 2014, and no obvious outflow or inflow period can be identified from sea level variations. There was no strong fluctuation in hydrostatic pressure, and thus sedimentary CH_4 release and CH_4 supersaturations in the water column were lower than in December 2014. Another difference is that the decrease in salinity and increase in CH_4 concentrations were observed between 10 and 20 m, which is at shallower depths compared to the MBI in December 2014, indicating that the saline water volume in the bottom layer was larger at the time of the sampling in November 2013.

The situation in March 2014 is different. We did not find any evidence for saline water inflow or hydrostatic pressure fluctuation, and the correlation between CH_4 concentration and salinity is poor (Fig. 4c; $r^2 = 0.43$, $p = 0.16$, $n = 6$). The occurrences of the unusual CH_4 profiles were accompanied by the enhanced Chlorophyll *a* concentrations in the upper waters. CH_4 production by widespread marine phytoplankton has been reported, and the phytoplankton might be a potential source of surface CH_4 supersaturations (Lenhart et al., 2016; Klintzsch et al., 2019). However, spring or autumn algae blooms at BE were often observed without CH_4 accumulation, and surface CH_4 contribution from phytoplankton

remains to be proven. Potential sources for the enhanced CH_4 in March 2014 are still unclear.

In summary, we suggest that saline water inflow and the subsequent upwelling of water are the most likely causes for the CH_4 surface accumulation in November 2013 and December 2014. Nonetheless, the occurrence of inflow does not necessarily lead to enhanced CH_4 concentrations in the upper waters. Inflow events are relatively common; for example, in 2013, besides the inflow in November, three other events with similar estimated inflow volumes were detected in January, February and April (Nausch et al., 2014), but no CH_4 anomaly was found during that period. The magnitude of the CH_4 anomalies might depend on the strength of the inflow events and other factors, such as storms and sediment resuspension. Besides, there is a high chance that the monthly sampling at BE only captured few CH_4 pulses. Inflow events usually last days to weeks, but the accumulated CH_4 in the upper layers might last even less time because of effective aerobic CH_4 oxidation (Steinle et al., 2017) and strong vertical mixing in winter. The occurrences of surface CH_4 accumulations at BE might be more frequent than have been observed.

4.3 Surface saturation and flux density

Surface CH_4 saturations are directly proportional to CH_4 concentrations in the surface water ($S_{CH_4} = 31.40 \times [CH_4] + 10.29$; $R^2 = 0.9794$, $n = 77$, $p < 0.0001$; Fig. 6a, b), despite the pronounced seasonal variations in temperature (Fig. 3). This indicates that the net CH_4 production at BE is overriding the temperature-driven variability in the CH_4 concentrations. Excluding the extreme value from December 2014, surface CH_4 saturations at BE varied between 129 % and 5563 %, with an average of 615 ± 688 %. The surface layer was supersaturated with CH_4 and thus emitting CH_4 to the atmosphere throughout the sampling period.

The coastal Baltic Sea, especially the southwestern part, is a hotspot for CH_4 emissions. Area-weighted mean CH_4 saturations for the entire Baltic Sea (113 % and 395 % in winter and summer 1992, respectively; Bange et al., 1994) were lower than at BE. Schmale et al. (2010) extensively investigated dissolved CH_4 distributions in the Baltic Sea and found that surface CH_4 supersaturations were stronger in the shallow western areas.

Sea-to-air CH_4 flux densities fluctuated between 0.3 and 746.3 µmol m^{-2} d^{-1}, with an average of 43.8 ± 88.7 µmol m^{-2} d^{-1} (excluding the extreme value in December 2014; Fig. 6c). Comparable results in saturation and flux density were observed at the pockmark sites in Eckernförde Bay (Bussmann and Suess, 1998). Although surface CH_4 saturations in this study are consistent with the previously published results by Bange et al. (2010; 554 ± 317 %), calculated CH_4 flux densities in this study are much higher than in Bange et al. (2010; 6.3–14.7 µmol m^{-2} d^{-1}). The discrepancy is derived from different flux calculation methods. Bange et al. (2010) adopted the equations by Raymond and Cole (2001) with a lower gas transfer velocity, and they used the median of surface CH_4 concentrations for computation, which eliminated the extreme values. Our results are in good agreement with the ones reported by Bange et al. (2010) if we adopt the same method.

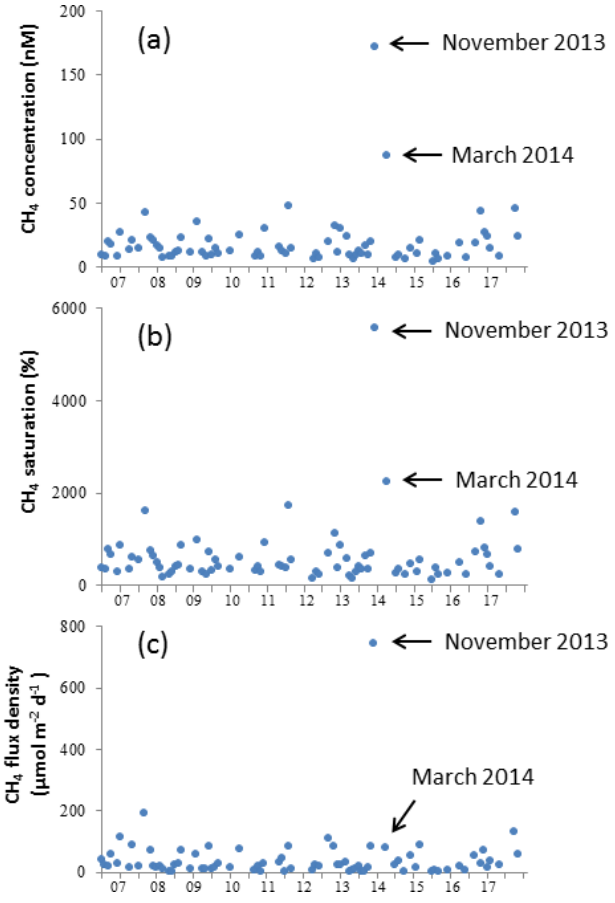

Figure 6. Inter-annual variations in dissolved CH_4 concentration **(a)**, saturation **(b)** and flux density **(c)** at BE during 2006–2017. Data collected from December 2014 are not shown.

CH_4 emissions from coastal waters could be roughly considered as the difference between the formation and oxidation of CH_4 in the water column and sediments. Although sediments are substantial CH_4 sources, most CH_4 is consumed before escaping to the atmosphere (Martens et al., 1999; Treude et al., 2005; Steinle et al., 2017). Treude et al. (2005) compared the potential and field rates of anaerobic oxidation of methane (AOM) in the sediments of Eckernförde Bay and suggested that the AOM-mediating organisms are capable of a fast response to changes in CH_4 supply. Steinle et al. (2017) reported that 70 %–95 % of dissolved CH_4 was effectively removed in the water column during summer stratification. Apart from the MBI-driven uplift of CH_4-enriched bottom water to the surface (see below), wind-

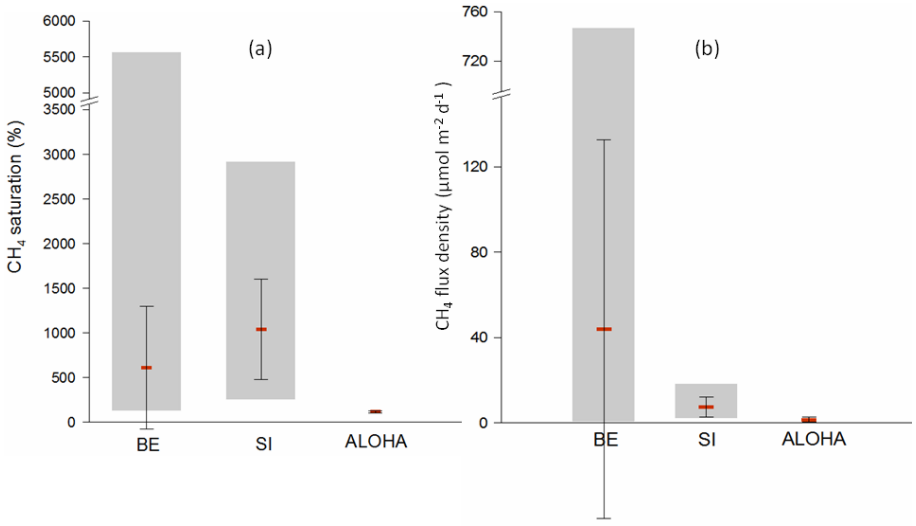

Figure 7. Comparison of surface CH_4 saturations **(a)** and flux densities **(b)** from time-series stations of BE, Saanich Inlet (SI) and ALOHA. For the computation of flux density, the equations of Nightingale et al. (2000) and Wanninkhof (2014) were used for SI and ALOHA, respectively. Data in December 2014 at the BE time series station were not included. Please note the break on the *y* axis for both charts.

driven upwelling events can lead to a ventilation of the accumulated CH_4 to the atmosphere. For example, Gülzow et al. (2013) observed elevated CH_4 concentrations in the Gotland Basin as a result of wind-induced upwelling. The influence of upwelling at BE, however, is more prominent due to the shallow water depth. In September 2012 and 2017, when upwelling occurred (see Sect. 4.1), sea-to-air CH_4 flux densities were 65.9 and 132.3 µmol m^{-2} d^{-1}, respectively, which were about 50 % and 200 % higher than the mean value.

Enhanced CH_4 saturations and associated emissions at BE were also strongly promoted by saline inflows (see Sect. 4.2). We found very high surface CH_4 saturation and flux density in November 2013 and December 2014 (Fig. 6). In December 2014, surface CH_4 saturations were as high as 19 770 % and the calculated flux density reached 3104.5 µmol m^{-2} d^{-1}. Inflows of saline waters usually occur in winter, when the well-ventilated water column, relatively low CH_4 oxidation rates and high wind speeds are all favorable for high CH_4 emissions (Wanninkhof, 2014; Steinle et al., 2017). Assuming that there was no continuous mixing or supply of CH_4 to the surface layer, it took about 3.3 d for the accumulated CH_4 to come back to equilibrium values under the calculated flux density, during which the annual CH_4 emissions from Eckernförde Bay increased by approximately 66 % in 2014. This is also in line with our speculation in Sect. 4.2 that the monthly sampling at BE might have missed some of the short-lived CH_4 pulses.

Moreover, methanogenesis in the sediments of Eckernförde Bay is sufficient for CH_4 bubble formation (Whiticar, 2002). Hydrostatic pressure fluctuations associated with saline water inflow could have triggered CH_4 seepage and gas bubble plumes from the seafloor to the atmosphere (Wever et al., 2006; Lohrberg et al., 2020). Gas ebullition sites were usually found accompanied by pockmark structures (Schneider von Deimling et al., 2011), and Jackson et al. (1998) provided sonar evidence for CH_4 ebullition in Eckernförde Bay. However, recently Lohrberg et al. (2020) reported a widespread CH_4 ebullition event in Eckernförde Bay and found no direct linkage between pockmarks and ebullitions. They estimated the bubble-driven CH_4 flux during a weak storm in the autumn of 2014 was 1916 µmol m^{-2} d^{-1}. These findings point to the fact that ebullition might be an important, but highly variable, additional CH_4 efflux to the atmosphere. However, our measurements did not capture gas bubbles, and, thus, the estimate of the overall CH_4 emissions resulting from the MBI might be too low. In this case, time-series monitoring of saline inflows and sea level variations, combined with continuous observation of CH_4 variability, especially in winter, are essential for quantifying CH_4 emissions from Eckernförde Bay.

4.4 Comparison with other time-series measurements

Besides this study, time-series measurements of CH_4 have also been reported from Saanich Inlet (SI), British Columbia, Canada (Capelle et al., 2019) and ALOHA station in the North Pacific Subtropical Gyre (Wilson et al., 2017).

Located in a seasonally anoxic fjord, the time-series station in SI has a similar hydrographic setting compared to BE but a deeper water depth (230 m; Capelle et al., 2019). Surface CH_4 saturations at SI fell in the lower end of the range observed here for BE (Fig. 7). Despite the fact that the mean surface saturation in SI was higher, CH_4 flux densities were much lower than at BE. Since the air–sea exchange approach of Nightingale et al. (2000) was used in both studies, the discrepancy results from the higher wind speeds at

BE. CH_4 saturations from ALOHA were only slightly supersaturated (close to the equilibrium saturation), and the flux densities were consequently low as well, which results from the fact that ALOHA is a deep-water ($\sim$ 4800 m) station located in the oligotrophic open ocean where potential strong CH_4 sources such as sedimentary release or methanogenesis under low O_2 in the water column are negligible (Wilson et al., 2017).

Wilson et al. (2017) analyzed the time-series CH_4 data from ALOHA during 2008–2016 and observed a decline in the surface CH_4 concentrations from 2013. They attributed the potential decrease in CH_4 production to fluctuations in phosphate concentrations. Capelle et al. (2019) also detected a significant decline in CH_4 concentrations in the upper water column over time at SI and proposed a link with the shoaling of the boundary of the hypoxic layer. However, no significant trend was detected in CH_4 concentrations or flux densities at BE (Fig. 6), despite the relatively long observation period. The different situations can be explained by the shallow water depth in Eckernförde Bay, which makes the CH_4 distribution sensitive to the variability in its sedimentary release and events such as MBI and wind-driven upwelling.

5 Conclusions

The CH_4 measurements at BE showed a strong temporal variability and variations with depths. A pronounced enhancement of the CH_4 concentrations was usually found in the bottom layer (15–25 m) during February, May–June and October, which indicates that the release from the sediments is the major source of CH_4. Organic matter and dissolved O_2 are usually considered as the main controlling factors in CH_4 production and consumption pathways, but we did not detect correlations of CH_4 with Chlorophyll *a* or O_2 during 2006–2017.

Obviously non-biological processes such as local wind-driven upwelling and the inflow of saline North Sea waters play a significant role in the observed variability in CH_4 at BE. However, these phenomena, which occur on relatively short timescales of day or weeks, were not frequently detected, most probably due to the monthly sampling frequency. The surface layer at BE was always supersaturated with CH_4, and therefore, BE was a persistent and strong, but highly variable, source of CH_4 to the atmosphere. We did not detect significant temporal trends in CH_4 concentrations or emissions, despite ongoing environmental changes (warming, deoxygenation) in Eckernförde Bay. Overall, the CH_4 variability at BE is driven by a complex interplay of various biological (i.e., methanogenesis, oxidation) and physical (i.e., upwelling, inflow events) processes. Continuous observations at BE, with an emphasis on the period when upwelling and saline inflow usually occur, is therefore of great importance for quantifying CH_4 variability and the associated emissions as well as for predicting future CH_4 variability in the SW Baltic Sea.

Data availability. Data are available from the Boknis Eck database at https://www.bokniseck.de//database-access (Bange and Malien, 2020) and the MEMENTO (MarinE MethanE and NiTrous Oxide) database at https://memento.geomar.de (Kock and Bange, 2015).

Author contributions. XM, MS, STL and HWB designed the study and participated in the fieldwork. CH_4 measurements and data processing were performed by XM, MS and STL. XM wrote the article with contributions from MS, STL and HWB.

Competing interests. The authors declare that they have no conflict of interest.

Acknowledgements. The authors thank the captains and crews of the RV *Littorina* and *Polarfuchs* as well as the many colleagues and numerous students who helped with the sampling and measurements of the BE time series through various projects. Special thanks go to Annette Kock for her help with sampling, measurements and data analysis. The time series at BE was supported by DWK Meeresforschung (1957–1975), HELCOM (1979–1995), BMBF (1995–1999), the Institut für Meereskunde (1999–2003), IfM-GEOMAR (2004–2011) and GEOMAR (2012–present). The current CH_4 measurements at BE are supported by the EU BONUS INTEGRAL project which receives funding from BONUS (Art 185), funded jointly by the EU, the German Federal Ministry of Education and Research, the Swedish Research Council Formas, the Academy of Finland, the Polish National Centre for Research and Development, and the Estonian Research Council. The Boknis Eck Time Series Station (https://www.bokniseck.de, last access: 2 July 2020) is run by the Chemical Oceanography Research Unit of GEOMAR, Helmholtz Centre for Ocean Research Kiel. The sea level data used in this study were made available by the EMODnet Physics project (https://www.emodnet-physics.eu/map, last access: 2 July 2020), funded by the European Commission Directorate-General for Maritime Affairs and Fisheries.

Financial support. This research has been supported by the China Scholarship Council (grant no. 201306330056) and the BONUS INTEGRAL project (grant no. 03F0773B).

The article processing charges for this open-access publication were covered by a Research Centre of the Helmholtz Association.

Review statement. This paper was edited by Gwenaël Abril and reviewed by two anonymous referees.

References

Ahmerkamp, S., Winter, C., Janssen, F., Kuypers, M. M., and Holtappels, M.: The impact of bedform migration on benthic oxygen fluxes, J. Geophys. Res.-Biogeo, 120, 2229–2242, https://doi.org/10.1002/2015JG003106, 2015.

Bange, H. W. and Malien, F.: Boknis Eck Time-series Database, Kiel Datamanagement Team, available at: https://www.bokniseck.de//database-access, last access: 23 March 2020.

Bange, H. W., Bartell, U. H., Rapsomanikis, S., and Andreae, M. O.: Methane in the Baltic and North Seas and a reassessment of the marine emissions of methane, Global Biogeochem. Cy., 8, 465–480, https://doi.org/10.1029/94GB02181, 1994.

Bange, H. W., Bergmann, K., Hansen, H. P., Kock, A., Koppe, R., Malien, F., and Ostrau, C.: Dissolved methane during hypoxic events at the Boknis Eck Time Series Station (Eckernförde Bay, SW Baltic Sea), Biogeosciences, 7, 1279–1284, https://doi.org/10.5194/bg-7-1279-2010, 2010.

Barnes, J., Ramesh, R., Purvaja, R., Nirmal Rajkumar, A., Senthil Kumar, B., Krithika, K., Ravichandran, K., Uher, G., and Upstill-Goddard, R.: Tidal dynamics and rainfall control N_2O and CH_4 emissions from a pristine mangrove creek, Geophys. Res. Lett., 33, L15405, https://doi.org/10.11029/12006GL026829, 2006.

Belkin, I. M.: Rapid warming of large marine ecosystems, Prog. Oceanogr., 81, 207–213, https://doi.org/10.1016/j.pocean.2009.04.011, 2009.

Bernard, B. B., Brooks, J. M., and Sackett, W. M.: Natural gas seepage in the Gulf of Mexico, Earth Planet Sc. Lett., 31, 48–54, 1976.

Borges, A. V., Champenois, W., Gypens, N., Delille, B., and Harlay, J.: Massive marine methane emissions from near-shore shallow coastal areas, Sci. Rep.-UK, 6, 27908, https://doi.org/10.1038/srep27908, 2016.

Bussmann, I. and Suess, E.: Groundwater seepage in Eckernförde Bay (Western Baltic Sea): Effect on methane and salinity distribution of the water column, Cont. Shelf Res., 18, 1795–1806, https://doi.org/10.1016/S0278-4343(98)00058-2, 1998.

Capelle, D. W., Hallam, S. J., and Tortell, P. D.: Time-series CH_4 measurements from Saanich Inlet, BC, a seasonally anoxic fjord, Mar. Chem., 215, 103664, https://doi.org/10.1016/j.marchem.2019.103664, 2019.

Carstensen, J., Andersen, J. H., Gustafsson, B. G., and Conley, D. J.: Deoxygenation of the Baltic Sea during the last century, P. Natl. Acad. Sci. USA, 111, 5628–5633, https://doi.org/10.1073/pnas.1323156111, 2014.

Conley, D. J., Carstensen, J., Aigars, J., Axe, P., Bonsdorff, E., Eremina, T., and Lannegren, C.: Hypoxia is increasing in the coastal zone of the Baltic Sea, Environ. Sci. Technol., 45, 6777–6783, https://doi.org/10.1021/es201212r, 2011.

Dale, A. W., Flury, S., Fossing, H., Regnier, P., Røy, H., Scholze, C., and Jørgensen, B. B.: Kinetics of organic carbon mineralization and methane formation in marine sediments (Aarhus Bay, Denmark), Geochim. Cosmochim. Ac., 252, 159–178, https://doi.org/10.1016/j.gca.2019.02.033, 2019.

David, H. A.: Further applications of range to analysis of variance, Biometrika, 38, 393–409, 1951.

Egger, M., Riedinger, N., Mogollon, J. M., and Jørgensen, B. B.: Global diffusive fluxes of methane in marine sediments, Nat. Geosci., 11, 421–425, https://doi.org/10.1038/s41561-018-0122-8, 2018.

Fleming-Lehtinen, V. and Laamanen, M.: Long-term changes in Secchi depth and the role of phytoplankton in explaining light attenuation in the Baltic Sea, Estuar. Coast Shelf S., 102, 1–10, https://doi.org/10.1016/j.ecss.2012.02.015, 2012.

Grasshoff, K., Kremling, K., and Ehrhardt, M.: Methods of seawater analysis, 3rd edition, WILEY-VCH, Weihheim, Germany, 1999.

Gülzow, W., Rehder, G., Schneider von Deimling, J., Seifert, S., and Tóth, Z.: One year of continuous measurements constraining methane emissions from the Baltic Sea to the atmosphere using a ship of opportunity, Biogeosciences, 10, 81–99, https://doi.org/10.5194/bg-10-81-2013, 2013.

Hansen, H. P., Giesenhagen, H. C., and Behrends, G.: Seasonal and long-term control of bottom water oxygen deficiency in a stratified shallow-coastal system, ICES J. Mar. Sci., 56, 65–71, https://doi.org/10.1006/jmsc.1999.0629, 1999.

HELCOM: State of the Baltic Sea – Second HELCOM holistic assessment 2011–2016, Baltic Sea Environ. Proc., 1–155, 2018.

Hovland, M., Judd, A. G., and Burke Jr., R. A.: The global flux of methane from shallow submarine sediments, Chemosphere, 26, 559–578, https://doi.org/10.1016/0045-6535(93)90442-8, 1993.

Hsu, S. A., Meindl, E. A., and Gilhousen, D. B.: Determining the power-law wind-profile exponent under near-neutral stability conditions at sea, J. Appl. Meteorol., 33, 757–765, https://doi.org/10.1175/1520-0450(1994)033<0757:DTPLWP>2.0.CO;2, 1994.

IPCC: Climate Change 2013: The physical science basis. Contribution of Working Group I to the fifth assessment report of the Intergovernmental Panel on Climate Change, Cambridge University Press, Cambridge, UK and New York, NY, 2013.

Jackson, D. R., Williams, K. L., Wever, T. F., Friedrichs, C. T., and Wright, L. D.: Sonar evidence for methane ebullition in Eckernförde Bay, Cont. Shelf Res., 18, 1893–1915, https://doi.org/10.1016/S0278-4343(98)00062-4, 1998.

Jähne, B., Heinz, G., and Dietrich, W.: Measurements of the diffusion coefficients of sparingly soluble gases in water, J. Geophys. Res.-Ocean., 92, 10767–10776, https://doi.org/10.1029/JC092iC10p10767, 1987.

Judd, A. G., Hovland, M., Dimitrov, L. I., Garcia Gil, S., and Jukes, V.: The geological methane budget at continental margins and its influence on climate change, Geofluids, 2, 109–126, https://doi.org/10.1046/j.1468-8123.2002.00027.x, 2002.

Klintzsch, T., Langer, G., Nehrke, G., Wieland, A., Lenhart, K., and Keppler, F.: Methane production by three widespread marine phytoplankton species: release rates, precursor compounds, and potential relevance for the environment, Biogeosciences, 16, 4129–4144, https://doi.org/10.5194/bg-16-4129-2019, 2019.

Kock, A. and Bange, H. W.: Counting the ocean's greenhouse gas emissions, Eos, 96, 10–13, https://doi.org/10.1029/2015EO023665, 2015.

Lenhart, K., Klintzsch, T., Langer, G., Nehrke, G., Bunge, M., Schnell, S., and Keppler, F.: Evidence for methane production by the marine algae Emiliania huxleyi, Biogeosciences, 13, 3163–3174, https://doi.org/10.5194/bg-13-3163-2016, 2016.

Lennartz, S. T., Lehmann, A., Herrford, J., Malien, F., Hansen, H. P., Biester, H., and Bange, H. W.: Long-term trends at the Boknis Eck time-series station (Baltic Sea), 1957–2013: does climate change counteract the decline in eutrophication?,

Biogeosciences, 11, 6323–6339, https://doi.org/10.5194/bg-11-6323-2014, 2014.

Levipan, H. A., Quiñones, R. A., Johansson, H. E., and Urrutia, H.: Methylotrophic methanogens in the water column of an upwelling zone with a strong oxygen gradient off central Chile, Microbes Environ., 22, 268–278, 2007.

Lohrberg, A., Schmale, O., Ostrovsky, I., Niemann, H., Held, P., and Schneider von Deimling, J.: Discovery and quantification of a widespread methane ebullition event in a coastal inlet (Baltic Sea) using a novel sonar strategy, Sci. Rep.-UK, 10, 4393, https://doi.org/10.1038/s41598-020-60283-0, 2020.

Maher, D. T., Cowley, K., Santos, I. R., Macklin, P., and Eyre, B. D.: Methane and carbon dioxide dynamics in a subtropical estuary over a diel cycle: Insights from automated in situ radioactive and stable isotope measurements, Mar. Chem., 168, 69–79, https://doi.org/10.1016/j.marchem.2014.10.017, 2015.

Maltby, J., Steinle, L., Löscher, C. R., Bange, H. W., Fischer, M. A., Schmidt, M., and Treude, T.: Microbial methanogenesis in the sulfate-reducing zone of sediments in the Eckernförde Bay, SW Baltic Sea, Biogeosciences, 15, 137–157, https://doi.org/10.5194/bg-15-137-2018, 2018.

Martens, C. S., Albert, D. B., and Alperin, M. J.: Stable isotope tracing of anaerobic methane oxidation in the gassy sediments of Eckernförde Bay, German Baltic Sea, Am. J. Sci., 299, 589–610, 1999.

Mohrholz, V., Naumann, M., Nausch, G., Krüger, S., and Gräwe, U.: Fresh oxygen for the Baltic Sea-An exceptional saline inflow after a decade of stagnation, J. Marine Syst., 148, 152–166, https://doi.org/10.1016/j.jmarsys.2015.03.005, 2015.

Naqvi, S. W. A., Bange, H. W., Farías, L., Monteiro, P. M. S., Scranton, M. I., and Zhang, J.: Marine hypoxia/anoxia as a source of CH_4 and N_2O, Biogeosciences, 7, 2159–2190, https://doi.org/10.5194/bg-7-2159-2010, 2010.

Nausch, G., Naumann, M., Umlauf, L., Mohrholz, V., and Siegel, H.: Hydrographisch-hydrochemische Zustandseinschätzung der Ostsee 2013, Leibniz-Institut für Ostseeforschung Warnemünde, Germany, 2014.

Nightingale, P. D., Malin, G., Law, C. S., Watson, A. J., Liss, P. S., Liddicoat, M. I., Boutin, J., and Upstill-Goddard, R. C.: In situ evaluation of air-sea gas exchange parameterizations using novel conservative and volatile tracers, Global Biogeochem. Cy., 14, 373–387, https://doi.org/10.1029/1999GB900091, 2000.

Nittrouer, C. A., Lopez, G. R., Wright, L. D., Bentley, S. J., D'Andrea, A. F., Friedrichs, C. T., Craig, N. I., and Sommerfield, C. K.: Oceanographic processes and the preservation of sedimentary structure in Eckernförde Bay, Baltic Sea. Cont. Shelf Res., 18, 1689–1714, https://doi.org/10.1016/S0278-4343(98)00054-5, 1998.

Orsi, T. H., Werner, F., Milkert, D., Anderson, A. L., and Bryant, W. R.: Environmental overview of Eckernförde bay, northern Germany, Geo-Mar. Lett., 16, 140–147, 1996.

Pimenov, N. V., Ul'yanova, M. O., Kanapatskii, T. A., Mitskevich, I. N., Rusanov, I. I., Sigalevich, P. A., Nemirovskaya, I. A., and Sivkov, V. V.: Sulfate reduction, methanogenesis, and methane oxidation in the upper sediments of the Vistula and Curonian Lagoons, Baltic Sea, Microbiology, 82, 224–233, https://doi.org/10.1134/S0026261713020136, 2013.

Raymond, P. A. and Cole, J. J.: Gas exchange in rivers and estuaries: Choosing a gas transfer velocity, Estuaries, 24, 312–317, https://doi.org/10.2307/1352954, 2001.

Reeburgh, W. S.: Oceanic methane biogeochemistry, Chem. Rev., 107, 486–513, https://doi.org/10.1021/cr050362v, 2007.

Rehder, G., Keir, R. S., Suess, E., and Pohlmann, T.: The multiple sources and patterns of methane in North Sea waters, Aquat. Geochem., 4, 403–427, https://doi.org/10.1023/A:1009644600833, 1998.

Reindl, A. R., and Bolałek, J.: Methane flux from sediment into near-bottom water in the coastal area of the Puck Bay (Southern Baltic), Oceanol. Hydrobiol. St., 41, 40–47, https://doi.org/10.2478/s13545-012-0026-y, 2012.

Sandén, P. and Håkansson, B.: Long-term trends in Secchi depth in the Baltic Sea, Limnol. Oceanogr., 41, 346–351, https://doi.org/10.4319/lo.1996.41.2.0346, 1996.

Saunois, M., Bousquet, P., Poulter, B., Peregon, A., Ciais, P., Canadell, J. G., Dlugokencky, E. J., Etiope, G., Bastviken, D., Houweling, S., Janssens-Maenhout, G., Tubiello, F. N., Castaldi, S., Jackson, R. B., Alexe, M., Arora, V. K., Beerling, D. J., Bergamaschi, P., Blake, D. R., Brailsford, G., Brovkin, V., Bruhwiler, L., Crevoisier, C., Crill, P., Covey, K., Curry, C., Frankenberg, C., Gedney, N., Hoglund-Isaksson, L., Ishizawa, M., Ito, A., Joos, F., Kim, H. S., Kleinen, T., Krummel, P., Lamarque, J. F., Langenfelds, R., Locatelli, R., Machida, T., Maksyutov, S., McDonald, K. C., Marshall, J., Melton, J. R., Morino, I., Naik, V., O'Doherty, S., Parmentier, F. J. W., Patra, P. K., Peng, C. H., Peng, S. S., Peters, G. P., Pison, I., Prigent, C., Prinn, R., Ramonet, M., Riley, W. J., Saito, M., Santini, M., Schroeder, R., Simpson, I. J., Spahni, R., Steele, P., Takizawa, A., Thornton, B. F., Tian, H. Q., Tohjima, Y., Viovy, N., Voulgarakis, A., van Weele, M., van der Werf, G. R., Weiss, R., Wiedinmyer, C., Wilton, D. J., Wiltshire, A., Worthy, D., Wunch, D., Xu, X. Y., Yoshida, Y., Zhang, B. W., Zhang, Z., and Zhu, Q.: The global methane budget 2000–2012, Earth Syst. Sci. Data, 8, 697–751, https://doi.org/10.5194/essd-8-697-2016, 2016.

Schmale, O., Schneider von Deimling, J., Gülzow, W., Nausch, G., Waniek, J. J., and Rehder, G.: Distribution of methane in the water column of the Baltic Sea, Geophys. Res. Lett., 37, L12604, https://doi.org/10.1029/2010GL043115, 2010.

Schmaljohann, R.: Methane dynamics in the sediment and water column of Kiel Harbour (Baltic Sea), Mar. Ecol. Prog. Ser., 131, 263–273, https://doi.org/10.3354/meps131263, 1996.

Schneider von Deimling, J., Gülzow, W., Ulyanova, M., Klusek, Z., and Rehder, G.: Detection and monitoring of methane ebullition, BONUS-Baltic GAS Final report WP 3.3, 1–11, 2011.

Scranton, M. I. and Farrington, J. W.: Methane production in the waters off Walvis Bay, J. Geophys. Res., 82, 4947–4953, https://doi.org/10.1029/JC082i031p04947, 1977.

Siedler, G. and Peters, H.: Properties of sea water: physical properties, in: Oceanography, edited by: Sündermann, J., Springer, Berlin, Germany, 233–264, 1986.

Smetacek, V.: The annual cycle of Kiel Bight plankton: A long-term analysis, Estuaries, 8, 145–157, 1985.

Smetacek, V., von Bodungen, B., von Bröckel, K., Knoppers, B., Martens, P., Peinert, R., Pollehne, F., Stegmann, P., and Zeitzschel, B.: Seasonality of plankton growth and sedimentation, in: Seawater-Sediment Interactions in Coastal Waters,

edited by: Rumohr, J., Walger, E., and Zeitzschel, B., Springer, Berlin, Germany, 34–56, 1987.

Steinle, L., Maltby, J., Treude, T., Kock, A., Bange, H. W., Engbersen, N., Zopfi, J., Lehmann, M. F., and Niemann, H.: Effects of low oxygen concentrations on aerobic methane oxidation in seasonally hypoxic coastal waters, Biogeosciences, 14, 1631–1645, https://doi.org/10.5194/bg-14-1631-2017, 2017.

Sturm, K., Werner, U., Grinham, A., and Yuan, Z.: Tidal variability in methane and nitrous oxide emissions along a subtropical estuarine gradient, Estuar. Coast Shelf S., 192, 159–169, https://doi.org/10.1016/j.ecss.2017.04.027, 2017.

Treude, T., Krüger, M., Boetius, A., and Jørgensen, B. B.: Environmental control on anaerobic oxidation of methane in the gassy sediments of Eckernförde Bay (German Baltic), Limnol. Oceanogr., 50, 1771–1786, https://doi.org/10.4319/lo.2005.50.6.1771, 2005.

Upstill-Goddard, R. C., Barnes, J., Frost, T., Punshon, S., and Owens, N. J.: Methane in the southern North Sea: Low-salinity inputs, estuarine removal, and atmospheric flux, Global Biogeochem. Cy., 14, 1205–1217, https://doi.org/10.1029/1999GB001236, 2000.

Wanninkhof, R.: Relationship between wind speed and gas exchange over the ocean revisited, Limnol. Oceanogr.-Method., 12, 351–362, https://doi.org/10.4319/lom.2014.12.351, 2014.

Weber, T., Wiseman, N. A., and Kock, A.: Global ocean methane emissions dominated by shallow coastal waters, Nat. Commun., 10, 4584, https://doi.org/10.1038/s41467-019-12541-7, 2019.

Wever, T. F., Lühder, R., Voß, H., and Knispel, U.: Potential environmental control of free shallow gas in the seafloor of Eckernförde Bay, Germany, Mar. Geol., 225, 1–4, https://doi.org/10.1016/j.margeo.2005.08.005, 2006.

Whiticar, M. J.: Diagenetic relationships of methanogenesis, nutrients, acoustic turbidity, pockmarks and freshwater seepages in Eckernförde Bay, Mar. Geol., 182, 29–53, https://doi.org/10.1016/S0025-3227(01)00227-4, 2002.

Wiesenburg, D. A. and Guinasso Jr., N. L.: Equilibrium solubilities of methane, carbon monoxide, and hydrogen in water and sea water, J. Chem. Eng. Data, 24, 356–360, 1979.

Wilson, S. T., Ferrón, S., and Karl, D. M.: Interannual variability of methane and nitrous oxide in the North Pacific Subtropical Gyre, Geophys. Res. Lett., 44, 9885–9892, https://doi.org/10.1002/2017GL074458, 2017.

WMO: Scientific assessment of ozone depletion: 2018, World Meteorological Organization, Geneva, Switzerland, Global Ozone Research and Monitoring Project–Report No. 58, 588 pp., 2018.

Xiao, K. Q., Beulig, F., Roy, H., Jørgensen, B. B., and Risgaard-Petersen, N.: Methylotrophic methanogenesis fuels cryptic methane cycling in marine surface sediment, Limnol. Oceanogr., 63, 1519–1527, https://doi.org/10.1002/lno.10788, 2018.

Chapter 3

A multi-year observation of nitrous oxide at the Boknis Eck Time Series Station in the Eckernförde Bay (southwestern Baltic Sea)

Biogeosciences, 16, 4097–4111, 2019
https://doi.org/10.5194/bg-16-4097-2019

Biogeosciences
Open Access
EGU

A multi-year observation of nitrous oxide at the Boknis Eck Time Series Station in the Eckernförde Bay (southwestern Baltic Sea)

Xiao Ma[1], **Sinikka T. Lennartz**[1,a], **and Hermann W. Bange**[1]

[1]GEOMAR Helmholtz Centre for Ocean Research Kiel, Düsternbrooker Weg 20, 24105 Kiel, Germany
[a]now at: ICBM, University of Oldenburg, Oldenburg, Germany

Correspondence: Xiao Ma (mxiao@geomar.de)

Received: 30 April 2019 – Discussion started: 23 May 2019
Revised: 19 September 2019 – Accepted: 26 September 2019 – Published: 25 October 2019

Abstract. Nitrous oxide (N_2O) is a potent greenhouse gas, and it is involved in stratospheric ozone depletion. Its oceanic production is mainly influenced by dissolved nutrient and oxygen (O_2) concentrations in the water column. Here we examined the seasonal and annual variations in dissolved N_2O at the Boknis Eck (BE) Time Series Station located in Eckernförde Bay (southwestern Baltic Sea). Monthly measurements of N_2O started in July 2005. We found a pronounced seasonal pattern for N_2O with high concentrations (supersaturations) in winter and early spring and low concentrations (undersaturations) in autumn when hypoxic or anoxic conditions prevail. Unusually low N_2O concentrations were observed during October 2016–April 2017, which was presumably a result of prolonged anoxia and the subsequent nutrient deficiency. Unusually high N_2O concentrations were found in November 2017 and this event was linked to the occurrence of upwelling which interrupted N_2O consumption via denitrification and potentially promoted ammonium oxidation (nitrification) at the oxic–anoxic interface. Nutrient concentrations (such as nitrate, nitrite and phosphate) at BE have been decreasing since the 1980s, but oxygen concentrations in the water column are still decreasing. Our results indicate a close coupling of N_2O anomalies to O_2 concentration, nutrients, and stratification. Given the long-term trends of declining nutrient and oxygen concentrations at BE, a decrease in N_2O concentration, and thus emissions, seems likely due to an increasing number of events with low N_2O concentrations.

1 Introduction

Long-term observation with regular measurement intervals can be an effective way to monitor seasonal and inter-annual variabilities as well as to decipher short- and long-term trends of an ecosystem, which are required to make projections of the future ecosystem development (e.g. see Ducklow et al., 2009). Recently, multi-year time series measurements of nitrous oxide (N_2O), a potent greenhouse gas and a major threat to ozone depletion (IPCC, 2013; Ravishankara et al., 2009), have been reported from the coastal upwelling areas off central Chile (Farías et al., 2015), off Goa (Naqvi et al., 2010), in the North Pacific Subtropical Gyre (Wilson et al., 2017), and in Saanich Inlet (Capelle et al., 2018).

N_2O production in the ocean is generally dominated by microbial nitrification ($NH_4^+ \rightarrow NO_2^- \rightarrow NO_3^-$) and denitrification ($NO_3^- \rightarrow NO_2^- \rightarrow N_2O \rightarrow N_2$). During bacterial or archaeal nitrification, N_2O is produced as a by-product with enhanced N_2O production under low-oxygen (O_2) conditions (e.g. Goreau et al., 1980; Löscher et al., 2012). N_2O is produced as an intermediate during bacterial denitrification (Codispoti et al., 2005). N_2O could be further consumed via denitrification to dinitrogen; however, this process is inhibited with the presence of O_2 because of the low O_2 tolerance of the enzyme involved (Bonin et al., 1989). This incomplete pathway is called partial denitrification and can lead to N_2O accumulation (e.g. Naqvi et al., 2000; Farías et al., 2009).

The oceans including coastal areas contribute $\sim 25\,\%$ of the natural and anthropogenic N_2O emissions (IPCC, 2013), with disproportionately high emissions from coastal and estuarine areas (Bange, 2006). N_2O emissions from coastal

areas strongly depend on nitrogen inputs (Seitzinger and Kroeze, 1998; Zhang et al., 2010). The increasing input of nitrogen (i.e. eutrophication) has become a worldwide problem in coastal waters leading to enhanced productivity and severe O_2 depletion caused by enhanced degradation of organic matter (Breitburg et al., 2018; Rabalais et al., 2014). The decline in O_2 concentration (i.e. deoxygenation), either in coastal waters or the open ocean, might result in favourable conditions for N_2O production (Codispoti et al., 2001; Nevison et al., 2003). The results of a model study by Kroeze and Seitzinger (1998) indicated a significant increase in N_2O in European coastal waters for 2050. Moreover, it has been suggested that N_2O production and emissions are very likely to increase in the near future, especially in the shallow suboxic or anoxic coastal systems (Naqvi et al., 2000; Bange, 2006). However, model projections show a net decrease in future global oceanic N_2O emission during the 21st century (Martinez-Rey et al., 2015; Landolfi et al., 2017; Battaglia and Joos, 2018).

The Baltic Sea is a nearly enclosed, marginal sea with a very limited access to the open ocean via the North Sea. The restricted water exchange with the North Sea and extensive human activities, such as agriculture, industrial production, and sewage discharge in the catchment area led to high inputs of nutrients to the Baltic Sea. As a result, the areas affected by anoxia have been expanding in the deep basins of the central Baltic Sea (Carstensen et al., 2014). In order to control this situation, the Helsinki Commission (HELCOM) was established in 1974 and a series of measures have been taken to prevent anthropogenic nutrient input into the Baltic Sea. Consequently, the nutrient inputs (by riverine loads, direct point sources, and, for nitrogen, atmospheric deposition) to the Baltic Sea are declining (HELCOM, 2018a). However, the number of low-O_2 (i.e. hypoxic or anoxic) events in coastal waters of the Baltic Sea is increasing and deoxygenation is still going on (Conley et al., 2011; Lennartz et al., 2014). The deoxygenation in the Baltic Sea can affect the production and consumption of N_2O. Our group has been monitoring dissolved N_2O concentrations at the Boknis Eck Time Series Station, located in Eckernförde Bay (southwestern Baltic Sea), for more than a decade. In this study, we present monthly measurements of N_2O and biogeochemical parameters such as nutrients and O_2 from July 2005 to December 2017. The major objectives of our study were: (1) to decipher the seasonal pattern of N_2O distribution in the water column, (2) to identify short-term and long-term trends of the N_2O concentrations, (3) to explore the potential role of nutrients and O_2 for N_2O production and consumption, and (4) to quantify the sea-to-air N_2O flux density at the time series station.

2 Material and methods

2.1 Study site

Sampling at the Boknis Eck (BE) Time Series Station (https://www.bokniseck.de) started on 30 April 1957 and, therefore, it is one of the oldest continuously operated time series stations in the world. The BE station is located at the entrance of Eckernförde Bay (54°31′ N, 10°02′ E; Fig. 1) in the southwestern Baltic Sea. The water depth of the sampling site is 28 m. Various physical, chemical, and biological parameters are measured on a monthly basis (Lennartz et al., 2014). There is no significant river runoff to Eckernförde Bay. Hence, the hydrographical conditions are mainly dominated by saline water input from the North Sea and less saline water from the Baltic Proper, which is typical for that region. Seasonal stratification usually starts to develop in April and lasts until October, during which hypoxia or even anoxia (characterized by the presence of hydrogen sulfide, H_2S) sporadically occurs, as a result of restricted vertical water exchange and bacterial decomposition of organic matter in the bottom water (Hansen et al., 1999; Lennartz et al., 2014). Thus, BE is a natural laboratory to study the influence of O_2 variations and anthropogenic nutrient loads on N_2O production and consumption.

2.2 Sample collection and measurement

Monthly sampling of N_2O at the BE Time Series Station started in July 2005. Triplicate samples were collected from six depths (1, 5, 10, 15, 20, and 25 m). Seawater was drawn from 5 L Niskin bottles into 20 mL brown glass vials after overflow. The vials were sealed with rubber stoppers and aluminium caps. The bubble-free samples were poisoned with 50 µL of a saturated mercury chloride ($HgCl_2$) solution and then stored in a cool, dark place until measurement. The general storage time before measurements of the N_2O concentrations was less than 3 months.

The static headspace equilibrium method was adopted to measure the dissolved N_2O concentrations in the vials. A 10 mL helium (99.9999 %, AirLiquide, Düsseldorf, Germany) headspace was created in each vial with a gas-tight glass syringe (VICI Precision Sampling, Baton Rouge, LA, USA). Samples were vibrated with a vortex (G-560E, Scientific Industries Inc., NY, USA) for 20 s and then left for at least 2 h until equilibrium. A 9.5 mL subsample of the headspace was subsequently injected into a GC-ECD (gas chromatograph equipped with an electron capture detector) system (Hewlett-Packard 5890 Series II, Agilent Technologies, Santa Clara, CA, USA), which was calibrated with two standard gas mixtures (N_2O in synthetic air, 320 and 1000 ppb, Deuste Steininger GmbH, Mühlhausen, Germany and Westfalen AG, Münster, Germany) prior to the measurement. The average precision of the measurements, calculated as the median standard deviation from triplicate measure-

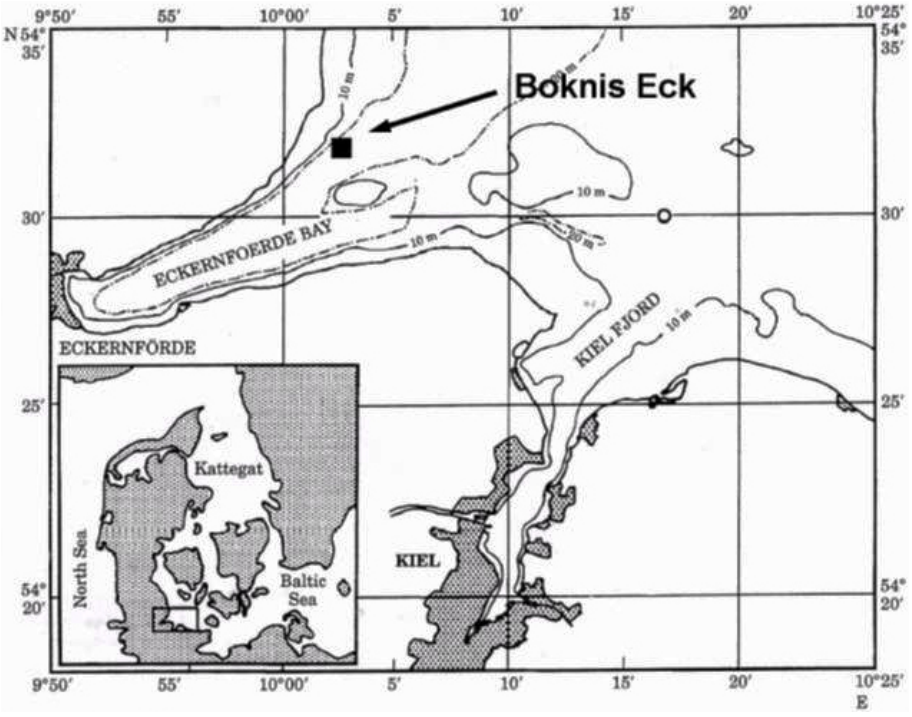

Figure 1. Location of the Boknis Eck Time Series Station in the Eckernförde Bay, southwestern Baltic Sea. (Map from Hansen et al., 1999.)

ments, was 0.4 nM. Triplicates with a standard deviation of > 10 % were omitted. More details about the N_2O measurement can be found in Kock et al. (2016). Dissolved oxygen (O_2) concentrations were measured by Winkler titrations (Grasshoff et al., 1999). Nutrient concentrations were measured by segmented continuous-flow analysis (SCFA; Grasshoff et al., 1999). A more detailed summary of the parameters measured and methods applied can be found in Lennartz et al. (2014).

2.3 Times series analysis

A time series can be decomposed into three main components, i.e. trend, cycle, and residual component (Schlittgen and Streitberg, 2001). We used the Mann–Kendall test and wavelet analysis to detect the trend and periodical cycles in the time series data, respectively. As for the residual component, we highlight unusual high or low N_2O concentrations during 2005–2017 and discuss the potential causes for these events.

2.3.1 Wavelet analysis

In order to decipher periodical cycles of the parameters collected at the BE Time Series Station, a wavelet analysis method was adopted. Wavelet analysis enables the detection of the period and the temporal occurrence of repeated cycles in time series data. One of the requirements for wavelet analysis is a regular, continuous time series. Since there are data missing (maximum 2 months in a row) in the BE time series, due to terrible weather or the ship's unavailability, missing data were interpolated from the previous and following months. Sampling time varied for every month (usually 20–40 d interval) but for the statistical analysis data were assumed to be regularly spaced as the uncertainty introduced was not significant (< 5 %). Considering the band width in both frequency and time domain, a Morlet mother wavelet with a wave number of 6 was chosen (Torrence and Compo, 1998). The mother wavelet was then scaled between the frequency of a half-year cycle and the length of the time series with a step size of 0.25. The wavelet analysis was conducted with the MATLAB code by Torrence and Compo (2004). More information about the method can be found on the website http://paos.colorado.edu/research/wavelets/ (last access: 23 October 2019).

2.3.2 Mann–Kendall test

Mann–Kendall test (MKT) is a non-parametric statistical test to assess the significance of monotonic trends for time series measurements. It tests the null hypothesis that all variables are randomly distributed against the alternative hypothesis that a monotonic trend, either increase or decrease, exists in the time series on a given significance level α (here $\alpha = 0.05$). MKT is flexible for data with missing values and the results are not impacted by the magnitude of extreme values, which makes it a widely used test in hydrology and climatology (e.g. Xu et al., 2003; Yang et al., 2004). How-

ever, MKT is sensitive to serial correlation in the time series. The presence of positive serial correlation would increase the probability of trend detection even though no such trend exists (Kulkarni and von Storch, 1995). In order to avoid this situation, data from 12 months were tested individually. It is assumed that there is no residual effect left from the same month last year, considering that the nitrogen species are rapidly biologically cycled. The MATLAB function from Simone (2009) was used for the MKT.

2.4 Calculation of saturation and sea-to-air flux density

N_2O saturations (S_{N_2O}, %) were calculated as

$$S_{N_2O} = 100 \times N_2O_{obs}/N_2O\,eq., \quad (1)$$

where N_2O_{obs} and N_2O eq. (nM) are the observed and equilibrated N_2O concentrations in seawater, respectively. N_2O eq. was computed as a function of surface seawater temperature, in situ salinity (Weiss and Price, 1980), and the dry mole fractions of atmospheric N_2O at the time of the sampling. Since the atmospheric N_2O mole fractions were not measured at the BE Time Series Station, atmospheric dry mole fractions of N_2O were derived from the monthly average of N_2O data at Mace Head, Ireland, instead (AGAGE, Advanced Global Atmospheric Gases Experiment, http://agage.mit.edu/, last access: 23 October 2019).

N_2O flux density (F_{N_2O}, μmol m^{-2} d^{-1}) was calculated as

$$F_{N_2O} = k_{N_2O} \times (N_2O_{obs} - N_2O\,eq.), \quad (2)$$

where k_{N_2O} (cm h^{-1}) is the gas transfer velocity calculated with the method given by Nightingale et al. (2000), as a function of the wind speed and the Schmidt number (Sc). The wind speed data were obtained from Kiel lighthouse (see https://www.geomar.de/service/wetter/, last access: 23 October 2019), which is approximately 20 km away from the BE Time Series Station. The wind speed was normalized to 10 m (u_{10}) to calculate k_{N_2O} (Hsu et al., 1994). k_{N_2O} was adjusted by multiplying with $(Sc/600)^{-0.5}$, and Sc was computed as

$$Sc = v/D_{N_2O}, \quad (3)$$

$$D_{N_2O} = 3.16 \times 10^{-6} e^{-18370/RT}, \quad (4)$$

where v is the kinematic viscosity of seawater, which is calculated from the empirical equations given in Siedler and Peters (1986), and D_{N_2O} is the diffusion coefficient of N_2O in seawater. R is the universal gas constant and T is the water temperature in kelvin.

3 Result and discussion

3.1 Overview

N_2O concentrations at the BE Time Series Station showed significant temporal and depth-dependent variations from 2005 to 2017 (Fig. 2). N_2O concentrations fluctuated between 1.2 and 37.8 nM, with an overall average of 13.9 ± 4.2 nM. This value was higher than the results from the surface water of Station ALOHA (5.9–7.4 nmol kg^{-1}, average 6.5±0.3 nmol kg^{-1}; Wilson et al., 2017), which is reasonable considering the weak anthropogenic impact in the North Pacific Subtropical Gyre. The N_2O concentrations at BE were much lower than those measured at the time series station in the coastal upwelling area off Chile (2.9–492 nM, average 39.4±29.2 nM in the oxyclines and 37.6±23.3 nM in the bottom waters; Farías et al., 2015) and a quasi-time-series station off Goa (Naqvi et al., 2010), where significant N_2O accumulations are observed in subsurface waters at both locations. Our measurements were comparable to the time series station from Saanich Inlet (∼ 0.5–37.4 nM, average 14.7 nM; Capelle et al., 2018), a seasonally anoxic fjord which has similar hydrographic conditions as BE.

NO_2^- concentrations fluctuated between below the detection limit of 0.1 and 1.6 μM, with an average of 0.2 ± 0.3 μM. NO_3^- concentrations varied from below the detection limit of 0.3 to 17.9 μM, with an average of 2.0 ± 2.8 μM. The temporal and spatial distributions of nitrite (NO_2^-) and nitrate (NO_3^-) were similar during 2005–2017. A clear O_2 seasonality can be seen with severe O_2 depletion in the bottom waters during summer and autumn. Anoxia with the presence of H_2S were detected in September and October 2005, September 2007, September and October 2014, and September–November 2016. All of the extremely low N_2O concentrations (< 5 nM) were observed in the bottom waters in autumn, coinciding with hypoxia or anoxia, while the high N_2O concentrations (> 20 nM) sporadically occurred at different depths either in spring or autumn.

3.2 Seasonal cycle

Significant cycles at different frequencies were detected via wavelet analysis at the BE Time Series Station during 2005–2017 (Fig. 3). A half-year NO_2^- cycle sporadically occurred in 2007–2009, 2013, and 2015. There is a seasonal NO_2^- variability (at the frequency of 1 year) between 2007 and 2016 (times before 2007 and after 2016 were outside the conic line), except during 2010–2012, when high NO_2^- concentrations were not observed in winter (Fig. 2). A biennial cycle of NO_2^- could be observed as well during 2008–2015. The NO_3^- concentrations were dominated by an annual cycle and a minor half-year cycle. The biennial cycle only occurred in 2008 and 2009. A remarkable seasonal variability in dissolved O_2 prevailed all the time, which is also obvious from the time series data shown in Fig. 2. The annual N_2O cycle became gradually more and more evident until 2014, then declined and reoccurred less intensely in 2016. The periodical cycle was also present at other frequencies, indicated by the broadening of the red area before 2015 in Fig. 2d. For example, a biennial N_2O cycle occurred during 2013–2015.

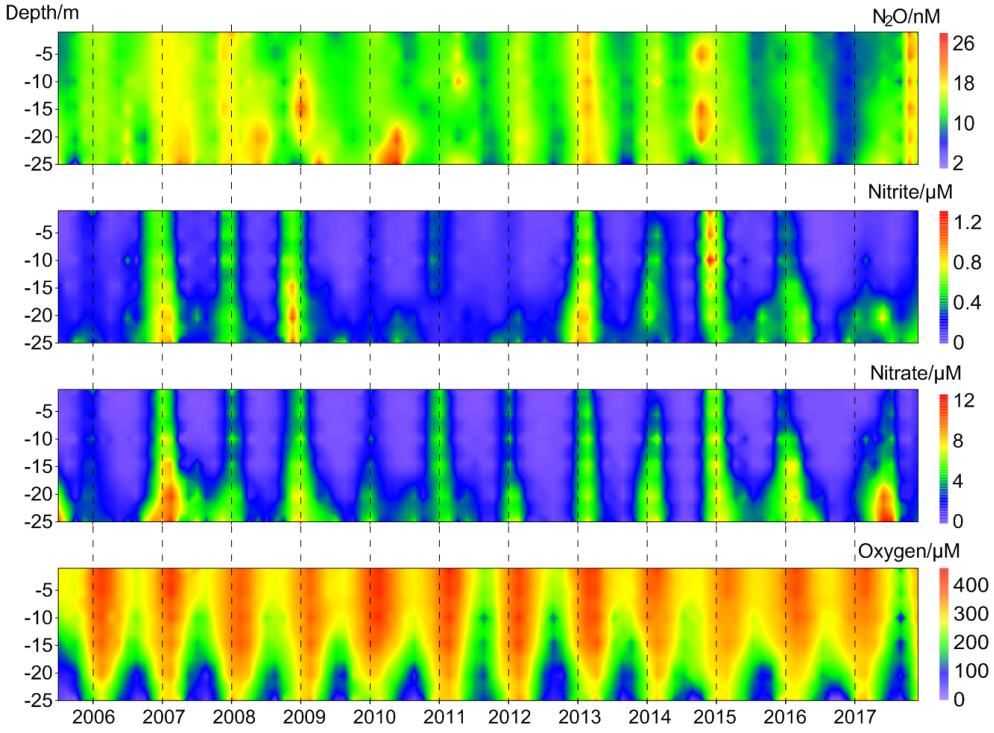

Figure 2. Vertical distributions of dissolved O_2, NO_2^-, NO_3^-, and N_2O from the BE Time Series Station during 2005–2017.

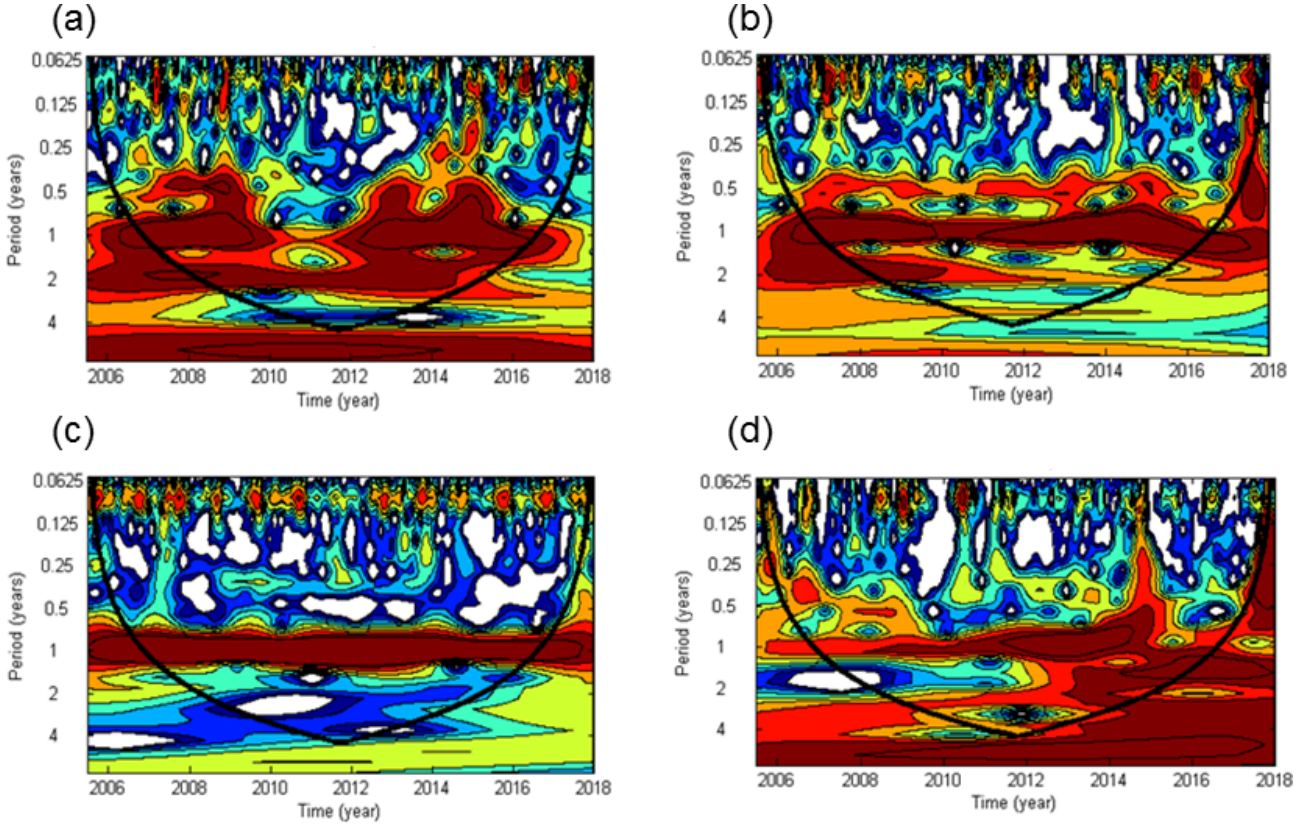

Figure 3. Wavelet power spectra of NO_2^- **(a)**, NO_3^- **(b)**, dissolved O_2 **(c)**, and N_2O **(d)** from the BE Time Series Station. Red areas indicate high power and blue areas indicate low power. The black conic line indicates the significant area where boundary effects can be excluded.

The half-year cycles of NO_2^- and NO_3^- were probably associated with algae blooms which usually occur in each spring and autumn (Figs. S1 and S2 in the Supplement). Since the time between the two blooms differed between years, the cycles were weak and thus not present in every year. Due to the fact that there was no half-year O_2 cycle at all, nutrients apart from O_2 might be the "drivers" of the sporadic half-year N_2O cycle in 2008 and 2015 because N_2O production depends on the concentration of the bioavailable nitrogen compounds (Codispoti et al., 2001).

Generally the wavelet analysis indicated a strong annual cycle for NO_2^-, NO_3^-, dissolved O_2, and N_2O at the BE Time Series Station, which enabled us to explore the seasonal pattern with annual mean data. Although extreme values were excluded as a result of averaging, the smoothed results generally reflect the seasonality of these parameters. Here, we focus on the annual cycle.

The annual mean vertical distribution of dissolved O_2, NO_2^-, NO_3^-, and N_2O are shown in Fig. 4. Due to the development of stratification, the mixed layer was shallow in summer and deep in late autumn and winter. O_2 depletion was observed in bottom waters from late spring until late autumn. The seasonal variations in NO_2^- and NO_3^- were significantly correlated with each other ($[NO_3^-] = 11.59[NO_2^-] - 0.51$, $R^2 = 0.80$, $n = 72$, $p < 0.0001$) and high concentrations were observed for both in winter. Minimum N_2O concentrations were found in the bottom waters during September and October, presumably as a result of consumption during denitrification under anoxic condition (Codispoti et al., 2005). High N_2O concentrations were observed in late spring and late autumn, respectively. In late spring N_2O accumulated in the bottom waters because the stratification prevented mixing of the water column. In late autumn, however, N_2O could be ventilated to the surface and thus emitted to the atmosphere due to the breakdown of the stratification. The high N_2O concentrations could be attributed to enhanced N_2O production via nitrification and/or denitrification within the oxic–anoxic interface (Goreau et al., 1980; Codispoti et al., 1992). Since there is no clear O_2 concentration threshold, N_2O production from both nitrification and the onset of denitrification overlap at oxic–anoxic interface. To this end, direct N_2O production measurements (i.e. nitrification and denitrification rates) are required to decipher which process dominates the formation of the different N_2O maxima.

High N_2O concentrations prevailed all over the water column in winter and early spring. NH_4^+ is released from the sediment into bottom waters due to the degradation of organic matter, especially after the autumn algae bloom (Figs. S1 and S2 in the Supplement). The stratification usually completely breaks down at this time of the year and the water column becomes oxygenated. Denitrification is inhibited by the presence of high concentrations of dissolved O_2 ($> 20\,\mu mol\,L^{-1}$, which is higher than the O_2 threshold of about $10\,\mu mol\,L^{-1}$; Tiedje, 1988) and thus nitrification is presumably responsible for the high N_2O concentrations in winter and early spring.

3.3 Trend analysis

The MKTs were conducted for the surface (1 m) and bottom (25 m) N_2O concentrations and saturations of the individual 12 months, respectively. Significant decreasing trends were detected for the concentrations in the bottom waters for February and August (Table 1a), and for the saturations in the surface for September and in the bottom for August and November (Table 1b). These results indicated that some systematical changes in N_2O took place at BE. For example, the significant decrease in N_2O concentration/saturation in August might be associated with the increasing temperature, which reinforces the stratification and accelerates O_2 consumption in the bottom waters (Lennartz et al., 2014). As a result, hypoxia/anoxia starts earlier and thus enables the onset of denitrification to consume N_2O. During most of the months, trends in N_2O concentration and saturation were not significant during 2005–2017.

A significant nutrient decline has been observed at the BE Time Series Station since the mid-1980s; however, Lennartz et al. (2014) found that bottom O_2 concentrations were still decreasing over the past 60 years. The ongoing oxygen decline was attributed to the temperature-enhanced O_2 consumption in the bottom water (Meier et al., 2018) and a prolongation of the stratification period at the BE Time Series Station (Lennartz et al., 2014). Please note that the trends in nutrients and O_2 concentrations were detected based on the data collection, which lasted for approximately 30 and 60 years, respectively, while the N_2O observations at BE Time Series Station have lasted for only 12.5 years. Further MKT analysis for nutrients, temperature, and oxygen for months with significant trends in N_2O concentrations did not show any significant results ($p > 0.05$). The significant trends in N_2O concentrations thus do not seem to be directly related to one of these parameters, and we cannot state a reason for the significant trends of N_2O concentration in February and the N_2O saturation in September and November at this point. Presumably, a longer monitoring period for N_2O is required to detect corresponding trends in N_2O and oxygen or nutrients.

3.4 Extreme events

3.4.1 Low N_2O concentrations during October 2016–April 2017

Besides the low N_2O concentrations occurring in autumn, we observed a band of pronounced low N_2O concentrations which started in October 2016 and lasted until April 2017 (Fig. 5). In this period N_2O concentrations varied between 5.5 and 13.9 nM, with an average of 8.4 ± 2.0 nM. This is approximately 40 % lower than the average N_2O concentration

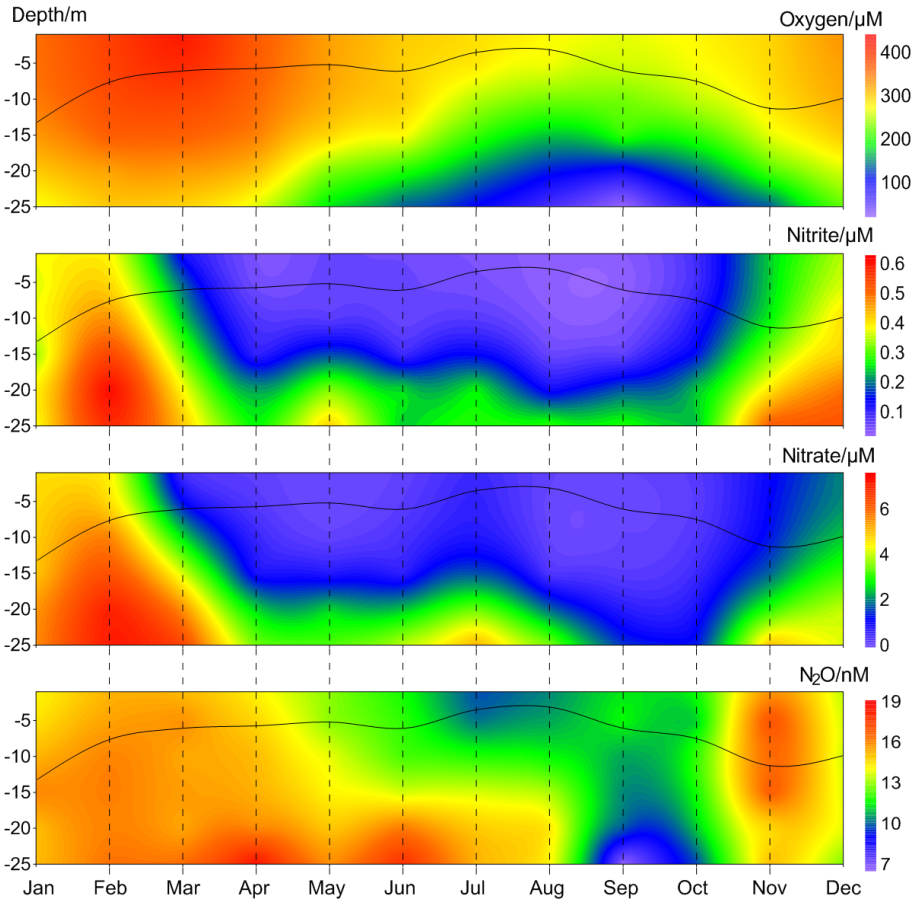

Figure 4. Average vertical distributions of dissolved O_2, NO_2^-, NO_3^-, and N_2O from the BE Time Series Station during 2005–2017. The black line indicates the mixed layer depth, which was calculated based on a potential density anomaly of 0.15 kg m^{-3} from the sea surface (1 m).

during the entire measurement period 2005–2017. The average N_2O saturation during 2005–2017 was 111 ± 30 %, while from October 2016 to April 2017 the N_2O saturations were as low as 43 %–93 % (average 62 ± 10 %).

Undersaturated N_2O waters have been previously reported from the Baltic Sea: Rönner (1983) observed a N_2O surface saturation of 79 % in the central Baltic Sea and attributed the undersaturation to upwelling of N_2O-depleted waters. Bange et al. (1998) found a minimum N_2O saturation of 91 % in the southern Baltic Sea where the hydrographic conditions were significantly influenced by riverine runoff. Walter et al. (2006) reported a mean N_2O saturation of 79 ± 11 % for shallow stations (< 30 m) in the southwestern Baltic Sea in October 2003. The low-N_2O event at BE was unusual because the concentrations were much lower than those reported values and it lasted for more than half a year.

Although the observed temperatures and salinities during October 2016–April 2017 were comparable to other years (Fig. S1), it is difficult to evaluate the role of physical mechanism in the low-N_2O event because of insufficient data for water mass exchange at the BE Time Series Station. Here we mainly focused on the chemical or biological processes. Anoxia events with the presence of H_2S were observed in the bottom waters for 3 months in a row during September–November 2016. This is an unusual long period and is unprecedented at the BE Time Series Station. In December 2016 the stratification did not completely break down. Although the water column was generally oxygenated, bottom O_2 concentrations were the lowest observed during the past 12.5 years. Considering the classical view of N_2O consumption via denitrification under hypoxic and anoxic conditions, we inferred that denitrification accounted for low N_2O concentrations in the bottom layer. However, the question of where the low N_2O concentration water in the upper layers came from still remains.

In September 2016, low N_2O concentrations were only observed in the bottom waters where the anoxia occurred. However, the situation was different in the following months. During October/November 2016, N_2O concentrations were homogeneously distributed in the water column. Although the stratification gradually started to break down in late autumn, the density gradient was still strong enough to keep

Table 1. The results of the Mann–Kendall test for the surface and bottom N_2O concentrations and saturations of the 12 individual months.

(a) MKT results for N_2O concentrations								
Month	Jan		Feb		Mar		Apr	
Depth (m)	1	25	1	25	1	25	1	25
p	0.09	0.19	0.11	0.03(–)	0.19	0.63	0.09	0.30
Month	May		Jun		Jul		Aug	
Depth (m)	1	25	1	25	1	25	1	25
p	0.63	0.24	0.15	0.95	0.16	0.16	0.20	0.03(–)
Month	Sep		Oct		Nov		Dec	
Depth (m)	1	25	1	25	1	25	1	25
p	0.25	0.76	0.36	0.76	0.67	0.16	0.10	0.30
(b) MKT results for N_2O saturations								
Month	Jan		Feb		Mar		Apr	
Depth (m)	1	25	1	25	1	25	1	25
p	0.37	0.24	0.15	0.15	0.19	0.63	0.11	0.19
Month	May		Jun		Jul		Aug	
Depth (m)	1	25	1	25	1	25	1	25
p	0.19	1	0.37	0.54	0.10	0.43	0.20	0.02(–)
Month	Sep		Oct		Nov		Dec	
Depth (m)	1	25	1	25	1	25	1	25
p	0.04(–)	0.85	0.06	0.43	0.20	0.03(–)	0.16	0.36

p indicates the p value of the test, which is the probability, under the null hypothesis, of obtaining a value of the test statistic as extreme or more extreme than the value computed from the sample. (–) indicates a rejection of the null hypothesis at α significance level and a decreasing trend is detected.

the bottom waters at anoxic conditions and prevented the low-N_2O-concentration water to reach the surface. Thus we inferred that the unusual low N_2O concentrations in the upper layers (above 20 m) were probably resulting from advection of adjacent waters. Due to the fact that the upper layers were well-mixed and oxygenated, in situ N_2O consumption in the water column could be neglected. We suggest, therefore, that the N_2O-depleted waters were resulting from consumption of N_2O in bottom waters elsewhere and then they were upwelled and transported to BE. Hence, N_2O consumption via denitrification might have been, directly or indirectly, responsible for the low N_2O concentrations during October–November 2016.

In December 2016, the bottom waters were ventilated with O_2. Although N_2O consumption by denitrification should have been inhibited by the high concentrations of O_2 (Codispoti et al., 2001), the N_2O concentrations did not restore to their normal level under suboxic conditions. Since January 2017, the whole water column was well mixed and oxygenated. Usually a significant nutrient supply could be observed starting in November (Fig. 4) as a result of remineralization and vertical mixing, but the average NO_2^- and NO_3^- concentrations during November 2016–April 2017 were 0.2 and 1.4 µM, respectively, which was about 50 % and 60 % lower than in other years. Ammonium (NH_4^+) and chlorophyll a concentrations during this period were comparable to those of other years (Fig. S1). Secchi depth, a proxy of water transparency, was 3.8 m in March 2017, which is only slightly lower compared to the monthly average value for March (4.5 ± 1.8 m). There is no exceptional spring algae bloom and thus we infer that assimilative uptake of nutrients by phytoplankton was not responsible for the low nutrient concentrations. The nutrient deficiency might be attributed to enhanced nitrogen removal processes like denitrification or anammox (Voss et al., 2005; Hietanen et al., 2007; Hannig et al., 2007) during the prolonged period of anoxia in autumn 2016. During the low-N_2O event, we found that N_2O concentrations were positively correlated with both NO_2^- ($[N_2O] = 7.02[NO_2^-] + 7.36$, $R^2 = 0.29$, $n = 24$, $p < 0.01$) and NO_3^- ($[N_2O] = 0.80[NO_3^-] + 7.36$, $R^2 = 0.51$, $n = 24$, $p < 0.0001$). These results indicate that the development and maintenance of the low N_2O concentration was closely associated with nutrient deficiency. Especially after the breakdown of the stratification, when denitrification was no longer a significant N_2O sink, nutrients might have become a limiting factor for N_2O production.

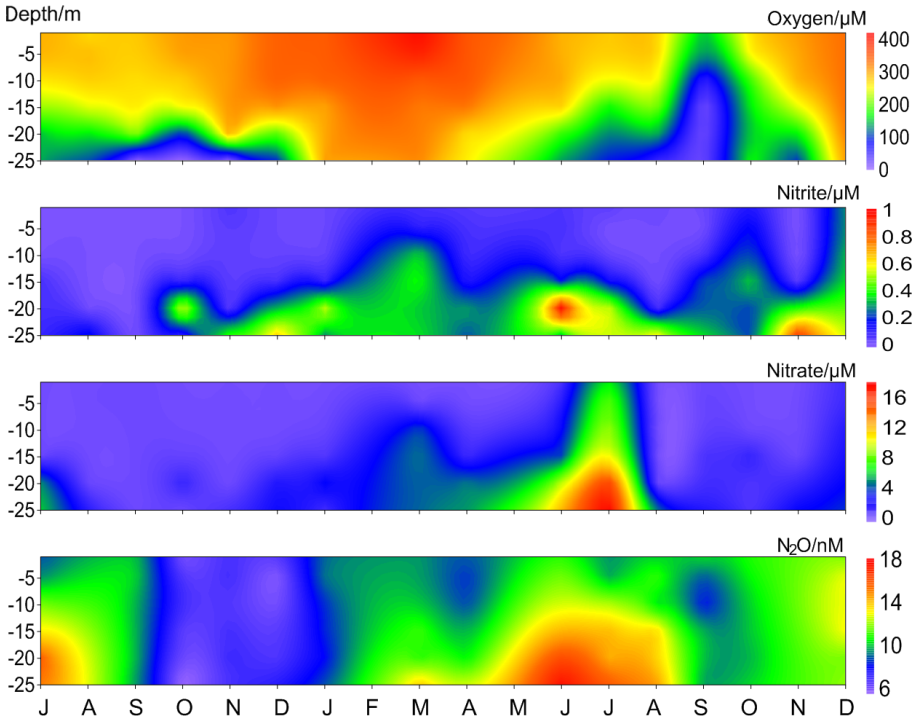

Figure 5. Vertical distribution of dissolved O_2, NO_2^-, NO_3^-, and N_2O from the BE Time Series Station during July 2016–December 2017. Please note that the high N_2O concentrations in November 2017 were removed for better visualization.

In general, the low-N_2O-concentration event during October 2016–April 2017 can be divided into two parts: in the stratified waters during October–November 2016, O_2 played a dominant role and N_2O was consumed via denitrification under anoxic conditions. In the well-mixed water column during December 2016–April 2017, nutrient deficiency seemed to have constrained N_2O production via nitrification under suboxic/oxic conditions.

In recent years a novel biological N_2O consumption pathway, called N_2O fixation, which transforms N_2O into particulate organic nitrogen via its assimilation, has been reported (Farías et al., 2013). This process can take place under extreme environmental conditions even at very low N_2O concentrations. Cornejo et al. (2015) reported that N_2O fixation might play a major role in the coastal zone off central Chile where seasonally occurring surface N_2O undersaturation was observed. The relatively high N_2 fixation rates in the Baltic Sea (Sohm et al., 2011) highlight the potential role of N_2O fixation (Farías et al., 2013). However, we cannot quantify the role of biological N_2O fixation for the N_2O depletion in the Baltic Sea due to the absence of N_2O assimilation measurements.

3.4.2 High N_2O concentrations in November 2017

High N_2O concentrations were observed at the BE Time Series Station in November 2017. The average value reached 35.4±1.5 nM, which was the highest concentration measured during the entire sampling period from 2005 to 2017. Dissolved N_2O was homogeneously distributed in the water column, but this event did not last long. In December, dissolved N_2O returned to normal levels and the average concentration in the water column was comparable to that of other years. Average N_2O saturation in November 2017 was 322 ± 10 %, which was also the highest for the past 12.5 years. This value was much higher than the maximum surface N_2O saturation reported by Rönner (1983) in the central Baltic Sea but was comparable to the results observed in the southern Baltic Sea (312 %; Bange et al., 1998). Bange et al. (1998) linked the enhanced N_2O concentrations to riverine runoff because those samples were collected in an estuarine area; however, the riverine influence around the BE Time Series Station is negligible. As a result, the impact of fresh water input can be excluded.

Dissolved O_2 seemed to play a dominant role in the high N_2O concentrations. Enhanced N_2O production usually occurred at the oxic–anoxic interface, which was closely linked to the development of water column stratification. In general the breakdown of the stratification is faster than its establishment at the BE Time Series Station. As a result, it took about half a year for bottom O_2 saturation to gradually decrease from ∼ 80 % to almost 0 % (i.e. anoxia) but only 2 months to restore normal saturation level in 2010 (Fig. 6). In late autumn, surface water penetrated into the deep layers via vertical mixing and eroded the oxic–anoxic interface. The entire

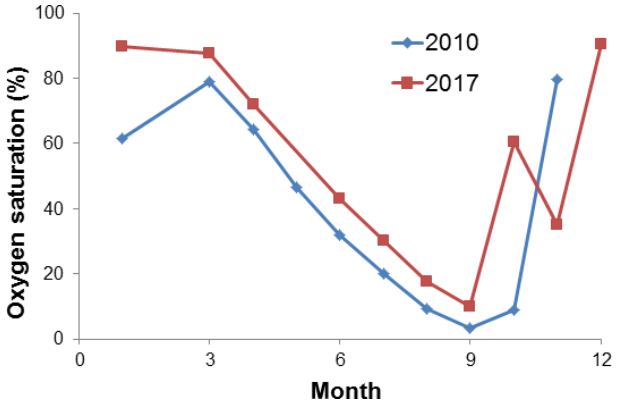

Figure 6. Variations of bottom O_2 saturation in 2010 (blue) and 2017 (red).

water column quickly became oxygenated and the enhanced N_2O production was stopped.

Hypoxia or anoxia at BE is usually observed in the bottom waters in autumn, but in September 2017 hypoxic water (O_2 saturation < 20 %, which was close to the criterion for hypoxia; see Naqvi et al., 2010) was found in the subsurface layer (10 m) as well. Surface O_2 saturation was only ∼ 50 %, which was the lowest during the sampling period 2005–2017. The density gradient of the water column in September 2017 was much lower than in other years. These results indicate the occurrence of an upwelling event at BE Time Series Station in autumn 2017, which might be a result of the saline water inflow from the North Sea considering the change of salinity in the water column (Fig. S1). Strong vertical mixing has interrupted the hypoxia/anoxia and bottom O_2 saturation reached ∼ 60 % in October 2017. The presence of O_2 prevented N_2O consumption via denitrification; as a result, we did not observe a significant N_2O decline during that period (Fig. 5).

Considering the fact that a significant autumn algae bloom was observed in autumn 2017 (as indicated by high chlorophyll *a* concentrations, see Fig. S1), severe O_2 depletion in the bottom water could be expected. Although the bottom O_2 saturation was only slightly lower in November than in October, we speculate that even lower O_2 saturation (but not anoxia) might have occurred between October and November. The "W-shaped" O_2 saturation curve (see Fig. 6) suggests that the stratification did not completely break down in October and that there might have been a reestablishment of the oxic–anoxic interface providing favourable conditions for enhanced N_2O production. Due to the degradation of organic nitrogen, NH_4^+ is released from the sediment into bottom waters (Dale et al., 2011), especially in autumn when O_2 is low (Fig. S2). NH_4^+ concentrations in November 2017 were lower than in other years (Fig. S1), and NO_2^- concentrations were higher (Fig. 5), indicating that nitrification occurred in bottom waters. To this end, we suggest that the reestablishment of the oxic–anoxic interface promoted ammonium oxidation (the first step of nitrification). In this case, N_2O could have temporary accumulated because its consumption via denitrification was blocked. Meanwhile, the relatively low density gradient (i.e. low stratification) allowed upward mixing of the excess N_2O to the surface. However, we inferred that this phenomenon would only last for a few days due to the rapid breakdown of stratification at the BE Time Series Station.

Due to the development of the pronounced stratification, the oxic–anoxic interface prevailed in summer/early autumn as well, but we did not observe N_2O accumulation during these months. One of the potential explanations is that enhanced N_2O production only took place within particular depths where strong O_2 gradient existed, but our vertical sampling resolution was too low to capture this event. Also enhanced N_2O production might be covered by the weak mixing which brought low-N_2O water from the bottom to the surface.

The upwelling event played different roles in autumn 2016 and 2017. First, upwelling took place somewhere else but at BE because of the strong density and O_2 gradient in the water column during autumn 2016. Second, bottom water remained anoxic in autumn 2016, while the compensated water for upwelling in 2017 penetrated through stratification and brought O_2 into bottom water (Fig. 6), which caused enhanced N_2O production. Similarly, autumn upwelling was detected in 2011 and 2012 when we found relatively low O_2 concentrations in subsurface layers (10 m) (Fig. 2), but we did not observe an increase in bottom O_2 concentrations and N_2O concentrations remained low during that time. These upwelling events seem to be driven by saline water inflow considering the prominent increase in salinity, but the mechanism that dominates O_2 input into bottom water before the stratification break down remains unclear.

3.5 Flux density

During 2005–2017, surface N_2O saturations at the BE Time Series Station varied from 56 % to 314 % (69 %–194 % excluding the extreme values discussed in Sect. 3.4), with an average of 111 ± 30 % (111 ± 20 % without the extreme values). Generally the water column at BE was slightly oversaturated with N_2O. Our results are in good agreement with the estimated mean surface N_2O saturation for the European shelf (113 %; Bange, 2006).

We found a weak seasonal cycle for surface N_2O concentrations, with high N_2O concentrations occurring in winter and early spring and low concentrations occurring in summer/autumn, but no such cycle for N_2O saturation (Figs. 4, 7). The seasonality in concentration but not in saturation could be largely attributed to the effect of temperature on N_2O solubility: in summer when surface N_2O concentrations are low, N_2O saturations are increased by the relative high temperature and vice versa in winter. Although salinity also affects N_2O solubility, its contribution is negligible compared to temperature. Temperature alleviated the fluctua-

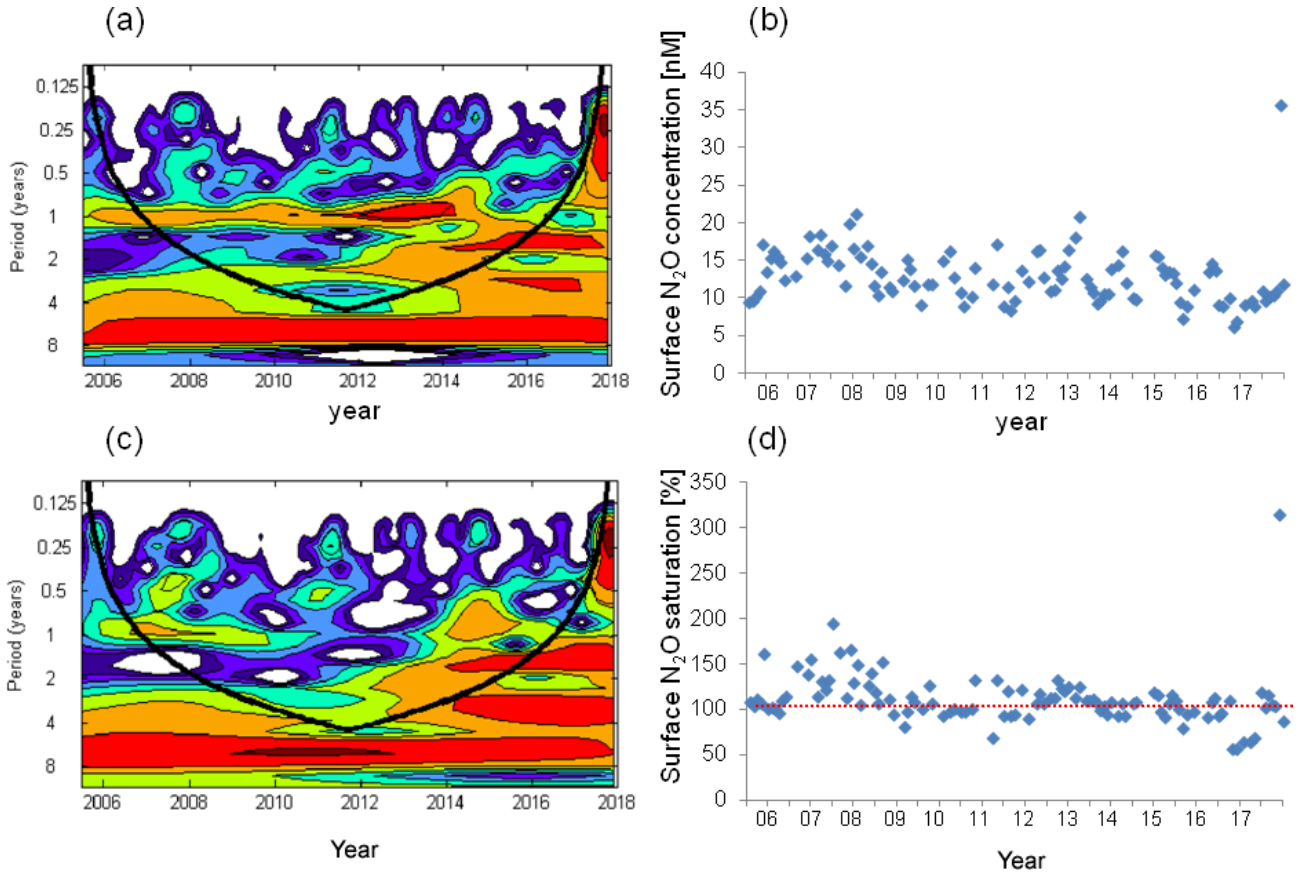

Figure 7. Wavelet analysis and the variation in surface N_2O concentrations **(a, b)** and surface N_2O saturations **(c, d)**. The dashed red line in **(d)** indicates the saturation of 100 %.

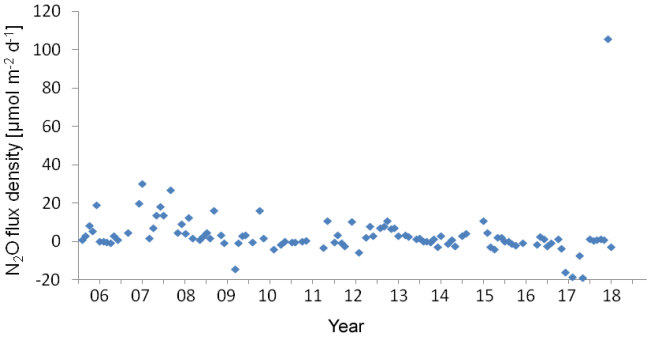

Figure 8. Variation of N_2O flux density at the BE Time Series-Station during 2005–2017. Negative values indicated N_2O influx from the atmosphere and positive values indicated N_2O efflux to the atmosphere.

tion of surface N_2O saturation and thus affected the sea-to-air N_2O fluxes. We conclude that temperature plays a modulating role for N_2O emissions.

The wind speed (u_{10}) at the BE Time Series Station ranged from 1.1 to 14.0 m s^{-1}, with an average of 7.0 ± 2.7 m s^{-1}. N_2O flux densities varied from -19.0 to 105.7 μmol m^{-2} d^{-1} (-14.1 to 30.3 μmol m^{-2} d^{-1} without the extreme values), with an average of 3.5 ± 12.4 μmol m^{-2} d^{-1} (3.3 ± 6.5 μmol m^{-2} d^{-1} without the extreme values). However, the true emissions might have been underestimated because our monthly sampling resolution is insufficient to capture short-term N_2O accumulation events due to the fast breakdown of stratification in autumn. The uncertainty introduced in the flux density computation was estimated to be 20 % (Wanninkhof, 2014). The flux densities at the BE Time Series Station are comparable to those reported by Bange et al. (1998, 0.4 to 7.1 μmol m^{-2} d^{-1}) from the coastal waters of the southern Baltic Sea but are slightly lower than the average N_2O flux density reported by Rönner (1983, 8.9 μmol m^{-2} d^{-1}) from the central Baltic Sea. Please note that the results of Rönner (1983) were obtained only from the summer season and therefore are probably biased because of missing seasonality.

In December 2014, a strong saline water inflow from the North Sea was observed, which was the third strongest ever recorded (Mohrholz et al., 2015). Although the salinity in December 2014 was comparable to other years, a remarkable increase in salinity was observed in the following several months. However, we did not detect a significant N_2O

anomaly or enhanced emission during that time. Similarly, Walter et al. (2006) investigated the impact of the North Sea water inflow on N_2O production in the southern and central Baltic Sea in 2003. The oxygenated water ventilated the deep Baltic Sea and shifted anoxic to oxic condition which led to enhanced N_2O production, but the accumulated N_2O was unlikely to reach the surface due to the presence of a permanent halocline (Walter et al., 2006).

Although we observed an extremely high N_2O flux density in November 2017, the low-N_2O-concentration (< 10 nM) events have become more and more frequent during the past 12.5 years (Fig. 2). This phenomenon seldom occurred before 2011, but remarkable low N_2O concentrations can be seen in 2011 and 2013, and to a lesser extent in 2012 and 2014. Similar events lasted for several months in 2015 and for even more than half a year during 2016–2017. The most striking feature was that the low-N_2O-concentration water was not only detected in bottom waters but also at surface which would significantly impact the air–sea N_2O flux densities. Although the MKT result did not give a significant trend for the N_2O flux densities, the data presented in Fig. 8 suggest a potential decline of N_2O flux densities from the coastal Baltic Sea, challenging the conventional view that N_2O emissions from coastal waters would most probably increase in the future, which was based on the hypothesis of increasing nutrient loads into coastal waters. Due to an effective reduction of nutrient inputs, the severe eutrophication condition in the Baltic Sea has been alleviated (HELCOM, 2018b), but ongoing deoxygenation points to the fact that it will take a longer time for coastal ecosystems to feedback to reduced nutrient inputs because other environmental changes such as warming may override decreasing eutrophication (Lennartz et al., 2014).

4 Conclusions

The seasonal and inter-annual N_2O variations at the BE Time Series Station from July 2005 to December 2017 were driven by the prevailing O_2 regime and nutrient availability. We found a pronounced seasonal cycle with low N_2O concentrations (undersaturations) occurring in hypoxic or anoxic bottom waters in autumn and enhanced concentrations (supersaturations) all over the water column in winter and early spring. Significant decreasing trends for N_2O concentrations were found for few months, while most of the year no significant trend was detectable in the period of 2005–2017. During 2005–2017, no significant trends were present for O_2 or nutrients either, but these parameters all show significant decreasing trends on longer timescales (~ 60 years) at BE. Our results show the strong coupling of N_2O with O_2 and nutrient concentrations, and suggest similar changes on comparable timescales. Further monitoring of N_2O at BE Time Series Station is thus important to detect changes. Further studies on N_2O production and consumption by nitrification and denitrification and analysis of the characteristic N_2O isotope signature might be very helpful to decipher the potential roles of O_2 and nutrients for N_2O cycling.

Temperature plays a modulating role for the N_2O emission at the BE Time Series Station. Although the hydrographic condition at BE is generally dominated by the inflow of saline North Sea water, this did not affect N_2O production and its emissions to the atmosphere. It seems that events with extremely low N_2O concentrations and thus reduced N_2O emissions became more frequent in recent years. Our results provide a new perspective on potential future patterns of N_2O distribution and emissions in coastal areas. Continuous measurement at the BE Time Series Station with a focus on late autumn would be of great importance for monitoring and understanding the future changes in N_2O concentrations and emissions in the southwestern Baltic Sea.

Data availability. Data are available from the Boknis Eck Database: https://www.bokniseck.de (Bange and Malien, 2019) and MEMENTO (the MarinE MethanE and NiTrous Oxide database, https://memento.geomar.de, Kock and Bange, 2015, last accessed: 23 October 2019).

Supplement. The supplement related to this article is available online at: https://doi.org/10.5194/bg-16-4097-2019-supplement.

Author contributions. XM, STL, and HWB designed the study and participated in the fieldwork. N_2O measurements and data processing were done by XM and STL. XM wrote the article with contributions from STL and HWB.

Competing interests. The authors declare that they have no conflict of interest.

Acknowledgements. The authors thank the captain and crew of the RV *Littorina* and *Polarfuchs* as well as the many colleagues and numerous students who helped with the sampling and measurements of the BE time series through various projects. Special thanks to Anette Kock for her help with sampling, measurements, and data analysis. The time series at BE was supported by DWK Meeresforschung (1957–1975), HELCOM (1979–1995), BMBF (1995–1999), the Institut für Meereskunde (1999–2003), IfM-GEOMAR (2004–2011), and GEOMAR (2012–present). The current N_2O measurements at BE are supported by the EU BONUS INTEGRAL project which receives funding from BONUS (Art 185), funded jointly by the EU, the German Federal Ministry of Education and Research, the Swedish Research Council Formas, the Academy of Finland, the Polish National Centre for Research and Development, and the Estonian Research Council. The Boknis Eck Time Series Station (https://www.bokniseck.de, last access: 23 October 2019) is run by the Chemical Oceanography Research Unit of GEOMAR, Helmholtz Centre for Ocean Research Kiel.

Financial support. Xiao Ma is grateful to the financial support provided by the China Scholarship Council (grant no. 201306330056) and the BONUS INTEGRAL (grant no. 03F0773B).

Review statement. This paper was edited by S. Wajih A. Naqvi and reviewed by two anonymous referees.

References

Bange, H. W.: Nitrous oxide and methane in European coastal waters, Estuar. Coast. Shelf S., 70, 361–374, https://doi.org/10.1016/j.ecss.2006.05.042, 2006.

Bange, H. W., Dahlke, S., Ramesh, R., Meyer-Reil, L. A., Rapsomanikis, S., and Andreae, M. O.: Seasonal study of methane and nitrous oxide in the coastal waters of the southern Baltic Sea, Estuar. Coast. Shelf S., 47, 807–817, https://doi.org/10.1006/ecss.1998.0397, 1998.

Bange, H. W. and Malien, F.: Boknis Eck Timeseries Database, Kiel Datamanagement Team, http://www.bokniseck.de/, last accessed: 23 October 2019.

Battaglia, G. and Joos, F.: Marine N_2O emissions from nitrification and denitrification constrained by modern observations and projected in multimillenial global warming simulations, Global Biogeochem. Cy., 32, 92–121, https://doi.org/10.1002/2017GB005671, 2018.

Bonin, P., Gilewicz, M., and Bertrand, J. C.: Effects of oxygen on each step of denitrification on Pseudomonas nautica, Can. J. Microbiol., 35, 1061–1064, https://doi.org/10.1139/m89-177, 1989.

Breitburg, D., Levin, L. A., Oschlies, A., Grégoire, M., Chavez, F. P., Conley, D. J., Garçon, V., Gilbert, D., Gutiérrez, D., Isensee, K., Jacinto, G. S., Limburg, K. E., Montes, I., Naqvi, S. W. A., Pitcher, G. C., Rabalais, N. N., Roman, M. R., Rose, K. A., Seibel, B. A., Telszewski, M., Yasuhara, M., and Zhang, J.: Declining oxygen in the global ocean and coastal waters, Science, 359, eaam7240, https://doi.org/10.1126/science.aam7240, 2018.

Capelle, D. W., Hawley, A. K., Hallam, S. J., and Tortell, P. D.: A multi-year time-series of N_2O dynamics in a seasonally anoxic fjord: Saanich Inlet, British Columbia, Limnol. Oceanogr., 63, 524–539, https://doi.org/10.1002/lno.10645, 2018.

Carstensen, J., Andersen, J. H., Gustafsson, B. G., and Conley, D. J.: Deoxygenation of the Baltic Sea during the last century, P. Natl. Acad. Sci. USA, 111, 5628–5633, https://doi.org/10.1073/pnas.1323156111, 2014.

Codispoti, L. A., Elkins, J. W., Yoshinari, T., Fredrich, G., Sakamoto, C., and Packard, T.: On the nitrous oxide flux from productive regions that contain low oxygen waters, in: Oceanography of the Indian Ocean, edited by: Desai, B. N., Oxford Univ. Press, New York, 271–284, 1992.

Codispoti, L. A., Brandes, J. A., Christensen, J. P., Devol, A. H., Naqvi, S. W. A., Paerl, H. W., and Yoshinari, T.: The oceanic fixed nitrogen and nitrous oxide budgets: Moving targets as we enter the anthropocene?, Sci. Mar., 65, 85–105, https://doi.org/10.3989/scimar.2001.65s285, 2001.

Codispoti, L. A., Yoshinari, T., and Devol, A. H.: Suboxic respiration in the oceanic water column, in: Respiration in aquatic ecosystems, edited by: del Giorgio, P. A. and Williams, P. J., Oxford Univ. Press, New York, 225–247, 2005.

Conley, D. J., Carstensen, J., Aigars, J., Axe, P., Bonsdorff, E., Eremina, T., and Lannegren, C.: Hypoxia is increasing in the coastal zone of the Baltic Sea, Environ. Sci. Technol., 45, 6777–6783, https://doi.org/10.1021/es201212r, 2011.

Cornejo, M., Murillo, A. A., and Farías, L.: An unaccounted for N_2O sink in the surface water of the eastern subtropical South Pacific: Physical versus biological mechanisms, Prog. Oceanogr., 137, 12–23, https://doi.org/10.1016/j.pocean.2014.12.016, 2015.

Dale, A. W., Sommer, S., Bohlen, L., Treude, T., Bertics, V. J., Bange, H. W., Pfannkuche, O., Schorp, T., Mattsdotter, M., and Wallmann, K.: Rates and regulation of nitrogen cycling in seasonally hypoxic sediments during winter (Boknis Eck, SW Baltic Sea): Sensitivity to environmental variables, Estuar. Coast. Shelf S., 95, 14–28, https://doi.org/10.1016/j.ecss.2011.05.016, 2011.

Ducklow, H. W., Doney, S. C., and Steinberg, D. K.: Contributions of long-term research and time-series observations to marine ecology and biogeochemistry, Annu. Rev. Mar. Sci., 1, 279–302, https://doi.org/10.1146/annurev.marine.010908.163801, 2009.

Farías, L., Castro-González, M., Cornejo, M., Charpentier, J., Faúndez, J., Boontanon, N., and Yoshida, N.: Denitrification and nitrous oxide cycling within the upper oxycline of the eastern tropical South Pacific oxygen minimum zone, Limnol. Oceanogr., 54, 132–144, https://doi.org/10.4319/lo.2009.54.1.0132, 2009.

Farías, L., Faúndez, J., Fernández, C., Cornejo, M., Sanhueza, S., and Carrasco, C.: Biological N_2O fixation in the Eastern South Pacific Ocean and marine cyanobacterial cultures, Plos One, 8, e63956, https://doi.org/10.1371/journal.pone.0063956, 2013.

Farías, L., Besoain, V., and García-Loyola, S.: Presence of nitrous oxide hotspots in the coastal upwelling area off central Chile: an analysis of temporal variability based on ten years of a biogeochemical time series, Environ. Res. Lett., 10, 044017, https://doi.org/10.1088/1748-9326/10/4/044017, 2015.

Goreau, T. J., Kaplan, W. A., Wofsy, S. C., McElroy, M. B., Valois, F. W., and Watson, S. W.: Production of NO_2^- and N_2O by nitrifying bacteria at reduced concentrations of oxygen, Appl. Environ. Microb., 40, 526–532, 1980.

Grasshoff, K., Kremling, K., and Ehrhardt, M.: Methods of seawater analysis, 3rd edition, WILEY-VCH, Weihheim, Germany, 208–225, 1999.

Hannig, M., Lavik, G., Kuypers, M. M. M., Woebken, D., Martens-Habbena, W., and Jürgens, K.: Shift from denitrification to anammox after inflow events in the central Baltic Sea, Limnol. Oceanogr., 52, 1336–1345, 2007.

Hansen, H. P., Giesenhagen, H. C., and Behrends, G.: Seasonal and long-term control of bottom water oxygen deficiency in a stratified shallow-coastal system, ICES J. Mar. Sci., 56, 65–71, https://doi.org/10.1006/jmsc.1999.0629, 1999.

HELCOM: Sources and pathways of nutrients to the Baltic Sea, Baltic Sea Environ. Proc., 153, 4–46, 2018a.

HELCOM: State of the Baltic Sea – Second HELCOM holistic assessment 2011–2016, Baltic Sea Environ. Proc., 155, 41–58, 2018b.

Hietanen, S. and Lukkari, K.: Effects of short-term anoxia on benthic denitrification, nutrient fluxes and phosphorus forms in coastal Baltic sediment, Aquat. Microb. Ecol., 49, 293–302, https://doi.org/10.3354/ame01146, 2007.

Hsu, S. A., Meindl, E. A., and Gilhousen, D. B.: Determining the power-law wind-profile exponent under near-neutral stability conditions at sea, J. Appl. Meteorol., 33, 757–765, 1994.

IPCC: Climate Change 2013: The physical science basis. Contribution of Working Group I to the fifth assessment report of the Intergovernmental Panel on Climate Change, Cambridge University Press, Cambridge, UK and New York, NY, 467–552, 2013.

Kock, A. and Bange, H. W.: Counting the ocean's greenhouse gas emissions, Eos (Washington DC), 96, 10–13, https://doi.org/10.1029/2015EO023665, 2015.

Kock, A., Arévalo-Martínez, D. L., Löscher, C. R., and Bange, H. W.: Extreme N_2O accumulation in the coastal oxygen minimum zone off Peru, Biogeosciences, 13, 827–840, https://doi.org/10.5194/bg-13-827-2016, 2016.

Kroeze, C. and Seitzinger, S. P.: Nitrogen inputs to rivers, estuaries and continental shelves and related nitrous oxide emissions in 1990 and 2050: a global model, Nutr. Cycl. Agroecosys., 52, 195–212, 1998.

Kulkarni, A. and Von Storch, H.: Monte Carlo experiments on the effect of serial correlation on the Mann-Kendall test of trend, Meteorol. Z., 4, 82–85, 1995.

Landolfi, A., Somes, C. J., Koeve, W., Zamora, L. M., and Oschlies, A.: Oceanic nitrogen cycling and N_2O flux perturbations in the Anthropocene, Global Biogeochem. Cy., 31, 1236–1255, https://doi.org/10.1002/2017GB005633, 2017.

Lennartz, S. T., Lehmann, A., Herrford, J., Malien, F., Hansen, H. P., Biester, H., and Bange, H. W.: Long-term trends at the Boknis Eck time series station (Baltic Sea), 1957–2013: does climate change counteract the decline in eutrophication?, Biogeosciences, 11, 6323–6339, https://doi.org/10.5194/bg-11-6323-2014, 2014.

Löscher, C. R., Kock, A., Könneke, M., LaRoche, J., Bange, H. W., and Schmitz, R. A.: Production of oceanic nitrous oxide by ammonia-oxidizing archaea, Biogeosciences. 9, 2419–2429, https://doi.org/10.5194/bg-9-2419-2012, 2012.

Martinez-Rey, J., Bopp, L., Gehlen, M., Tagliabue, A., and Gruber, N.: Projections of oceanic N_2O emissions in the 21st century using the IPSL Earth system model, Biogeosciences, 12, 4133–4148, https://doi.org/10.5194/bg-12-4133-2015, 2015.

Meier, H. M., Väli, G., Naumann, M., Eilola, K., and Frauen, C.: Recently accelerated oxygen consumption rates amplify deoxygenation in the Baltic Sea, J. Geophys. Res.-Ocean., 123, 3227–3240, https://doi.org/10.1029/2017JC013686, 2018.

Mohrholz, V., Naumann, M., Nausch, G., Krüger, S., and Gräwe, U.: Fresh oxygen for the Baltic Sea-An exceptional saline inflow after a decade of stagnation, J. Marine Syst., 148, 152–166, https://doi.org/10.1016/j.jmarsys.2015.03.005, 2015.

Naqvi, S. W. A., Jayakumar, D. A., Narvekar, P. V., Naik, H., Sarma, V. V. S. S., D'souza, W., Joseph, S., and George, M. D.: Increased marine production of N_2O due to intensifying anoxia on the Indian continental shelf, Nature, 408, 346–349, 2000.

Naqvi, S. W. A., Bange, H.W., Farías, L., Monteiro, P. M. S., Scranton, M. I., and Zhang, J.: Marine hypoxia/anoxia as a source of CH_4 and N_2O, Biogeosciences, 7, 2159–2190, https://doi.org/10.5194/bg-7-2159-2010, 2010.

Nevison, C., Butler, J. H., and Elkins, J. W.: Global distribution of N_2O and the ΔN_2O-AOU yield in the subsurface ocean, Global Biogeochem. Cy., 17, 1119, https://doi.org/10.1029/2003GB002068, 2003.

Nightingale, P., G. Malin, C. S. Law, A. J. Watson, P. S. Liss, M. I. Liddicoat, J. Boutin, and R. C. Upstill-Goddard: In situ evaluation of air-sea gas exchange parameterizations using novel conservative and volatile tracers, Global Biogeochem. Cy., 14, 373–387, https://doi.org/10.1029/1999GB900091, 2000.

Rabalais, N. N., Cai, W.-J., Carstensen, J., Conley, D. J., Fry, B., Hu, X., Quinones-Rivera, Z., Rosenberg, R., Slomp, C. P., Turner, R. E., Voss, M., Wissel, B., and Zhang, J.: Eutrophication-driven deoxygenation in the coastal ocean, Oceanography, 27, 172–183, https://doi.org/10.5670/oceanog.2014.21, 2014.

Ravishankara, A. R., Danielm J., S., and Portmann, R. W.: Nitrous oxide (N_2O): the dominant ozone-depleting substance emitted in the 21st century, Science, 326, 123–125, https://doi.org/10.1126/science.1176985, 2009.

Rönner, U.: Distribution, production and consumption of nitrous oxide in the Baltic Sea, Geochim. Cosmochim. Ac., 47, 2179–2188, https://doi.org/10.1016/0016-7037(83)90041-8, 1983.

Schlittgen, R. and Streitberg, B. H. J.: Zeitreihenanalyse, Oldenburg Wissenschaftsverlag, Munich, Germany, 1–89, 2001.

Seitzinger, S. P. and Kroeze, C.: Global distribution of nitrous oxide production and N inputs in freshwater and coastal marine ecosystems, Global Biogeochem. Cy., 12, 93–113, 1998.

Siedler, G. and Peters, H.: Properties of sea water, in: Oceanography, edited by Sündermann J., Springer, Berlin, Heidelberg, 233–264, 1986.

Simone, F.: Mann-Kendall Test, MathWorks, https://ww2.mathworks.cn/matlabcentral/fileexchange/25531-mann-kendall-test (last access: 23 October 2019), 2009.

Sohm, J. A., Webb, E. A., and Capone, D. G.: Emerging patterns of marine nitrogen fixation, Nat. Rev. Microbiol., 9, 499–508, https://doi.org/10.1038/nrmicro2594, 2011.

Tiedje, J. M.: Ecology of denitrification and dissimilatory nitrate reduction to ammonium, in: Environmental Microbiology of Anaerobes, edited by: Zehnder, A. J. B., John Wiley & Sons, NY, 179–244, 1988.

Torrence, C. and Compo, G. P.: A practical guide to wavelet analysis, B. Am. Meteorol. Soc., 79, 61–78, 1998.

Torrence, C. and Compo, G. P.: Wavelet analysis, http://paos.colorado.edu/research/wavelets/ (last access: 23 October 2019), 2004.

Voss, M., Emeis, K. C., Hille, S., Neumann, T., and Dippner, J. W.: Nitrogen cycle of the Baltic Sea from an isotopic perspective, Global Biogeochem. Cy., 19, GB3001, https://doi.org/10.1029/2004GB002338, 2005.

Walter, S., Breitenbach, U., Bange, H. W., Nausch, G., and Wallace, D. W.: Distribution of N_2O in the Baltic Sea during transition from anoxic to oxic conditions, Biogeosciences, 3, 557–570, https://doi.org/10.5194/bg-3-557-2006, 2006.

Wanninkhof, R.: Relationship between wind speed and gas exchange over the ocean revisited, Limnol. Oceanogr.-Method., 12, 351–362, https://doi.org/10.4319/lom.2014.12.351, 2014.

Weiss, R. F. and Price, B. A.: Nitrous oxide solubility in water and seawater, Mar. Chem., 8, 347–359, https://doi.org/10.1016/0304-4203(80)90024-9, 1980.

Wilson, S. T., Ferrón, S., and Karl, D. M.: Interannual variability of methane and nitrous oxide in the North Pacific Subtropical Gyre, Geophys. Res. Lett., 44, 9885–9892, https://doi.org/10.1002/2017GL074458, 2017.

Xu, Z. X., Takeuchi, K., and Ishidaira, H.: Monotonic trend and step changes in Japanese precipitation, J. Hydrol., 279, 144–150, https://doi.org/10.1016/S0022-1694(03)00178-1, 2003.

Yang, D., Li, C., Hu, H., Lei, Z., Yang, S., Kusuda, T., Koike, T., and Musiake, K.: Analysis of water resources variability in the Yellow river of China during the last half century using the historical data, Water Resour. Res., 40, 1–12, https://doi.org/10.1029/2003WR002763, 2004.

Zhang, G.-L., Zhang, J., Liu, S.-M., Ren, J.-L., and Zhao, Y.-C.: Nitrous oxide in the Changjiang (Yangtze River) estuary and its adjacent marine area: Riverine input, sediment release and atmospheric fluxes, Biogeosciences, 7, 3505–3516, https://doi.org/10.5194/bg-7-3505-2010, 2010.

Chapter 4

Nitrous oxide and hydroxylamine measurements in the southwest Indian Ocean

Journal of Marine Systems 209 (2020) 103062

Contents lists available at ScienceDirect

Journal of Marine Systems

journal homepage: www.elsevier.com/locate/jmarsys

Nitrous oxide and hydroxylamine measurements in the Southwest Indian Ocean

Xiao Ma*, Hermann W. Bange, Gesa K. Eirund[1], Damian L. Arévalo-Martínez

GEOMAR Helmholtz Centre for Ocean Research Kiel, Düsternbrooker Weg 20, 24105 Kiel, Germany

ARTICLE INFO

Keywords:
Nitrous oxide
Hydroxylamine
Atmospheric gases
Air-water interface
Hydrography

ABSTRACT

The southwestern basin of the Indian Ocean (SWIO) remains a rather under-sampled region with regard to nitrogen-cycle processes. Here we present the results of extensive nitrous oxide (N_2O) measurements as well as the first reported open ocean measurements of hydroxylamine (NH_2OH). Enhanced N_2O sea-to-air fluxes were found in the zonal band between 5°S and 10°S as a result of wind-driven upwelling, and N_2O depth profiles showed supersaturation throughout the water column with a distinct maximum at about 1000 m. Excess N_2O (ΔN_2O) was found to be positively correlated with apparent oxygen utilization (AOU) and nitrate. Although the water column distribution of NH_2OH was highly variable, combined analysis with N_2O and nutrient data allows us to argue for nitrification as the major formation pathway of N_2O in the SWIO.

1. Introduction

Nitrous oxide (N_2O) is an atmospheric trace gas which significantly affects the global climate system due to its role as a greenhouse gas and the substrate of a major ozone-depleting precursor (NO radical) in the stratosphere (Ravishankara et al., 2009; Myhre et al., 2013). In the ocean, N_2O production is dominated by two microbial processes: nitrification and denitrification. During nitrification, N_2O is produced as a by-product during the oxidation of ammonium (NH_4^+) to nitrate (NO_3^-) via hydroxylamine (NH_2OH) and nitrite (NO_2^-) (see e.g. Bakker et al., 2014), which is performed by both ammonia-oxidizing archaea (AOA) and ammonia-oxidizing bacteria (AOB) (Santoro et al., 2011; Löscher et al., 2012). Although detailed metabolic processes have been proposed, it remains controversial to what extent one or the other nitrification pathway is predominant as N_2O source in various aquatic and soil environments (Löscher et al., 2012; Zhang et al., 2012; Smith et al., 2014; Banning et al., 2015; Li et al., 2015). Although nitrification occurs under oxic conditions, it has been shown that N_2O production increases with decreasing environmental oxygen (O_2) concentrations (see e.g. Elkins et al., 1978; Goreau et al., 1980; Lipschultz et al., 1981; Löscher et al., 2012). Denitrification is the sequential reduction of NO_3^- to gaseous nitrogen (N_2) via NO_2^-, nitric oxide (NO) and N_2O, and it occurs mostly under suboxic conditions ($0 < O_2 < 2$–$10\,\mu mol\,L^{-1}$; Codispoti et al., 2005). In this pathway, N_2O is produced as an intermediate and its accumulation is considered to be a result of incomplete denitrification (Naqvi et al., 2000; Farias et al., 2009; Babbin et al., 2015).

Unlike N_2O, NH_2OH is an intermediate in the nitrification pathway, being produced during the oxidation of NH_4^+ to NO_2^- (see above). During the so-called hydroxylamine pathway (Stein, 2011), N_2O is produced via the reaction: NH_2OH ($\rightarrow$NO) $\rightarrow N_2O$. A direct enzymatic pathway has been found from NH_2OH to N_2O in AOB *Nitrosomonas europaea* (Caranto et al., 2016), however, nitric oxide (NO) is not obligatory in this process and the mechanism is not yet well understood. Although combined physiological and stable isotope tracer analyses support NH_2OH metabolism in ammonia oxidation by AOA such as *Nitrosopumilus maritimus* (Vajrala et al., 2013), the hydroxylamine pathway remains to be proven due to the absence of genes encoding for hydroxylamine oxidoreductase, which is the known enzyme responsible for catalyzing the conversion of NH_4^+ to NO_2^- (Walker et al., 2010). While NH_2OH is considered to be a precursor for bacterial nitrification under oxic conditions (Yamazaki et al., 2014; Sabba et al., 2015), its relevance in archaeal nitrification is not known yet (Santoro et al., 2011).

The Indian Ocean (IO) is a complex basin which has a profound impact on climate variability both on regional and global scales (Schott et al., 2009). Yet, the IO is at present a comparatively under-sampled and poorly understood basin. This has, in turn, motivated the creation of international large-scale initiatives aiming to improve our current understanding of the IO system, as well as its economical and societal influence on the bordering countries (see e.g. Hood et al., 2016). The major upper ocean oceanographic regimes of the IO are the monsoon-

* Corresponding author.
E-mail address: mxiao@geomar.de (X. Ma).
[1] Present address: Institute for Atmospheric and Climate Science, ETH Zurich Universitätstrasse 16, 8092, Zurich, Switzerland.

https://doi.org/10.1016/j.jmarsys.2018.03.003
Received 31 March 2017; Received in revised form 30 November 2017; Accepted 17 March 2018
Available online 21 March 2018
0924-7963/

driven tropical and subtropical Northern Hemisphere circulation and the Southern Hemisphere subtropical gyre circulation. These two regimes are separated by the South Equatorial Current (SEC) which flows westward at about 10–12°S, transporting waters from the Pacific through the Indonesian Throughflow (ITF; Schott et al., 2009). The SEC plays a dominant role in the upper 1000 m and extends across the IO until the African coast where it separates in northward and southward-flowing branches (Stramma and Lutjeharms, 1997). A relevant open ocean feature of the Southwest IO (SWIO) is the occurrence of wind-driven upwelling at 5–10°S, which is part of a subtropical cell (STC) consisting of subduction and westward transport of ITF waters, northward transport after reaching the African coast (East African Coastal Current), and an eastward flow as part of the South Equatorial Countercurrent (SECC; Schott et al., 2009).

Although the IO is considered a key region for N_2O production and emissions to the atmosphere (Bange, 2009), a vast majority of the studies carried out so far have been concentrated on the northern sector, in particular the Arabian Sea, since the co-occurrence of coastal upwelling and weak ventilation leads to the formation of a prominent oxygen minimum zone (OMZ) and extremely high N_2O emissions to the atmosphere (see e.g. Law and Owens, 1990; Naqvi et al., 2000). Hence, except for the surface measurements of Weiss et al. (1992), N_2O measurements from the SWIO are scarce and therefore its role for the open ocean emissions is still unclear.

Here we present the first comprehensive set of surface and water column N_2O measurements in the SWIO, as well as depth profiles of NH_2OH for selected stations. While NH_2OH has been measured in coastal areas and estuaries (Butler et al., 1987; Butler et al., 1988; Gebhardt et al., 2004; Schweiger et al., 2007), here we report the first NH_2OH observations in the open ocean. The main objectives of this study are: 1) to investigate the surface and vertical distribution of N_2O concentrations in the SWIO, 2) to quantify N_2O sea-to-air fluxes from this area, and 3) to explore the role of NH_2OH in N_2O formation.

2. Study sites

The field work was carried out during two cruises on board of the German research vessel RV Sonne I: the first leg (SO234-2, 8th - 20th of July 2014) started from Durban (South Africa), stopped in Madagascar and ended in Port Louis (Mauritius), whereas the second leg (SO235, 23th of July - 07th of August 2014) continued from Port Louis in northward and eastward direction until Malé (Maldives). Our cruise tracks cover the area between about 1°N and 30°S, where the trade wind regime largely affects the hydrographic settings in the SWIO. The cruise tracks and sampling locations are depicted in Fig. 1.

3. Methods

3.1. Continuous measurements of N_2O

Surface measurements of dissolved N_2O were carried out continuously during SO234-2 and SO235 by means of an underway system as described in Arévalo-Martínez et al. (2013). Briefly, the analytical system consists of a shower-head equilibration system coupled to an N_2O/CO analyzer from Los Gatos Research Inc. (USA). A permanent supply of seawater from about 6 m depth was accomplished by installing a submersible pump (LOWARA, Xylem Inc., Germany) at the ship's hydrographic shaft. Atmospheric measurements were conducted in six-hour intervals by pumping air from about 20 m height into the system. The N_2O/CO analyzer was calibrated on board with a reference gas mixture which contained 367.58 ppb N_2O and daily measurements of gas cylinders with mixing ratios on the range 360–750 ppb N_2O were used to assess instrumental drift. The overall accuracy of the system was 0.1 nmol L^{-1} N_2O. Data handling as well as the procedures used to compute N_2O concentrations are explained in detail in Arévalo-Martínez et al. (2013) and references therein. N_2O flux densities (F_{N2O}, in nmol m^{-2} s^{-1}) were calculated with the expression:

$$F_{N2O} = k_{N2O}.\ \Delta C_{N2O} \quad (1)$$

where k_{N2O} is the gas transfer velocity and ΔC_{N2O} is the N_2O concentration difference (in nmol L^{-1}) between seawater and atmosphere. For the computation of k_{N2O} we used the parameterizations by Nightingale et al. (2000; hereafter N00) and Ho et al. (2006; hereafter HO_06) with underway wind speeds measured by the ship's weather station after standardizing them to 10 m height (Garrat, 1977). k_{N2O} was multiplied by the corrected Schmidt number (Sc) for N_2O ($Sc/600)^{-0.5}$, whereby Sc was computed according to Walter et al. (2004). We choose the N00 parameterization since it has been shown to be stable over a wide range of environmental conditions, whereas the HO_06 parameterization was chosen since it is particularly suitable for wind speeds above 15 m s^{-1} (Ho et al., 2006). Overall, k_{N2O} values were about 5% higher when computed with HO_06 and in consequence all N_2O flux density values presented in this study are reported as a range whereby the lower (higher) values were yielded from the use of N00 (HO_06). Atmospheric equilibrium concentration of N_2O (C_{atm}) was computed as a function of SST and in situ salinity (Weiss and Price, 1980) at the time of the measurements and the dry mole fractions of N_2O measured during the cruises. Our measured dry mole fractions (mean: 324.8 ± 0.9 ppb N_2O) were in fairly good agreement with the mean of 326 ppb N_2O for July–August 2014 at the NOAA's cooperative global air sampling network station at Mahe Island (4.68°S, 55.53°E, height: 2 masl; available online under: https://www.esrl.noaa.gov/gmd/dv/iadv/). N_2O saturations (N_2O_{sat}, in %) were calculated as:

$$N_2O_{sat} = 100 \times C_{sw}/C_{atm} \quad (2)$$

3.2. Depth profiles of N_2O and NH_2OH

Discrete N_2O samples were collected from 10 L Niskin Bottles mounted on a standard CTD-Rosette during SO235. Seawater was drawn into 20 mL dark septum bottles after rinsing them at least twice their volume and ensuring the absence of air bubbles. Subsequently, the vials were sealed with rubber stoppers and aluminum caps. Samples were poisoned immediately by adding 50 µL of a saturated solution of mercury chloride ($HgCl_2$), and were measured on board within 24 h using a gas chromatographic method as described in Kock et al. (2016). Samples were analyzed with a static headspace equilibration method. For this, a 10 mL Helium (99.9999%, AirLiquide, Düsseldorf, Germany) headspace was injected into each vial by using a gas-tight syringe (VICI Precision Sampling, Baton Rouge, LA). After allowing the sample headspace to equilibrate with the water phase (at least 2 h), a 9.5 mL gas subsample was injected into the GC/ECD (gas chromatograph/electron capture detector) through a 2 mL sample loop. Serial dilutions of two standard gas mixtures (573.8 and 1484 ppb N_2O in synthetic air; Deuste Steininger GmbH, Mühlhausen, Germany) were used to calibrate the ECD response on a daily basis both before and after the measurements, as described in Kock et al. (2016). The average precision of the measurements was 0.4 nmol L^{-1}. Data acquisition and the calculation of excess of N_2O (ΔN_2O) and apparent oxygen utilization (AOU) were done as in Walter et al. (2006).

Dissolved NH_2OH was measured during SO235 with the improved ferric ammonium sulfate (FAS) conversion method from Kock and Bange (2013). This method is based on the conversion of NH_2OH to N_2O while scavenging NO_2^- by adding a sulfanilamide/acetic acid solution (SA) to the samples, thus avoiding the significant bias which results from the use of the traditional FAS method. Sample collection and headspace creation were performed as for N_2O, but no $HgCl_2$ was added since the samples were processed immediately (< 30 min). The N_2O resulting from NH_2OH conversion was measured with GC/ECD as mentioned above. The NH_2OH concentration in the samples was calculated as follows:

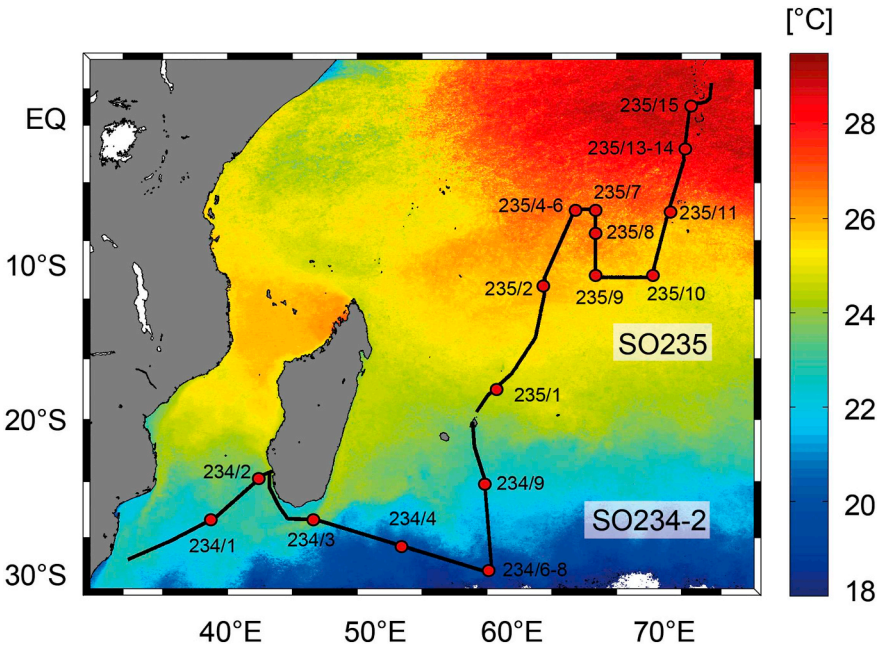

Fig. 1. Ship tracks and sampling locations during the SO234-2 and SO235 cruises. Cruise tracks are overlain on monthly mean MODIS-Aqua SST for July–August 2014 (4 km resolution, retrieved from the Goddard Earth Sciences Data and Information Services Center: http://disc.sci.gsfc.nasa.gov/giovanni/).

$$[NH_2OH] = ([N_2O]_{FAS} - [N_2O]_{BG})/RC \quad (3)$$

$$RC = m_{std} \times 2 \quad (4)$$

where $[N_2O]_{FAS}$ and $[N_2O]_{BG}$ are N_2O concentrations with and without FAS conversion. The factor of two in the calculation of the recovery factor (RC, Eq. (4)) derives from the stoichiometry of the reaction between NH_2OH and FAS. m_{std} is the regression slope of the standard addition. Four different standard solutions were diluted from a stock solution of hydroxylammonium chloride (p.a., Merck KGaA, Darmstadt, Germany, 20 mg per 100 mL, the exact concentration was calculated from the mass weight), which was prepared in an aqueous solution of acetic acid (p.a., Merck KGaA, 3 mL of acetic acid (glacial) per 1 L of MilliQ water, pH~3). A 100 µL volume of standard solution was added into the vials and the final concentrations fell between 0 and 100 nmol L^{-1}. The standard solutions were prepared one day before analysis and stored at 4 °C in the dark. The detection limit for NH_2OH was estimated to be approximately 0.6 nmol L^{-1}. Further details can be found in Kock and Bange (2013).

Dissolved O_2 concentrations were measured by using an optode attached to the CTD-Rosette. The optode was calibrated against discrete samples collected and measured on site by means of the Winkler method (Hansen, 1999; overall precision ± 0.5 µmol kg^{-1}). The inorganic nutrients NO_3^- and NO_2^- were measured on board with a QuAAtro auto-analyzer from SEAL Analytical (overall precision ± 0.2 µmol L^{-1}).

4. Results and discussion

4.1. Hydrological settings in the SWIO

Fig. 2a shows discrete T-S data with color coded dissolved O_2 concentrations during the SO235 cruise. Surface circulation in the SWIO is dominated by SEC and SECC (Wyrtki, 1973). Surface water with high temperature and salinity was identified as SECC Surface Water (SECCSW). Compared to the SECCSW, the SEC Surface Water (SECSW) is characterized by relatively low temperature and salinity. The low salinity may derive from excess precipitation over evaporation in the northeastern part of the IO or the influx of low salinity water through the Indonesian Archipelago, which is then advected with the SEC (Morales et al., 1997). Below the surface is the high salinity water which originates from the subtropical gyre. Subtropical Surface Water (SSW) extends northward and forms a shallow salinity maximum. Below the SSW, salinity was observed to decrease linearly with depth and these water masses were identified as South Indian Central Water (SICW). Antarctic Intermediate Water (AIW), formed at the Antarctic Convergence near 50°S, sinks and spreads in the depth 700 m or below (Morales et al., 1997).

As can be seen in Fig. 2b and c, there were marked differences in water properties of the southern and northernmost stations during SO235. Exceptionally high O_2 concentrations were observed at station 235/1, especially between the depths of 300 m and 600 m, with the SSW as the likely O_2 source from the south as a compensation for the western boundary Agulhas Current (Toole and Warren, 1993). In contrast, minimum O_2 concentrations of ca. 35 µmol L^{-1} were observed at station 235/15. Oxygen concentrations were the lowest between density 23–27 kg m^{-3} where Arabian Sea water penetrates. However, the southward intrusion of the Arabian Sea water is inhibited by the equatorial currents throughout the year (Kumar and Prasad, 1999). The presence of O_2 prevented N_2O metabolic pathways which are dominant under suboxic conditions, such as denitrification and dissimilatory reduction of NO_3^- to ammonium (DNRA). Hence, N_2O/NH_2OH variations could be attributed to nitrification in the water column.

4.2. Surface distribution and sea-air fluxes of N_2O

As expected from the open ocean location, surface N_2O concentrations were generally low, fluctuating between 5.8 and 8.0 nmol L^{-1} (mean ± SD: 6.9 ± 0.6 nmol L^{-1}). Nevertheless, surface waters of the SWIO at the time of sampling were mostly supersaturated with respect to atmospheric equilibrium (mean ± SD: 104.1 ± 2.8%), and slightly undersaturated waters were only found in a few areas at about 25–30°S (Fig. 3a). As can be seen in Table 1, our N_2O saturation values are well within the range of previous observations in the SWIO. The notable resemblance between our values and those from other studies, albeit the different analytical methods, years and part of the seasonal cycle in which the measurements were conducted (Supplementary Fig. 1), suggests a rather weak though permanent site for outgassing of N_2O to the atmosphere.

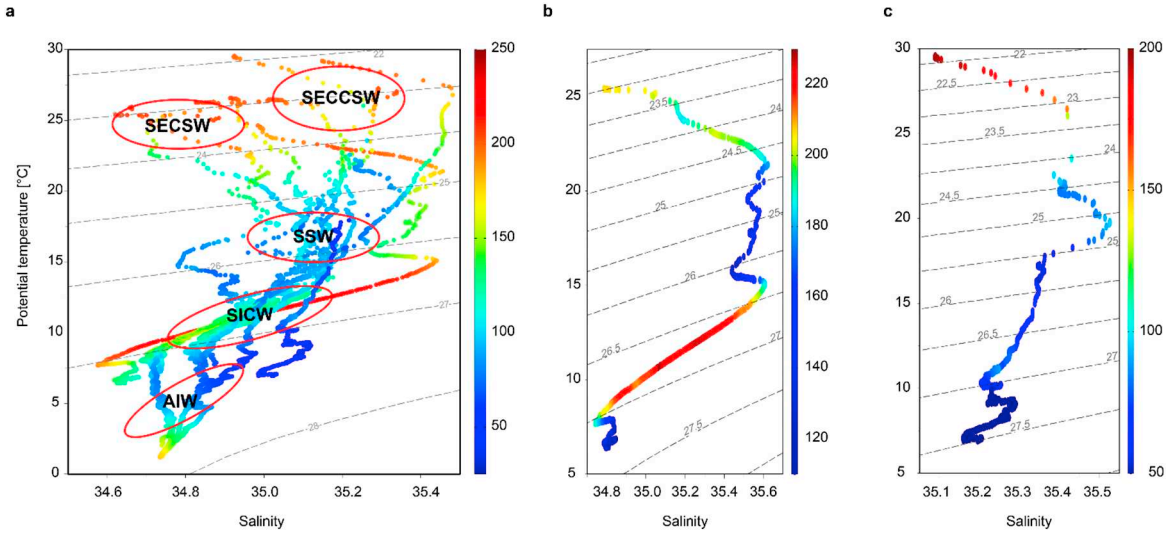

Fig. 2. T-S diagram for all the stations of the SO235 cruise. (a) The main water masses which can be identified are: SECCSW (South Equatorial Countercurrent Surface Water); SECSW (South Equatorial Current Surface Water); SSW (Subtropical Surface Water); SICW (South Indian Central Water); AIW (Antarctic Intermediate Water). (b) T-S diagram from station SO235/1. (c) T-S diagram from station SO235/15. The dashed lines in a-c indicate potential density (in kg m^{-3}) and the color bars depict in situ O_2 concentrations (in µmol kg^{-1}). (For interpretation of the references to color in this figure legend, the reader is referred to the web version of this article.)

It is worth noting, however, that although close-to-equilibrium N_2O concentrations/saturations were the predominant during our study, we observed enhanced N_2O saturations (up to 122.1%) at 5–10°S, coinciding with the location of the wind-driven open ocean upwelling area in the SWIO (Supplementary Fig. 1). Upwelling at this location is caused by Ekman pumping along the northern boundary of the southeast trade winds (which is also the boundary between the SECC and the SEC), and it constitutes one of the pathways for the transport of cold waters towards the tropical band as part of the IO STC (Schott et al., 2009). Since upwelling is rather weak in this area, it cannot be easily detected from satellite SST (e.g. see Fig. 1). However, depth profiles of physical properties during SO235 supported the occurrence of this process (Fig. 3b). Similar to our study, Butler et al. (1989) reported a mean N_2O saturation of 120% in the eastern IO, which could be associated with upwelling at about 8°S. Open ocean upwelling in the IO generally takes place at off-equatorial locations, as opposed to the Pacific and Atlantic oceans which experience seasonal upwelling of cold, subsurface waters in the equatorial region (Mitchell and Wallace, 1992). For comparison, mean N_2O saturations ranging from 104% to 125% (maximum 140%) have been reported for the equatorial Pacific (Elkins et al., 1978; Singh et al., 1979; Cline et al., 1987), whereas for the Atlantic counterpart Walter et al. (2004) reported values of up to 118% during boreal autumn (i.e. not during the upwelling season). More recently, Arévalo-Martínez et al. (2017) reported saturations up to 159% (mean 118%) for the same region of the Atlantic after the onset of the upwelling season. Although drawing a direct comparison between our data and data from equatorial systems is difficult because of the underlying oceanographic differences which characterize the SWIO, it could be argued that if the N_2O outgassing in the SWIO is a perennial feature (as upwelling is), the overall share of this area to the tropical marine emissions of N_2O can be higher than previously assumed. However, in the absence of long-term records which capture the annual variability across the tropical band of the three basins, this hypothesis remains to be proven.

Sea-to-air fluxes of N_2O at the time of sampling were highly variable and spanned a wide range of wind speeds (0.4–24.2 m s^{-1}, see Supplementary Fig. 2). Flux densities fluctuated between 0.0032 and 0.0078 and 2.34–2.62 nmol N_2O m^{-2} s^{-1} (mean ± SD: 0.51–0.54 ± 0.37–0.41 nmol N_2O m^{-2} s^{-1}), with the highest values north of 20°S. Our upper limit for N_2O flux seems fairly high, in particular considering that it is based on open ocean measurements (cf. Nevison et al., 2004). However, this can be explained by the high wind speeds encountered during the cruises, which reached up to 15 m s^{-1} at 10°S and 24.2 m s^{-1} at 15–20°S. These wind speeds agree well with observations and climatologic wind fields for the western IO (Collins et al., 2012; Fiehn et al., 2017) and suggest the potential for strong sea-to-air fluxes of N_2O and possibly other climate-relevant gases in the SWIO. Hence, the elevated wind speeds in the northern sector of our survey in conjunction with the enhanced gradient between the ocean and atmosphere due to upwelling resulted in the higher than expected N_2O fluxes to the atmosphere. It should be pointed out that for the flux density computation we used instantaneous, along-track wind speeds as measured by the ship's sensors. In order to objectively assess the magnitude of the N_2O fluxes out of the SWIO in longer time scales, climatologic winds and long-term observations of the sea-air gradient of N_2O in the SWIO (and in particular at 5–10°S) should be used. Thus, an estimation of the total N_2O emission from the whole region is not intended within this manuscript since upscaling the fluxes based on our single survey would not be representative.

Nevertheless, it is interesting to consider a potential contribution of the SWIO to the overall N_2O efflux from the neighboring northern IO (NIO), which is considered a strong source of this gas to the atmosphere (Bange et al., 2001a). Fiehn et al. (2017) showed that the atmospheric Monsoon circulation regime transports very short-lived substances emitted in the SWIO towards the north east (Bay of Bengal), where they ascend and reach the tropopause after about a month. Likewise their study showed that besides the NIO, the tropical west IO is also an important region for the transport of gases towards the stratosphere. Given that N_2O has a long residence time in the atmosphere (~121 years; Myhre et al., 2013), it is reasonable to assume that the emissions derived from the SWIO, and in particular those resulting from open ocean upwelling at 5–10°S, might get transported towards the stratosphere via either of the two above-mentioned entrainment regions. Moreover, it could be hypothesized that the large-scale transport of N_2O emitted to the atmosphere might be stronger during the summer months where steady southeasterly trade winds are dominant at the latitudes occupied during the sampling. Likewise, although our N_2O flux density values are about one order of magnitude lower than those reported for different locations of the NIO (e.g. Law and Owens, 1990; Naqvi et al., 1994; Naqvi et al., 2000; Bange et al., 2001a), it cannot be

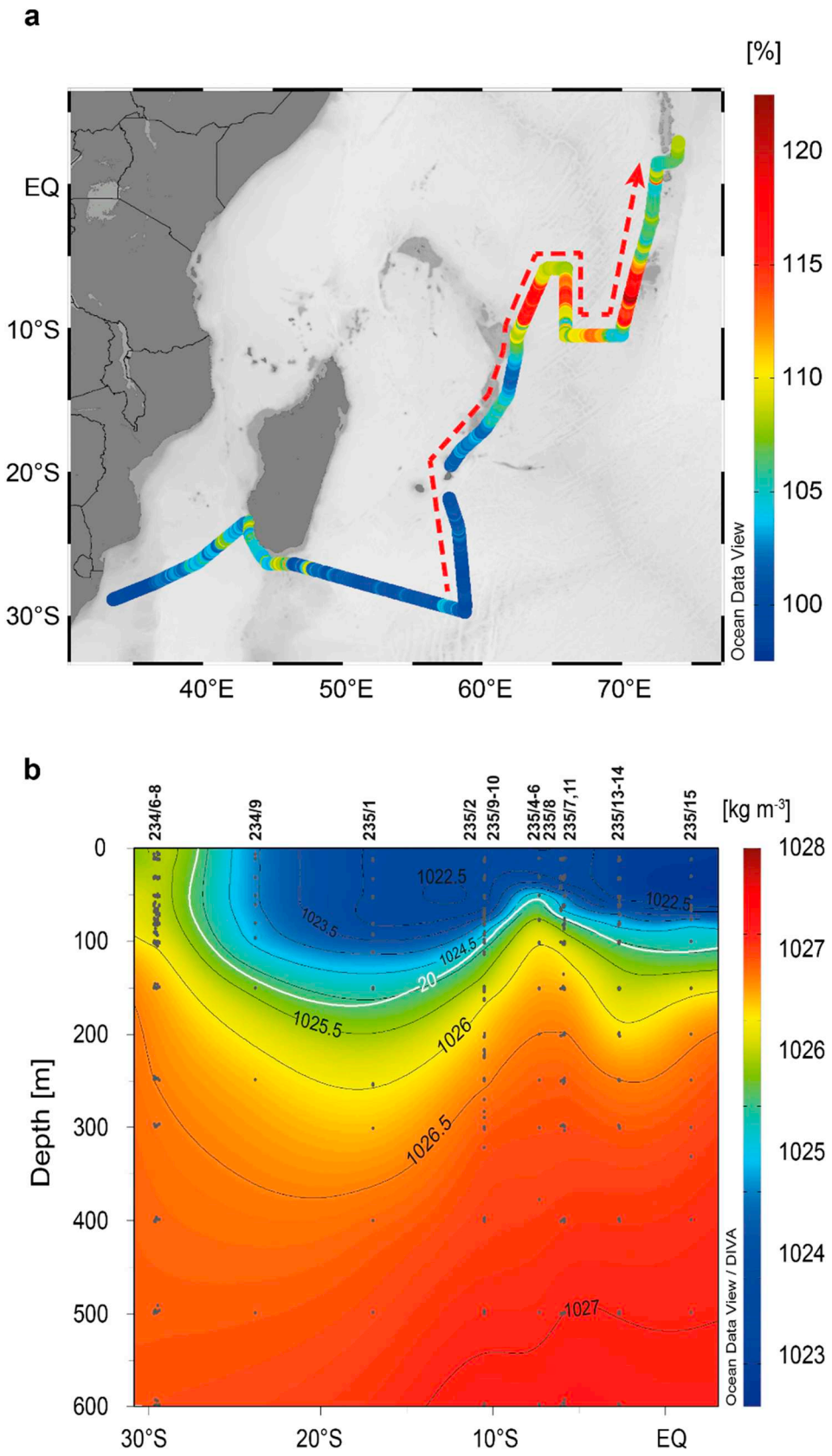

Fig. 3. Surface distribution of N_2O saturation in the SWIO. (a) N_2O saturation computed from along-track seawater and atmospheric measurements during SO234-2 and SO235. (b) Vertical distribution of potential density along a meridional transect between 30°S and 1°N with the 20 °C isotherm depicted as a white solid line. The red dashed line in (a) indicates the direction of the ship track shown in (b), whereas the upper numbers in (b) are the station numbers (c.f. Fig. 1). (For interpretation of the references to color in this figure legend, the reader is referred to the web version of this article.)

Table 1
Compilation of available N_2O saturation values from shipboard observations in the SWIO.

Cruise	Dates	Location	N_2O Saturation	
			($\bar{x}$ ± SD)	Range
Indomed Leg 4[a,c]	January 1978	4°N–20°S 50–59°E	105.8 ± 6.6%	96.8–127.9%
Indomed Leg 5[a,c]	January 1978	20–30°S 56–58°E	101.8 ± 1.4%	97.6–104.7%
RV/Meteor 32 legs 3–5[b,c]	May-Aug. 1995	5°N-30°S 31–76°E	103.8 ± 6.2%	98.0–127.8%
SO234-2 (this study)	July 2014	21–28°S 37–58°E	101.5 ± 1.8%	99.4–111.4%
SO235 (this study)	July-Aug. 2014	3°N–19°S 58–74°E	107.0 ± 3.9%	100.6–122.1%

[a] From Weiss et al. (1992).
[b] From Nevison et al. (2004).
[c] Saturation values were computed with data retrieved from the MEMENTO database (see Bange et al., 2009).

ruled out that overall the SWIO does contribute, at least temporarily, to the regional N_2O atmospheric budget of the NIO. At what extent the measured emissions at a given location in the NIO might actually correspond to air masses transported from the SWIO, as well as the efficiency with which N_2O is transported to the stratosphere at either of the major entrainment regions suggested by Fiehn et al. (2017), is still unclear and it should be addressed in future studies.

In summary, our surface data show that the SWIO was in general a rather weak, yet perennial and far-reaching (in terms of atmospheric transport) source of N_2O to the atmosphere at the time of sampling, with most of the outgassing taking place along the zonal band between 5°S and 10°S, where wind-driven upwelling led to enhanced dissolved concentrations of N_2O with respect to the overlying atmosphere.

4.3. Depth distribution of N_2O

N_2O distributions in the SWIO featured strong variations with water depth. Over the cruise track of SO235, N_2O concentrations increased in the upper 150 m and a subsurface N_2O maximum (mean ± SD: 30.6 ± 4.4 nmol L^{-1}) could be observed at about 200 m (Fig. 4). At Station 235/1, a distinct N_2O concentration decline was found at the depth between 400 and 500 m, coinciding with the intrusion of SSW waters with high O_2 concentrations (mean ± SD: 222.1 ± 2.8 µmol kg^{-1}; see also depth distribution of temperature and salinity in Supplementary Fig. 3). Maximum N_2O concentrations occurred in subsurface waters at Station 235/15, where O_2 concentrations were relatively low as a result of the Arabian Sea water intrusion.

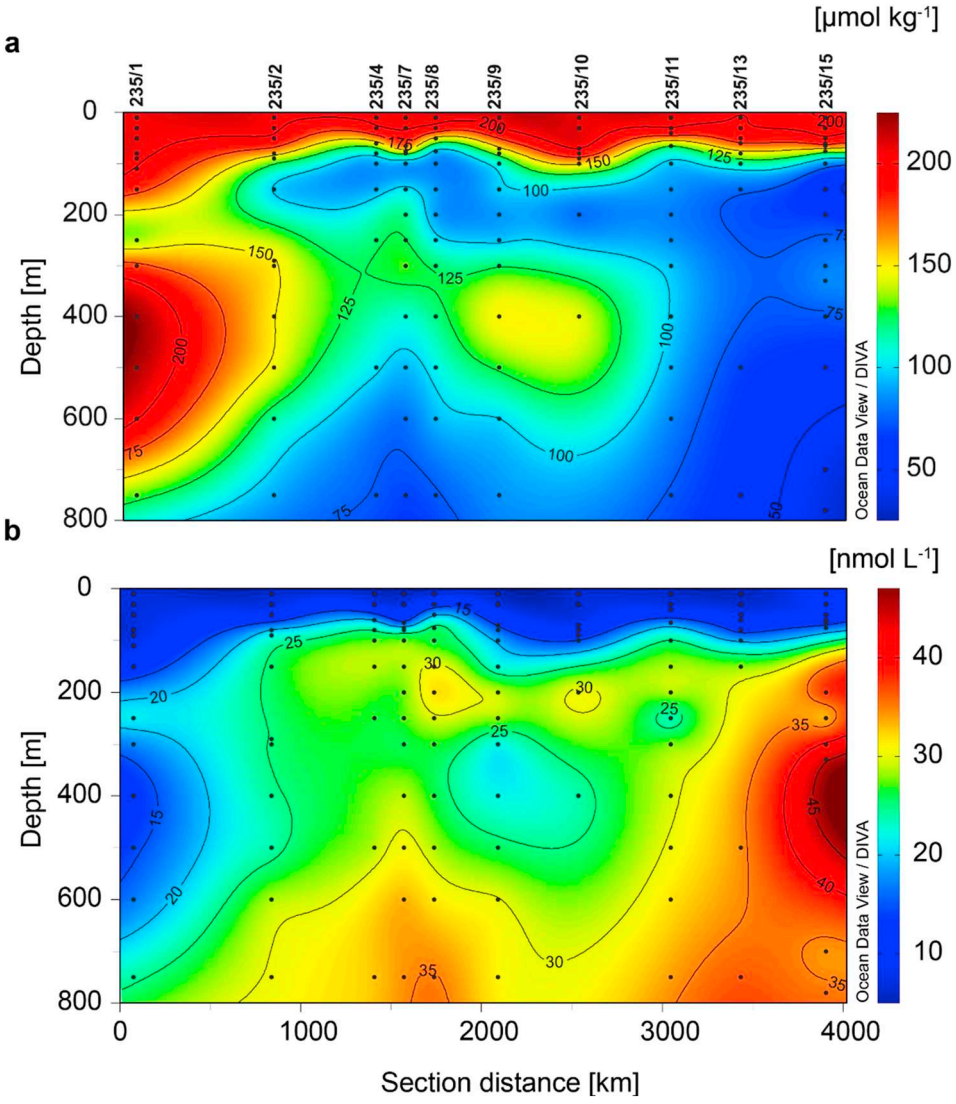

Fig. 4. Depth distributions of O_2 (a) and N_2O (b) concentrations during SO235. The numbers above panel (a) indicate the station numbers (c.f. Fig. 1).

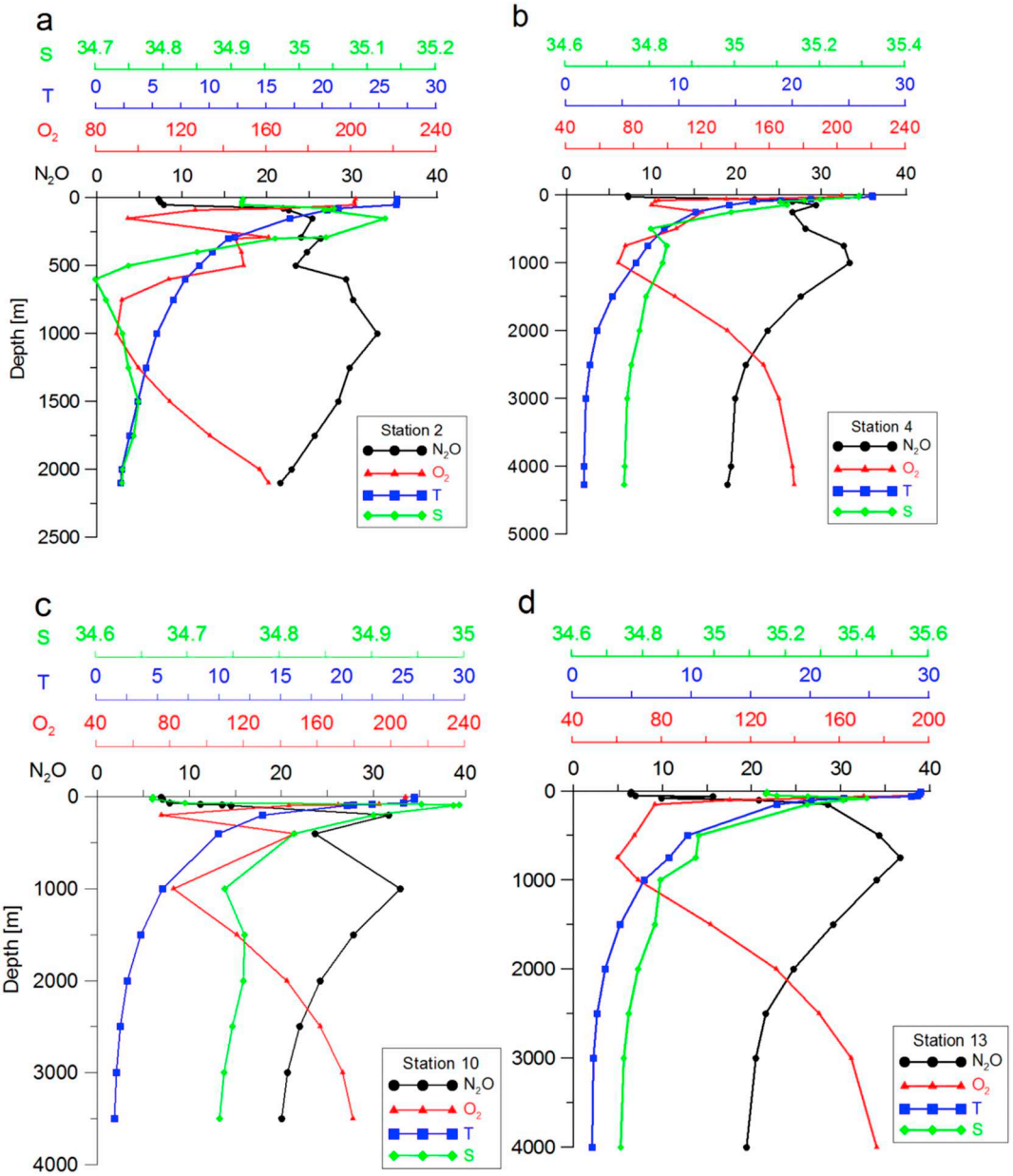

Fig. 5. Vertical distributions of salinity (S, green line), temperature (T, blue line, °C), dissolved oxygen (O_2, red line, μmol kg^{-1}) and N_2O (black line, nmol L^{-1}) at deep cast stations of SO235/2 (a), SO235/4 (b), SO235/10 (c) and SO235/13 (d). (For interpretation of the references to color in this figure legend, the reader is referred to the web version of this article.)

In deep stations we observed a pronounced N_2O maximum at about 1000 m (Fig. 5). Below 1000 m N_2O concentrations declined gradually with depth. Similar profiles were also found in the western Pacific (Butler et al., 1989), western and tropical North Atlantic (Yoshinari, 1976; Walter et al., 2006). Although the vertical distributions of N_2O varied at different stations, we observed a generally inverse relationship between N_2O and O_2.

In order to investigate the relationship between N_2O production and O_2 consumption, we used a simple regression analysis. The ΔN_2O was found to positively correlate with AOU (Fig. 6). We found different ΔN_2O/AOU ratios above and below 1000 m, and the slopes of the regression lines were 0.095 and 0.229 nmol μmol^{-1}, respectively. Similarly, Cline et al. (1987) observed systematic increases of ΔN_2O/AOU ratio in the eastern equatorial Pacific from the surface to the O_2 minimum depth. The variability in ΔN_2O/AOU ratios is more significant in the biologically active region. The data from Elkins et al. (1978) showed a ratio of about 0.36 nmol μmol^{-1} in the upwelling regions against 0.17 nmol μmol^{-1} elsewhere. Upstill-Goddard et al. (1999) found that a second-order polynomial fitted statistically best to the ΔN_2O/AOU relationship in the Arabian Sea, which indicates the N_2O formation via coupled nitrification-denitrification. Bange et al. (2001b) attributed the poor ΔN_2O/AOU correlations in the deep Arabian waters to a shift of N_2O production pathway from nitrification to denitrification. This idea was further supported by the changes of N_2O isotopic composition in the subtropical North Pacific gyre (Ostrom et al., 2000). More recently, Trimmer et al. (2016) provided isotopic and genetic evidence to link the exponential N_2O increase not only to decreasing O_2 but also to archaeal gene abundance. Our ΔN_2O/AOU ratios were comparable with the values reported for different tropical and subtropical regions (Table 2).

The slope of the linear regression between ΔN_2O and AOU is affected by various factors such as organic matter composition, variability in N_2O production pathways, and mixing of different water masses (Elkins et al., 1978). Our values for the ΔN_2O/AOU relationship implied

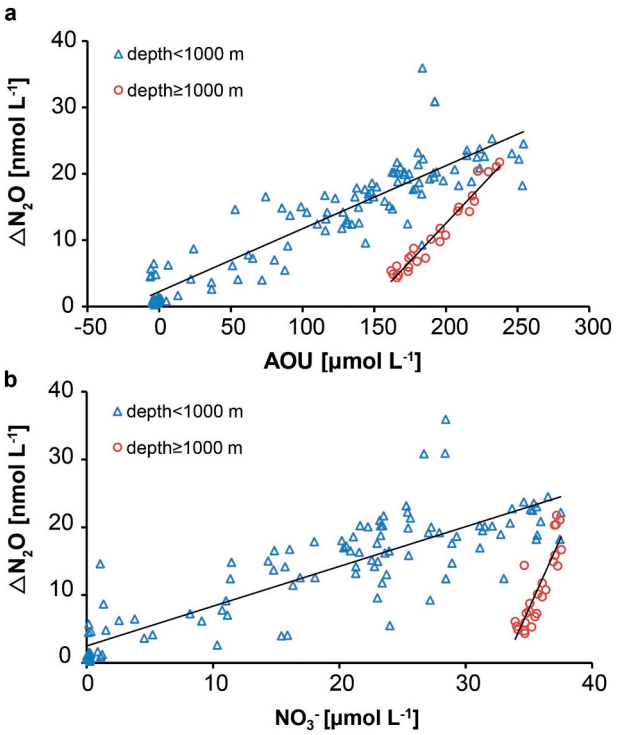

Fig. 6. ΔN_2O/AOU (a) and $\Delta N_2O/NO_3^-$ (b) relationships during SO235. Blue triangles and red circles represent data above and below 1000 m depth, respectively. The black lines show the corresponding regression lines for each subset of data: (a) $y = 0.095x + 2.252$, $r^2 = 0.842$, $n = 122$ (< 1000 m), $y = 0.229x - 33.237$, $r^2 = 0.953$, $n = 25$ (≥1000 m); (b) $y = 0.586x + 2.513$, $r^2 = 0.756$, $n = 122$ (< 1000 m), $y = 4.156x - 137.490$, $r^2 = 0.743$, $n = 25$ (≥1000 m). (For interpretation of the references to color in this figure legend, the reader is referred to the web version of this article.)

Table 2
ΔN_2O/AOU ratios in tropical and subtropical open ocean locations.

Reference	Region	Depth range [m]	Δ N_2O/AOU ratio [nmol μmol^{-1}]
Elkins et al. (1978)	Central Pacific	0–1000	0.168
Cline et al. (1987)	Eastern Equatorial Pacific	0–400	0.085–0.186
Butler et al. (1989)	West Pacific and East Indian Oceans	0–6000	0.124
Bange et al. (2001b)	Arabian Sea	0–150	0.080–0.106
		150–2000	0.061–0.095
		2000–4000	0.067–0.336
Charpentier et al. (2007)	South Pacific Subtropical Gyre	200–1000	0.0875
Forster et al. (2009)	Tropical Atlantic	0–300	0.106–0.121
This study	Southwest Indian Ocean	0–1000	0.0948
		1000–4000	0.2288

a higher yield of N_2O per mole O_2 consumed below 1000 m. However, it should be pointed out that mixing effects, which may also result in a rather linear ΔN_2O/AOU relationship (e.g. see Nevison et al., 2003; Yamagishi et al., 2005), could not be excluded.

Since NO_3^- is the final product of the nitrification sequence (Walter et al., 2006), its relationship to N_2O ($\Delta N_2O/NO_3^-$ ratio) can be used as an indicator of the extent at which this process is dominant for N_2O production (Bange and Andreae, 1999). Similar to the ΔN_2O/AOU relationship, we found positive correlations between ΔN_2O and NO_3^- concentrations during SO235 (Fig. 6), which together with the predominant O_2 concentrations and the apparent absence of denitrification (Codispoti et al., 2005) suggests that nitrification might be the major pathway of N_2O formation in the SWIO.

4.4. NH_2OH in the SWIO

Discrete NH_2OH samples were measured at stations 2, 4 and 10 during SO235 (cf. Fig. 1). The standard additions were conducted with water from 300 m depth at stations SO235/2 and SO235/4, and with water from 100 m depth at station SO235/10. The regression slopes varied between 0.34 and 0.40 (Supplementary Fig. 4), with the lowest slope at station SO235/10. Different intercepts were a result of different background N_2O concentrations. Our recovery factors ranged from 0.68 to 0.80, which is comparable to the values reported by Butler and Gordon (1986) (0.40–0.83), but considerably higher than the results from Schweiger et al. (2007) in the southwestern Baltic Sea (0.44–0.64). This may be explained by: 1) the higher concentrations of trace metals in coastal waters, which catalyze the decomposition of NH_2OH (Hughes and Nicklin, 1971; Bengtsson, 1973), and 2) the increased number of side reactions of NO_2^- with organic matter that favour N_2O production (Kock and Bange, 2013).

The vertical distribution of NH_2OH was highly variable across different stations (Fig. 7), with concentrations fluctuating between below detection limit and 6.76 nmol L^{-1}. We observed NH_2OH, N_2O and NO_3^- concentrations to increase with depth at station 235/2, whereas at station 235/4 there was a subsurface NH_2OH maximum at 100 m depth, followed by an abrupt decrease to values below detection limit at 500 m. N_2O and NO_3^- concentrations at station 235/4 had a distribution comparable to that of station 235/2. At station 235/10, NH_2OH concentration was close to or below detection limit in the upper 200 m, followed by an abrupt increase at 400 m. Vertical distributions of NO_2^- seemed uniform at these three stations with a subsurface maximum occurring at about 100 m. No uniform NH_2OH profiles were found and NH_2OH concentrations at station 235/2 were much higher than at the other two stations.

Our values were much lower than those observed in the Baltic Sea (0–179 nmol L^{-1}; Gebhardt et al., 2004; Schweiger et al., 2007), which was expected since our samples were from an open ocean area. However, we should point out that those values from the Baltic Sea were measured without the SA solution. The side reactions of NO_2^- can result in a significant bias, which may lead to an overestimation of the NH_2OH concentrations (Kock and Bange, 2013).

The concurrence of low NH_2OH and relatively high N_2O concentrations in the SWIO is not necessarily contradictory to the nitrification-dominated N_2O production. NH_2OH has a relatively short turnover time (< 8 h in natural seawater; Fiadeiro et al., 1967) and thus cannot accumulate in the water column. Either the low nitrification rate or the efficient consumption of NH_2OH would keep the steady-state concentration of hydroxylamine low. Besides, N_2O might be produced via non-NH_2OH involved pathways, like nitrifier-denitrification, or by AOA without NH_2OH formation. However, more direct evidence from isotopic or molecular studies is required to verify this hypothesis.

Although N_2O and NO_3^- profiles look similar at different stations, the fact that NH_2OH distributions vary suggests that the dominant N_2O pathway might be different. The yield of N_2O and NH_2OH is spatially variable, however, our sampling resolution was so coarse (only 6 depths per station) that subtle N_2O and NH_2OH production in the water column might be masked. A more detailed NH_2OH profile would be very helpful to investigate the NH_2OH/N_2O relationship and thus provide further insights into the marine nitrogen cycle.

4.5. Conclusions

Surface waters in the SWIO were mostly supersaturated with N_2O and enhanced saturations were observed between 5 and 10°S due to the wind-driven open ocean upwelling. The SWIO acted as a weak source for the atmospheric N_2O inventory at the time of sampling. N_2O

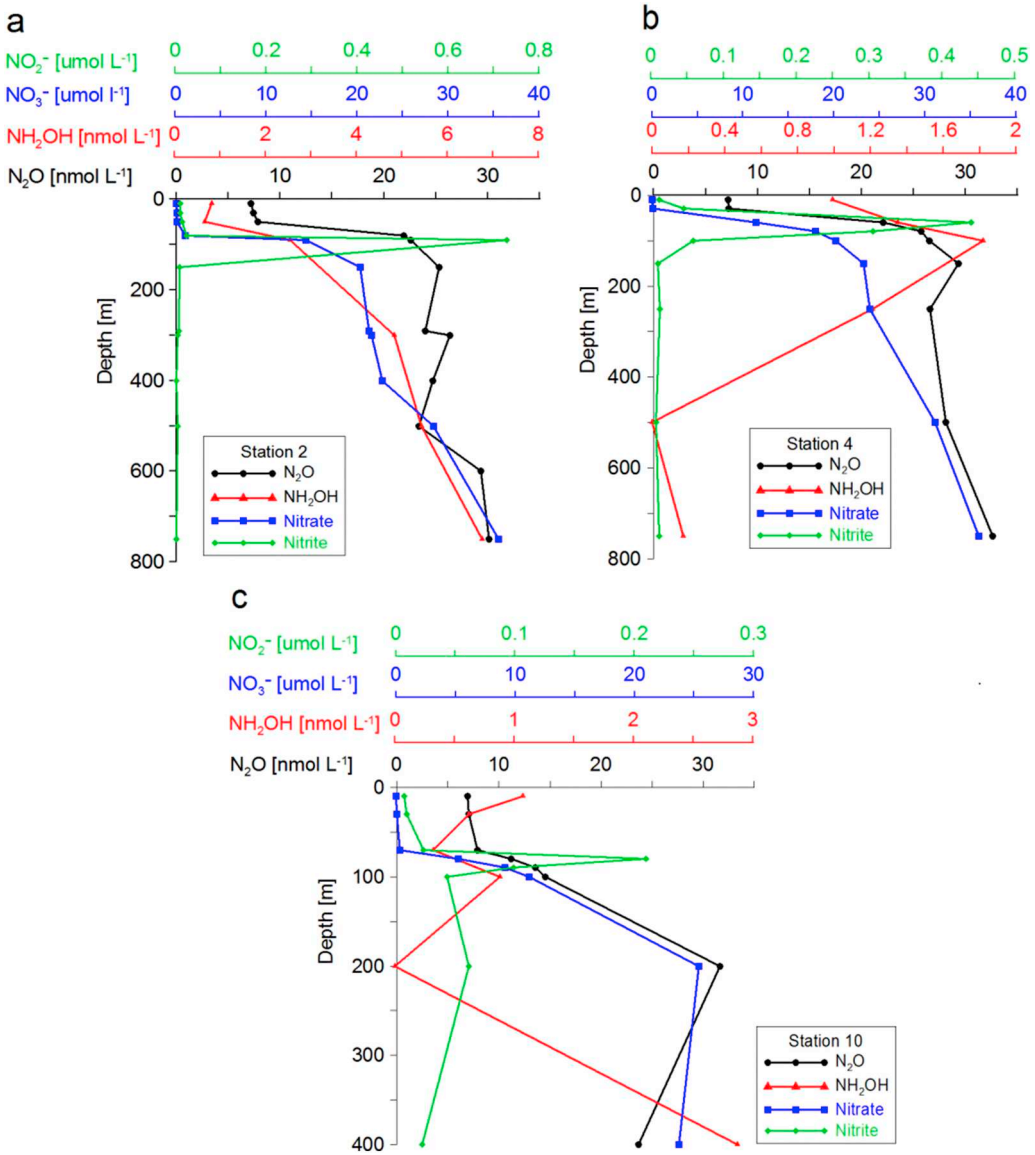

Fig. 7. Vertical distributions of NO_2^-, NO_3^-, N_2O and NH_2OH concentration at selected stations during SO235. Profiles from SO235/2 (a), SO235/4 (b) and SO235/10 (c) are shown.

distributions in the SWIO were negatively correlated with dissolved O_2 concentrations, and maximum N_2O concentrations were found at depths of about 1000 m. Linear relationships between ΔN_2O and AOU and between ΔN_2O and NO_3^- suggested that nitrification was the major N_2O formation pathway in the water column of the SWIO. However, NH_2OH concentrations varied at different stations and no straightforward relationship was found between NH_2OH and N_2O. To what extent NH_2OH is involved in the nitrification process remains to be proven.

Acknowledgements

We thank the captain and crew of the RV SONNE I for their assistance during sampling. We acknowledge the support of the co-chief scientists of SO235 (K. Krüger and B. Quack) and the chief scientist of SO234-2 (C. Marandino). We thank R. Link and M. Krüger for their technical support during the cruises as well as M. Lohmann, and G. Krahmann for providing O_2 and nutrient data. Thanks to T. Steinhoff for his technical support in the operation of our underway systems. We also thank A. Kock for her help in the design of the sampling strategy. We thank three anonymous reviewers for their helpful comments. This study was supported by funding provided by the Future Ocean Excellence Cluster at Kiel University (project CP0910) and the BMBF joint projects SOPRAN II and III (FKZ 03F0611A and FKZ 03F662A). X. Ma is also grateful to the China Scholarship Council for providing financial support (File No. 201306330056). D. L. Arévalo-Martínez received financial support from the EU FP7 project InGOS (Grant Agreement # 284274). The cruises SO234-2 and SO235 were funded by the BMBF (FKZ 03G235A).

Appendix A. Supplementary data

Supplementary data to this article can be found online at https://doi.org/10.1016/j.jmarsys.2018.03.003.

References

Arévalo-Martínez, D.L., Beyer, M., Krumbholz, M., Piller, I., Kock, A., Steinhoff, T., Körtzinger, A., Bange, H.W., 2013. A new method for continuous measurements of oceanic and atmospheric N_2O, CO and CO_2: performance of off-axis integrated cavity output spectroscopy (OA-ICOS) coupled to nondispersive infrared detection (NDIR). Ocean Sci. 9, 1071–1087. http://dx.doi.org/10.5194/os-9-1071-2013.

Arévalo-Martínez, D.L., Kock, A., Steinhoff, T., Brandt, P., Dengler, M., Fischer, T., Körtzinger, A., Bange, H.W., 2017. Nitrous oxide during the onset of the Atlantic Cold

Tongue. J. Geophys. Res. Oceans 122. http://dx.doi.org/10.1002/2016JC012238.
Babbin, A.R., Bianchi, D., Jayakumar, A., Ward, B.B., 2015. Rapid nitrous oxide cycling in the suboxic ocean. Science 348 (6239), 1127–1129. http://dx.doi.org/10.1126/science.aaa8380.
Bakker, D.C.E., Bange, H.W., Gruber, N., Johannessen, T., Upstill-Goddard, R.C., Borges, A.V., Delille, B., Löscher, C.R., Naqvi, W.A., Omar, A.M., Santana-Casiano, L.M., 2014. Air-sea interactions of natural long-lived greenhouse gases (CO_2, N_2O, CH_4). In: Liss, P.S., Johnson, M.T. (Eds.), Ocean-Atmosphere Interactions of Gases and Particles. Springer, pp. 113–169.
Bange, H.W., 2009. Nitrous oxide in the Indian Ocean. In: Wiggert, J.D., Hood, R.R., Naqvi, S.W.A., Brink, K.H., Smith, S.L. (Eds.), Indian Ocean Biogeochemical Processes and Ecological Variability. AGU Geophysical Monograph Series, 185, pp. 205–216. http://dx.doi.org/10.1029/GM185.
Bange, H.W., Andreae, M.O., 1999. Nitrous oxide in the deep waters of the world's oceans. Glob. Biogeochem. Cycles 13, 1127–1135.
Bange, H.W., Andreae, M.O., Lal, S., Law, C.S., Naqvi, S.W.A., Patra, P.K., Rixen, T., Upstill-Goddard, R.C., 2001a. Nitrous oxide emissions from the Arabian Sea: a synthesis. Atmos. Chem. Phys. 1, 61–71.
Bange, H.W., Rapsomanikis, S., Andreae, M.O., 2001b. Nitrous oxide cycling in the Arabian Sea. J. Geophys. Res. 106, 1053–1066.
Bange, H.W., Bell, T.G., Cornejo, M., Freing, A., Uher, G., Upstill-Goddard, R.C., Zhang, G.L., 2009. MEMENTO: a proposal to develop a database of marine nitrous oxide and methane measurements. Environ. Chem. 6, 195–197.
Banning, N.C., Maccarone, L.D., Fisk, L.M., Murphy, D.V., 2015. Ammonia-oxidising bacteria not archaea dominate nitrification activity in semi-arid agricultural soil. Sci. Rep. 5, 11146. http://dx.doi.org/10.1038/srep11146.
Bengtsson, G., 1973. Kinetics and mechanismof reaction between vanadium(V) and hydroxylamine within hydrogen ion concentration range 0.005–0.2 m. Acta Chem. Scand. 27, 3053–3060. http://dx.doi.org/10.3891/ACTA.CHEM.SCAND.27-3053.
Butler, J.H., Gordon, L.I., 1986. An improved gas chromatographic method for the measurement of hydroxylamine in marine and fresh waters. Mar. Chem. 19 (3), 229–243.
Butler, J.H., Jones, R.D., Garber, J.H., Gordon, L.I., 1987. Seasonal distributions and turnover of reduced trace gases and hydroxylamine in Yaquina Bay, Oregon. Geochim. Cosmochim. Acta 51 (3), 697–706.
Butler, J.H., Pequegnat, J.E., Gordon, L.I., Jones, R.D., 1988. Cycling of methane, carbon monoxide, nitrous oxide, and hydroxylamine in a meromictic, coastal lagoon. Estuar. Coast. Shelf Sci. 27 (2), 181–203.
Butler, J.H., Elkins, J.W., Thompson, T.M., 1989. Tropospheric and dissolved N_2O of the West Pacific and East Indian oceans during El Niño Southern Oscillation event of 1987. J. Geophys. Res. 94 (D12), 14865–14877.
Caranto, J.D., Vilbert, A.C., Lancaster, K.M., 2016. Nitrosomonas europaea cytochrome P460 is a direct link between nitrification and nitrous oxide emission. Proc. Natl. Acad. Sci. 113 (51), 14704–14709.
Charpentier, J., Farias, L., Yoshida, N., Boontanon, N., Raimbault, P., 2007. Nitrous oxide distribution and its origin in the central and eastern South Pacific Subtropical Gyre. Biogeosci. Discuss. 4 (3), 1673–1702.
Cline, J.D., Wisegarver, D.P., Kelly-Hansen, K., 1987. Nitrous oxide and vertical mixing in the equatorial Pacific during the 1982–1983 El Niño. Deep Sea Res. Part A 34 (5/6), 857–873.
Codispoti, L.A., Yoshinari, T., Devol, A.H., 2005. Suboxic respiration in the oceanic water column. In: Del Giorgio, P.A., Williams, P. (Eds.), Respiration in Aquatic Ecosystems. Oxford University Press, Oxford, pp. 225–247.
Collins, C., Reason, C.J.C., Hermes, J.C., 2012. Scatterometer and reanalysis wind products over the western tropical Indian Ocean. J. Geophys. Res. 117, C03045. http://dx.doi.org/10.1029/2011JC007531.
Elkins, J.W., Wofsy, S.C., McElroy, M.B., Kolb, C.E., Kaplan, W.A., 1978. Aquatic sources and sinks for nitrous oxide. Nature 275, 602–606.
Farias, L., Castro-Gonzalez, M., Cornejo, M., Charpentier, J., Faundez, J., Boontanon, N., Yoshida, N., 2009. Denitrification and nitrous oxide cycling within the upper oxycline of the eastern tropical South Pacific oxygen minimum zone. Limnol. Oceanogr. 54, 132–144.
Fiadeiro, M., Solorzan, L., Strickla, J.D., 1967. Hydroxylamine in seawater. Limnol. Oceanogr. 12, 555. http://dx.doi.org/10.4319/LO.1967.12.3.0555.
Fiehn, A., Quack, B., Hepach, H., Fuhlbrügge, S., Tegtmeier, S., Toohey, M., Atlas, Elliot, Krüger, K., 2017. Delivery of halogenated very short-lived substances from the west Indian Ocean to the stratosphere during the Asian summer monsoon. Atmos. Chem. Phys. 17, 6723–6741.
Forster, G., Upstill-Goddard, R.C., Gist, N., Robinson, C., Uher, G., Woodward, E.M.S., 2009. Nitrous oxide and methane in the Atlantic Ocean between 50°N and 52°S: latitudinal distribution and sea-to-air flux. Deep-Sea Res. II Top. Stud. Oceanogr. 56 (15), 964–976.
Garrat, J.R., 1977. Review of drag coefficients over oceans and continents. Mon. Weather Rev. 105, 915–929.
Gebhardt, S., Walter, S., Nausch, G., Bange, H.W., 2004. Hydroxylamine (NH_2OH) in the Baltic Sea. Biogeosci. Discuss. 1 (1), 709–724.
Goreau, T.J., Kaplan, W.A., Wofsy, S.C., McElroy, M.B., Valois, F.W., Watson, S.W., 1980. Production of NO_2^- and N_2O by nitrifying bacteria at reduced concentrations of oxygen. Appl. Environ. Microbiol. 40, 526–532.
Hansen, H.P., 1999. Determination of oxygen. In: Grasshoff, K.G., Kremling, K., Ehrhardt, M. (Eds.), Methods of Seawater Analysis. Wiley-VCH, Weinheim, Germany, pp. 75–90.
Ho, D.T., Law, C.S., Smith, M.J., Schlosser, P., Harvey, M., 2006. Measurements of air-sea gas exchange at high wind speeds in the Southern Ocean: implications for global parameterizations. Geophys. Res. Lett. 33, L16611. http://dx.doi.org/10.1029/2006GL026817.
Hood, R.H., Urban, E.R., McPhaden, M.J., Su, D., Raes, E., 2016. The 2nd international Indian Ocean expedition (IIOE-2): motivating new exploration in a poorly understood basin. Limnol. Oceanogr. Bull. 25, 117–124. http://dx.doi.org/10.1002/lob.10149.
Hughes, M.N., Nicklin, H.G., 1971. Autoxidation of hydroxylamine in alkaline solutions. J. Chem. Soc. A 164–168. http://dx.doi.org/10.1039/J19710000164.
Kock, A., Bange, H.W., 2013. Nitrite removal improves hydroxylamine analysis in aqueous solution by conversion with iron (III). Environ. Chem. 10, 64–71.
Kock, A., Arévalo-Martínez, D.L., Löscher, C.R., Bange, H.W., 2016. Extreme N_2O accumulation in the coastal oxygen minimum zone off Peru. Biogeosciences 13, 827–840. http://dx.doi.org/10.5194/bg-13-827-2016.
Kumar, S.P., Prasad, T.G., 1999. Formation and spreading of Arabian Sea high-salinity water mass. J. Geophys. Res. 104 (C1), 1455–1464.
Law, C.S., Owens, N.P.J., 1990. Significant flux of atmospheric nitrous oxide from the northwest Indian Ocean. Nature 346, 826–828.
Li, J., Nedwell, D.B., Beddow, J., Dumbrell, A.J., McKew, B.A., Thorpe, E.L., Whitby, C., 2015. amoA gene abundances and nitrification potential rates suggest that benthic ammonia-oxidizing bacteria and not archaea dominate N cycling in the Colne Estuary, United Kingdom. Appl. Environ. Microbiol. 81, 159–165.
Lipschultz, F., Zafiriou, O.C., Wofsy, S.C., McElroy, M.B., Valois, F.W., Watson, S.W., 1981. Production of NO and N_2O by soil nitrifying bacteria. Nature 294, 641–643.
Löscher, C.R., Kock, A., Könneke, M., LaRoche, J., Bange, H.W., Schmitz, R.A., 2012. Production of oceanic nitrous oxide by ammonia-oxidizing archaea. Biogeosciences 9, 2419–2429.
Mitchell, T.P., Wallace, J.M., 1992. The annual cycle in equatorial convection and sea surface temperature. J. Clim. 5, 1140–1156.
Morales, R.A., Barton, E.D., Heywood, K.J., 1997. Variability of water masses in the western Indian Ocean. Oceanogr. Lit. Rev. 2, 86.
Myhre, G.D., Schindell, D., Bréon, F.M., Collins, W., Fuglestvedt, J., Huang, J., Koch, D., Lamarque, J.F., Lee, D., Mendoza, B., Nakajima, T., Robock, A., Stephens, G., Takemura, T., Zhang, H., 2013. Anthropogenic and natural radiative forcing. In: Stocker, T.F., Qin, D., Plattner, G.K., Tignor, M., Allen, S.K., Boschung, J., Nauels, A., Xia, Y., Bex, V., Midgley, P.M. (Eds.), Climate Change 2013: The Physical Science Basis, Contribution of Working Group I to the Fifth Assessment Report of the Intergovernmental Panel on Climate Change. Cambridge University Press, Cambridge, United Kingdom and New York, USA, pp. 129–234.
Naqvi, S.W.A., Jayakumar, D.A., Nair, M.D., Kumar, M.D., George, M.D., 1994. Nitrous oxide in the western Bay of Bengal. Mar. Chem. 47, 269–278.
Naqvi, S.W.A., Jayakumar, D.A., Narvekar, P.V., Naik, H., Sarma, V.V.S.S., D'Souza, W., Joseph, S., George, M.D., 2000. Increased marine production of N_2O due to intensifying anoxia on the Indian continental shelf. Nature 408, 346–349.
Nevison, C., Butler, J.H., Elkins, J.W., 2003. Global distribution of N_2O and the ΔN_2O-AOU yield in the subsurface ocean. Glob. Biogeochem. Cycles 17 (4), 1119. http://dx.doi.org/10.1029/2003GB002068.
Nevison, C.D., Lueker, T.J., Weiss, R.F., 2004. Quantifying the nitrous oxide source from coastal upwelling. Glob. Biogeochem. Cycles 18, GB1018. http://dx.doi.org/10.1029/2003GB002110.
Nightingale, P.D., Malin, G., Law, C.S., Watson, A.J., Liss, P.S., Liddicoat, M.I., Boutin, J., Upstill-Goddard, R.C., 2000. In situ evaluation of air-sea gas exchange parameterizations using novel conservative and volatile tracers. Glob. Biogeochem. Cycles 14, 373–387.
Ostrom, N.E., Russ, M.E., Popp, B., Rust, T.M., Karl, D.M., 2000. Mechanisms of nitrous oxide production in the subtropical North Pacific based on determinations of the isotopic abundances of nitrous oxide and di-oxygen. Chemosphere Global Change Sci. 2 (3), 281–290.
Ravishankara, A.R., Daniel, J.S., Portmann, R.W., 2009. Nitrous oxide (N_2O): the dominant ozone-depleting substance emitted in the 21st century. Science 326, 123–125.
Sabba, F., Picioreanu, C., Pérez, J., Nerenberg, R., 2015. Hydroxylamine diffusion can enhance N_2O emissions in nitrifying biofilms: a modeling study. Environ. Sci. Technol. 49, 1486–1494.
Santoro, A.E., Buchwald, C., Mcllvin, M.R., Casciotti, K.L., 2011. Isotopic signature of N_2O produced by marine ammonia-oxidizing archaea. Science 333, 1282–1285.
Schott, F.A., Xie, S.P., McCreary Jr., J.P., 2009. Indian Ocean circulation and climate variability. Rev. Geophys. 47, RG1002. http://dx.doi.org/10.1029/2007RG000245.
Schweiger, B., Hansen, H.P., Bange, H.W., 2007. A time series of hydroxylamine (NH_2OH) in the southwestern Baltic Sea. Geophys. Res. Lett. 34, L24608. http://dx.doi.org/10.1029/2007GL031086.
Singh, H.B., Salas, L.J., Sri, H.S., 1979. The distribution of nitrous oxide (N_2O) in the global atmosphere and the Pacific Ocean. Tellus 31, 313–320.
Smith, J.M., Casciotti, K.L., Chavez, F.P., Francis, C.A., 2014. Differential contributions of archaeal ammonia oxidizer ecotypes to nitrification in coastal surface waters. ISME J. 8, 1704–1714.
Stein, L.Y., 2011. Surveying N_2O-producing pathways in bacteria. Methods Enzymol. 486, 131–152.
Stramma, L., Lutjeharms, J.R.E., 1997. The flow field of the subtropical gyre of the South Indian Ocean. J. Geophys. Res. Oceans 102, 5513–5530.
Toole, J.M., Warren, B.A., 1993. A hydrographic section across the subtropical South Indian Ocean. Deep-Sea Res. I Oceanogr. Res. Pap. 40, 1973–2019.
Trimmer, M., Chronopoulou, P.M., Maanoja, S.T., Upstill-Goddard, R.C., Kitidis, V., Purdy, K.J., 2016. Nitrous oxide as a function of oxygen and archaeal gene abundance in the North Pacific. Nat. Commun. 7, 13451. http://dx.doi.org/10.1038/ncomms13451.
Upstill-Goddard, R.C., Barnes, J., Owens, N.J.P., 1999. Nitrous oxide and methane during the 1994 SW monsoon in the Arabian Sea/northwestern Indian Ocean. J. Geophys. Res. Oceans 104, 30067–30084. http://dx.doi.org/10.1029/1999jc900232.
Vajrala, N., Martens-Habbena, W., Sayavedra-Soto, L.A., Schauer, A., Bottomley, P.J., Stahl, D.A., Arp, D.J., 2013. Hydroxylamine as an intermediate in ammonia oxidation

by globally abundant marine archaea. Proc. Natl. Acad. Sci. 110, 1006–1011.
Walker, C.B., De La Torre, J.R., Klotz, M.G., Urakawa, H., Pinel, N., Arp, D.J., Brochier-Armanet, C., Chain, P.S.G., Chan, P.P., Gollabgir, A., Hemp, J., Hugler, M., Karr, E.A., Konneke, M., Shin, M., Lawton, T.J., Martens-Habbena, W., Sayavedra-Soto, L.A., Lang, D., Sievert, S.M., Rosenzweig, A.C., Manning, G., Stahl, D.A., 2010. *Nitrosopumilus maritimus* genome reveals unique mechanisms for nitrification and autotrophy in globally distributed marine crenarchaea. Proc. Natl. Acad. Sci. 107, 8818–8823.
Walter, S., Bange, H.W., Wallace, D.W.R., 2004. Nitrous oxide in the surface layer of the tropical North Atlantic Ocean along a west to east transect. Geophys. Res. Lett. 31, L23S07. http://dx.doi.org/10.1029/2004GL019937.
Walter, S., Bange, H.W., Breitenbach, U., Wallace, D.W.R., 2006. Nitrous oxide in the North Atlantic Ocean. Biogeosciences 3, 607–619.
Weiss, R.F., Price, B.A., 1980. Nitrous oxide solubility in water and seawater. Mar. Chem. 8, 347–359.
Weiss, R.F., Van Woy, F.A., Salameh, P.K., 1992. Surface Water and Atmospheric Carbon Dioxide and Nitrous Oxide Observations by Shipboard Automated Gas Chromatography: Results from Expeditions between 1977 and 1990. Oak Ridge National Lab. TN (United States). Carbon Dioxide Information Analysis Center.
Wyrtki, K., 1973. Physical oceanography of the Indian Ocean. In: The Biology of the Indian Ocean. Springer Berlin Heidelberg, pp. 18–36.
Yamagishi, H., Yoshida, N., Toyoda, S., Popp, B.N., Westley, M.B., Watanabe, S., 2005. Contributions of denitrification and mixing on the distribution of nitrous oxide in the North Pacific. Geophys. Res. Lett. 32, L04603. http://dx.doi.org/10.1029/2004GL021458.
Yamazaki, T., Hozuki, T., Arai, K., Toyoda, S., Koba, K., Fujiwara, T., Yoshida, N., 2014. Isotopomeric characterization of nitrous oxide produced by reaction of enzymes extracted from nitrifying and denitrifying bacteria. Biogeosciences 11, 2679–2689.
Yoshinari, T., 1976. Nitrous oxide in the sea. Mar. Chem. 4 (2), 189–202.
Zhang, L.M., Hu, H.W., Shen, J.P., He, J.Z., 2012. Ammonia-oxidizing archaea have more important role than ammonia-oxidizing bacteria in ammonia oxidation of strongly acidic soils. ISME J. 6, 1032–1045.

Conclusions

The variability and emissions of CH_4 and N_2O are controlled by various factors and these factors are not independent from each other. The results presented in the thesis provide new perspectives for the understanding of dissolved CH_4/N_2O variability, and also give some clues about future developments of CH_4/N_2O emissions from coastal waters.

Temperature plays a modulating role for N_2O emissions, but not for CH_4. We have found a seasonal cycle for surface N_2O concentrations at BE, but not for surface N_2O saturations, while the variability in surface CH_4 concentrations and saturations are generally consistent during 2006–2017. As a result of global warming, the solubility of CH_4 and N_2O are decreasing. The background CH_4 concentrations/saturations are so high that the impact on CH_4 emissions seems negligible, but surface N_2O saturations are close to equilibrium and thus are more sensitive to seasonal and interannual temperature oscillations. This highlights that the respond of these two gases to global warming might be different.

Saline inflows and upwelling events exert a strong influence on the emissions of CH_4 and N_2O at BE. In November 2017, the N_2O flux density was about 30 times higher because of an upwelling event which brought N_2O-enriched bottom water to the surface. In December 2014, a strong MBI event significantly promoted CH_4 emissions from Eckernförde Bay, but its impact on the N_2O emissions was negligible. This can be explained by the dominant sedimentary CH_4 release. These kind of events (upwelling, MBI) are usually transient, but they contribute significantly to the overall sea-to-air CH_4/N_2O fluxes.

Dissolved O_2 is one of the major controlling factors for CH_4/N_2O variability in both coastal and open ocean settings: (i) At BE, the seasonal variations of CH_4/N_2O were closely linked to the development of hypoxic/anoxic events and (ii) In the SW Indian Ocean, we found a correlation between N_2O (ΔN_2O) and O_2 (AOU).

On the basis of the N_2O/AOU relationship and the NH_2OH measurements, nitrification was identified as the main pathway of N_2O in the SW Indian Ocean. Although NH_2OH profiles in the Indian Ocean seems highly variable, reliable measurement of NH_2OH can provide more information about the short-term dynamics of the marine nitrogen cycle.

Our results indicate that southwestern Baltic Sea is an important source of atmospheric CH_4/N_2O. Due to expanding hypoxia/anoxia, we suggest that N_2O emissions at BE are likely to decrease in the future, which challenges the traditional view that N_2O emissions

from coastal waters would most probably increase. The CH_4 concentrations were potentially increasing at BE during the study, which is different from the declining trend of CH_4 reported from other time series stations such as ALOHA and Saanich Inlet. The trends at BE might be caused by the shallow water depth (which leads to massive release of CH_4 to the water column) and the improved eutrophication status in the coastal Baltic Sea (HELCOM, 2018) (which leads to decreasing N_2O concentrations). However, neither of the trends mentioned above is significant based on our observations at BE. To verify the trends of CH_4/N_2O, continuation of the measurement at BE is mandatory.

Acknowledgements

First of all I would like to thank Prof. Dr. Hermann W. Bange. Talking to him makes me feel relax and peaceful, and he is always happy to give suggestions and comments. He is knowledgeable, thoughtful and patient. I cannot finish my PhD successfully without him.

I would like to thank Annette Kock, Damian L. Arévalo-Martínez and Sinikka T. Lennartz for their help in field investigations, lab works and writing. They are willing to share their ideas and I really learned a lot from them. Tobias Hahn, Dennis Booge, Tina Fiedler and Martina Lohmann offered me great help in daily life, especially in German translation. They are always patient to help me solve various problems. Thanks to Frank Malien and the crew of Littorina, BE cruises were smooth and successful during the past years. The work group “AG Bange” feels like a big family with a positive and friendly working atmosphere. I would also like to thank all the Chinese colleagues and friends. We had a good time together and they make me feel at home. Thanks to China Scholarship Council and BONUS INTEGRAL project for their financial support.

Last but not least, I would like to thank my family, who are always there for me. My parents and parents-in-law flew all the way to Germany to help take care of Mia, which was a big relief for us. Mingshuang is always supportive for my work and life. She sacrificed a lot to look after Mia during the corona crisis so that I can focus on my work.

Supplement of Biogeosciences, 16, 4097–4111, 2019
https://doi.org/10.5194/bg-16-4097-2019-supplement

Biogeosciences Open Access EGU

Supplement of

A multi-year observation of nitrous oxide at the Boknis Eck Time Series Station in the Eckernförde Bay (southwestern Baltic Sea)

Xiao Ma et al.

Correspondence to: Xiao Ma (mxiao@geomar.de)

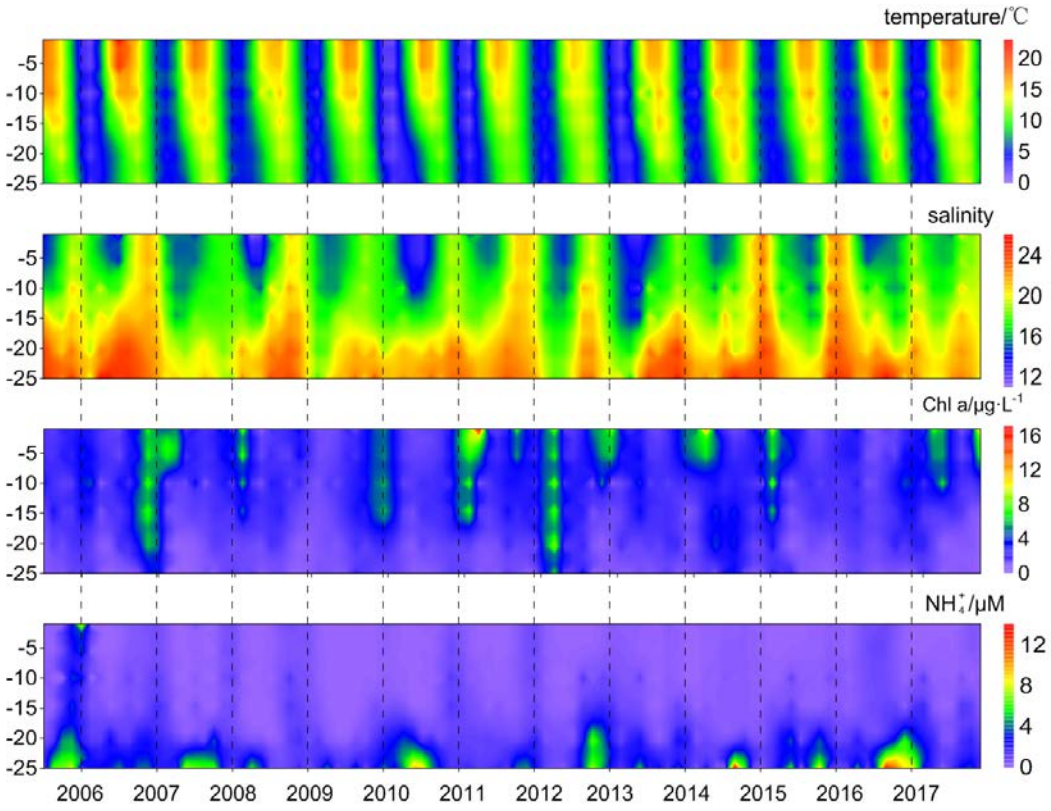

Supplementary Figure 1. Vertical distributions of temperature, salinity, chlorophyll *a* and NH_4^+ from the BE Time-Series Station during 2005–2017. Please note that high NH_4^+ concentrations (>20 μM/L, which are detected in the bottom water of October 2005, May 2006, October 2013, October 2014, October and November 2016) were removed for better visualization.

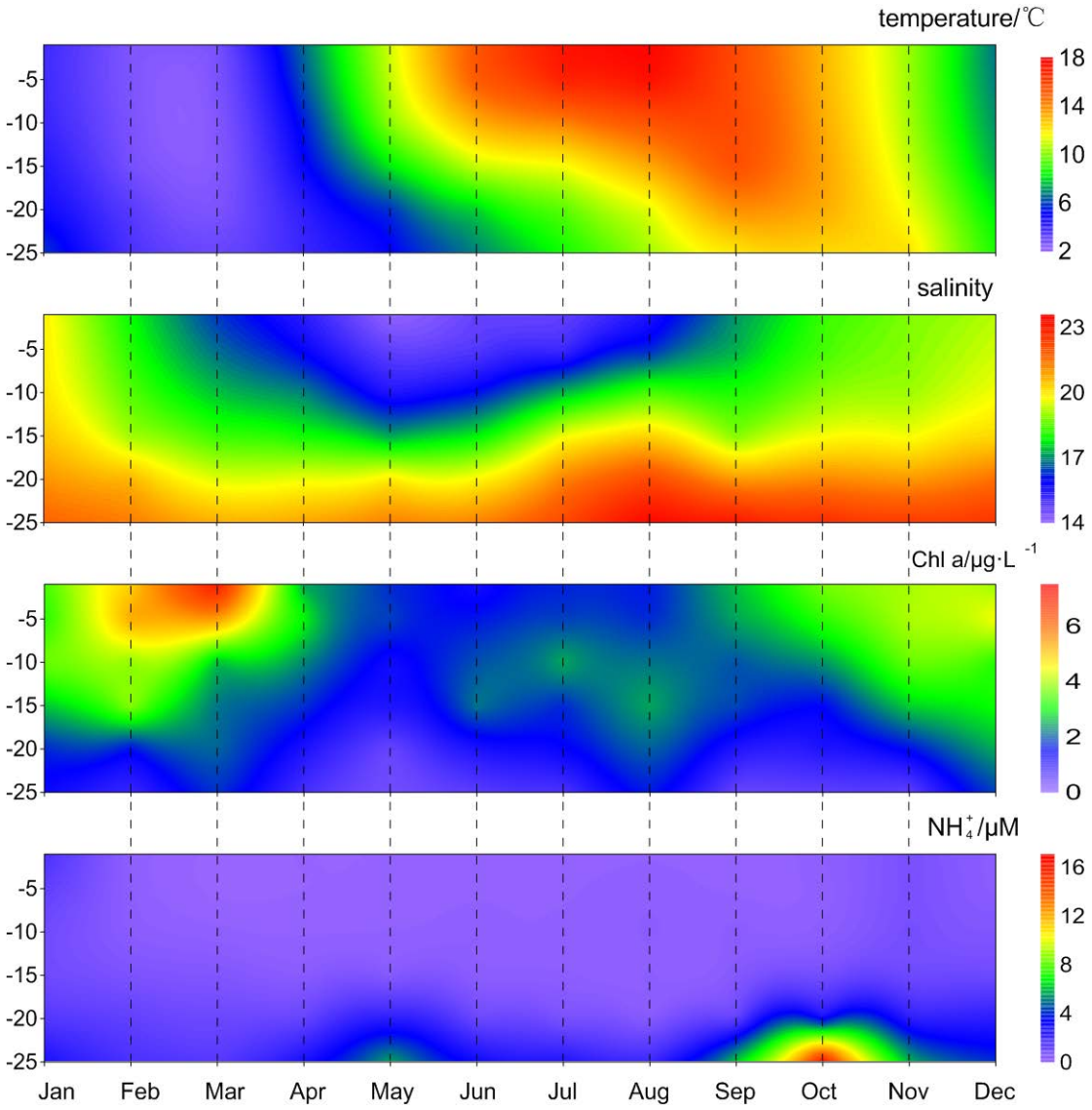

Supplementary Figure 2. Average vertical distributions of temperature, salinity, chlorophyll *a* and NH_4^+ from the BE Time-Series Station during 2005–2017

Supplementary material for: Nitrous Oxide and Hydroxylamine Measurements in the Southwest Indian Ocean

Xiao Ma, Hermann W. Bange, Gesa K. Eirund, and Damian L. Arévalo-Martínez

Contents

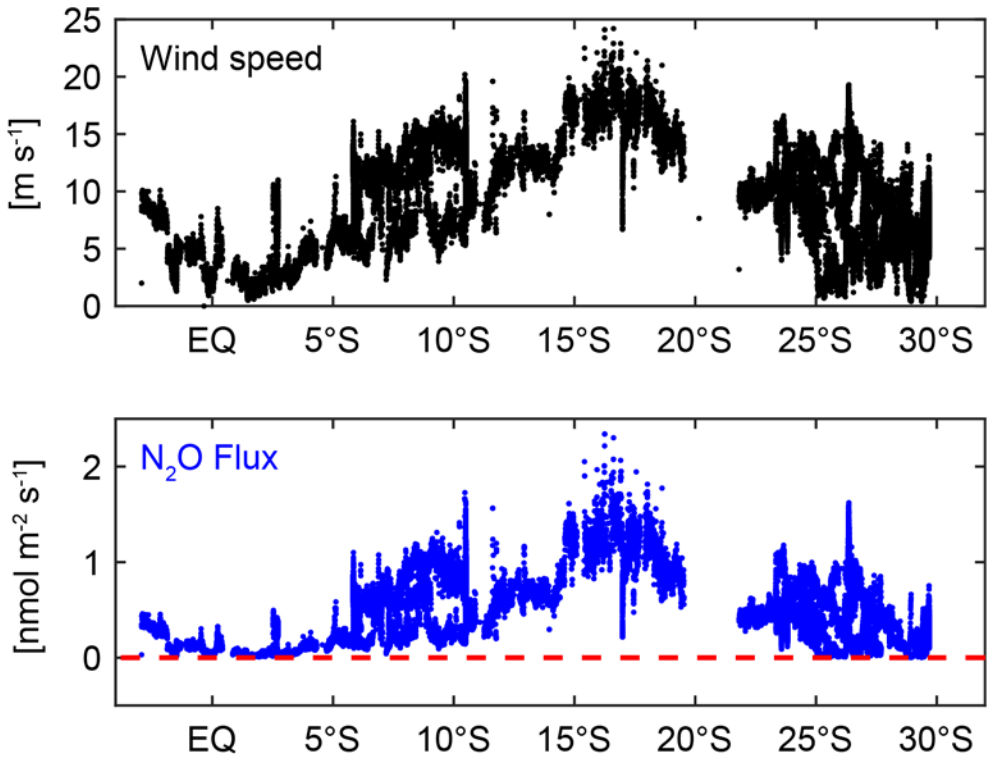

Supplementary Figure 1. Latitudinal distribution of wind speed and sea-to-air N_2O fluxes during the SO234-2 and SO235 cruises. Positive values in the lower panel indicate N_2O outgassing to the atmosphere.

- Supplementary Figure 2.

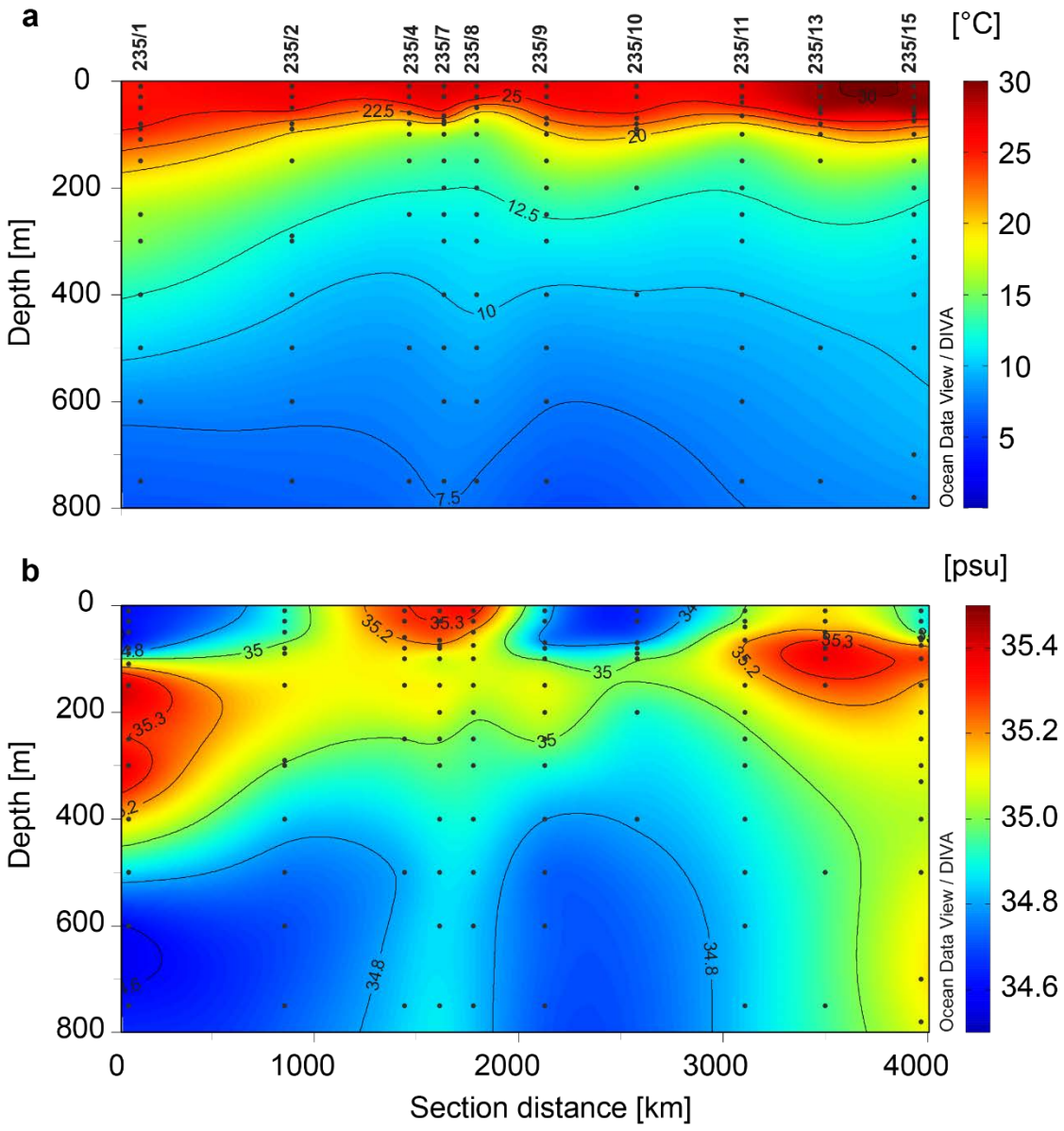

Supplementary Figure 2. Distributions of temperature (a) and salinity (b) during the SO235 cruise. Station numbers are indicated above panel (a) (c.f. Fig.1).

- Supplementary Figure 3.

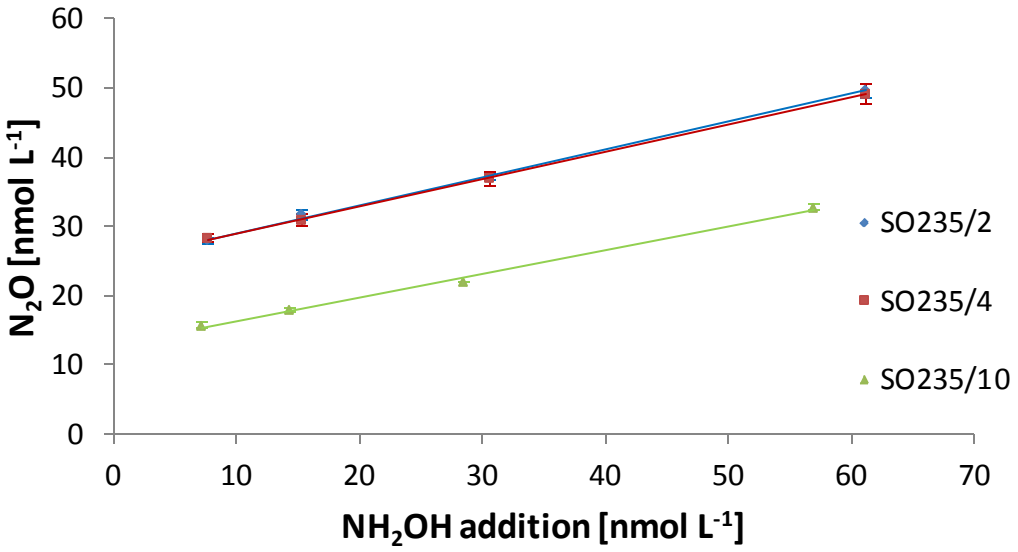

Supplementary Figure 3. NH_2OH standard additions during the SO235 cruise. Regression parameters are:

SO235/2 (blue) y = 0.400x + 25.096, r^2 = 0.998, SO235/4 (red) y = 0.391x + 25.161, r^2 = 0.999, and SO235/10 (green) y = 0.343x + 12.937, r^2 = 0.995.